

Summer 2003

Fabrication of cell culture scaffolds using micro/ nanotechnologies to study the attachment and alignment of smooth muscle cells

Mengyan Li

**FABRICATION OF CELL CULTURE SCAFFOLDS USING
MICRO/NANOTECHNOLOGIES TO STUDY
THE ATTACHMENT AND ALIGNMENT
OF SMOOTH MUSCLE CELLS**

by

Mengyan Li, M.S.

A Dissertation Presented in Partial Fulfillment
of the Requirements for the Degree
Ph.D. in Engineering

COLLEGE OF ENGINEERING AND SCIENCE
LOUISIANA TECH UNIVERSITY

August 2003

UMI Number: 3095971

Li, Mengyan

All rights reserved.

UMI[®]

UMI Microform 3095971

Copyright 2003 by ProQuest Information and Learning Company.

All rights reserved. This microform edition is protected against
unauthorized copying under Title 17, United States Code.

ProQuest Information and Learning Company
300 North Zeeb Road
P.O. Box 1346
Ann Arbor, MI 48106-1346

LOUISIANA TECH UNIVERSITY

THE GRADUATE SCHOOL

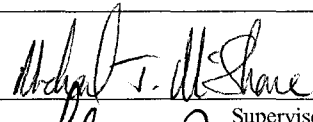
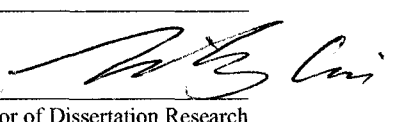
08/04/2003

Date

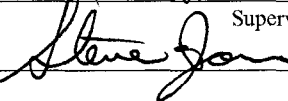
We hereby recommend that the dissertation prepared under our supervision by Mengyan Li

entitled Fabrication of Cell Culture Scaffolds Using Micro/Nanotechnologies to Study the Attachment and Alignment of Smooth Muscle Cells

be accepted in partial fulfillment of the requirements for the Degree of Ph.D. in Engineering

Supervisor of Dissertation Research

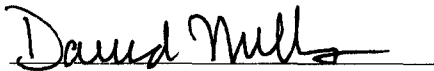


Head of Department

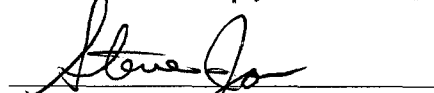
Biomedical Engineering

Department

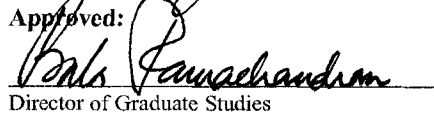
Recommendation concurred in:

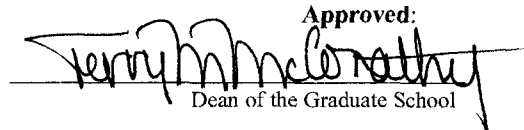






Advisory Committee

Approved: 
Director of Graduate Studies

Approved: 
Dean of the Graduate School


Dean of the College

ABSTRACT

This dissertation elaborates the design and fabrication of *in vitro* cell culture scaffolds using microfabrication and electrostatic layer-by-layer self-assembly (LbL) technologies, and develops the so-called layer-by-layer lift-off (LbL-LO) technique to control surface topography, surface properties, and underlying architectures of the scaffolds. Smooth muscle cells were cultured on the fabricated scaffolds with gelatin, fibronectin, and polyelectrolytes (PSS, PDDA, PAH, and PEI) as surface materials, multilayer polyelectrolytes as architectures, deposited in strip- and square-patterns. It was found that the exposed surface materials, which have different charge, hydrophobicity, and chemical structure (e.g., amino acid sequence), affect the adhesion of smooth muscle cells. Cells attached and grew on negatively-charged gelatin, PSS, and acid-treated glass surfaces rather than on positively-charged PDDA and PAH surfaces. The cell-adhesive proteins gelatin and fibronectin improve the attachment and further growth of smooth muscle cells, and cells attached to these surfaces showed more natural morphology than on PSS-coated surfaces. In addition, the underlying architectures of the polyelectrolyte thin films also significantly influence the cell morphologies and attachment. Cells on thicker nanofilms (20-bilayer) showed more elongated and spread-out morphology than on the thinner ones (e.g., 2-bilayer). Cells cultured on the gelatin- and fibronectin-coated strip patterns showed aligned patterns along the main axis of the strips. It was observed cells on 60 μ m wide strips had better alignment than on the 120 μ m strips. The

experimental results indicate that the LbL-LO technique is an efficient method to fabricate *in vitro* cell culture scaffolds with precise control of the surface properties and topography in three dimensions, and therefore, to study the cell behavior. The results of study suggest that a combination of micro/nanotechnologies for biosurface engineering has great potential in the application of tissue engineering and other related areas.

APPROVAL FOR SCHOLARLY DISSEMINATION

The author grants to the Prescott Memorial Library of Louisiana Tech University the right to reproduce, by appropriate methods, upon request, any or all portions of this Dissertation. It is understood that "proper request" consists of the agreement, on the part of the requesting party, that said reproduction is for his personal use and that subsequent reproduction will not occur without written approval of the author of this Dissertation. Further, any portions of the Dissertation used in books, papers, and other works must be appropriately referenced to this Dissertation.

Finally, the author of this Dissertation reserves the right to publish freely, in the literature, at any time, any or all portions of this Dissertation.

Author *Limengji*
Date *8/4/2003*

TABLE OF CONTENTS

ABSTRACT	iii
TABLE OF CONTENTS.....	vi
LIST OF TABLES.....	xi
LIST OF FIGURES	xii
LIST OF EQUATIONS.....	xviii
ACKNOWLEDGMENTS	xix
CHAPTER 1 INTRODUCTION	1
1.1 Overview.....	1
1.2 Research Review.....	3
1.3 Research Need and Motivation.....	8
CHAPTER 2 BACKGROUND	13
2.1 Tissue Engineering.....	13
2.1.1 What is Tissue Engineering?.....	13
2.1.2 Tissue Engineering Approaches.....	14
2.1.3 Motivations of Tissue Engineering.....	15
2.2 The Environment of Cells - Extracellular Matrix (ECM).....	16
2.2.1 Proteoglycans.....	17
2.2.2 Collagen.....	18

2.2.3	Elastin	20
2.2.4	Fibronectin	20
2.2.5	Laminin	22
2.3	Integrins	22
2.4	Cellular Interactions.....	24
2.4.1	Cell-Cell Interaction.....	24
2.4.2	Cell-ECM Interaction.....	25
2.5	Cellular Behavior	26
2.5.1	Cell Adhesion / Attachment.....	26
2.5.2	Cell Alignment / Orientation	27
2.5.3	Cell Migration / Mobility.....	28
2.5.4	Cell Growth / Spreading / Proliferation	28
2.5.5	Cell Differentiation	29
2.6	<i>In vitro</i> Cell Culture Scaffolds.....	29
2.6.1	Biomaterials	30
2.6.2	Biocompatibility	30
2.7	Surface Modification	31
2.7.1	Modification of Surface Topography.....	32
2.7.2	Modification of Surface Properties.....	33
2.8	Layer-by-Layer Self-Assembly.....	35
CHAPTER 3 EXPERIMENTAL DESIGN AND THEORIES		37
3.1	General Design.....	37
3.2	Biomaterials	38

3.2.1	Polymeric Materials and Surface Treatment.....	38
3.2.2	Protein-Surface Interactions.....	40
3.3	Layer-by-Layer Self-Assembly and Hydrophobic Interactions.....	42
3.3.1	Gibbs Free Energy of Film Formation.....	42
3.3.2	Energy Model.....	43
3.3.3	Correlation with Experimental Data	44
3.4	Electrostatic Layer-by-Layer Self-Assembly	46
3.4.1	Polyanion / Polycation Alternate Assembly	47
3.4.2	Multilayer Microencapsulation of Microspheres.....	48
3.4.3	Standard Assembly Procedure	49
3.5	Principles of Microfabrication	50
3.5.1	Photolithography and Inductively Coupled Plasma Etching	50
3.5.2	Soft Lithography	53
3.5.3	Hot-Embossing	54
3.6	Physical Surface Characterization	55
3.6.1	Contact Angle Analysis	55
3.6.2	Scanning Electron Microscopy (SEM)	56
3.6.3	Atomic Force Microscopy (AFM).....	57
3.7	Material Characterization.....	58
3.7.1	Quartz Crystal Microbalance (QCM)	58
3.7.2	Zeta-potential Analysis	60
3.7.3	Beer's Law – Concentration and Absorbance.....	61
3.8	Biological characterization	64

3.8.1	Staining Cells	64
3.8.2	Principle of Fluorescence.....	67
CHAPTER 4	MATERIALS AND METHODS.....	71
4.1	Materials and Instrumentation	71
4.2	Techniques and Methods	72
4.2.1	Conjugate Solution Preparation	72
4.2.2	Electrostatic Layer-by-Layer Self-Assembly	73
4.2.3	Layer-by-Layer & Lift-Off (LbL-LO).....	75
4.2.4	Monolayer Cell Culture	77
4.2.5	Cell Staining.....	78
4.2.6	Cell Density Counting.....	80
4.2.7	Measurement of Cell Roundness and Number of Pseudopodia.....	80
4.2.8	Statistical Analysis.....	81
CHAPTER 5	RESULTS AND DISCUSSION	82
5.1	Basic Studies on Layer-by-Layer Assembled Thin Films	82
5.1.1	Zeta-potential and UV-Vis Measurements of Gelatin at Different pH Values.....	82
5.1.2	QCM, Fluorescence Spectra, and Zeta-potential Measurements of FITC-gelatin.....	85
5.1.3	Contact Angle Measurements of Polyelectrolyte Multilayer Thin Films....	91
5.1.4	QCM Measurement of Fibronectin.....	97
5.1.5	Atomic Force Microscopy (AFM) Scan of Polyelectrolyte and Protein Thin Films.....	99
5.2	Fabrication of Cell Culture Scaffolds	108
5.2.1	Fabrication of Multilayer Thin Film Patterns on Planar Base Substrates..	108

5.2.2	Fabrication of PMMA Microchanneled Substrate.....	119
5.2.3	Fabrication of 3-D Microfluidic Cell Culture System on Silicon Substrate.....	121
5.3	Cell Culture on Engineered Scaffolds.....	123
5.3.1	Culture RASMCs on Planar Substrates	123
5.3.2	Culture Cells on Patterned Substrates.....	135
5.4	Cell Culture on other Substrates	150
5.4.1	Cells Cultured on PMMA Microchanneled Substrates.....	150
5.4.2	Cells Cultured in 3-D Silicon Microfluidic Cell Culture Systems	151
CHAPTER 6 CONCLUSIONS.....		154
REFERENCES		158
APPENDIX A MATERIALS, CHEMICALS, AND SUPPLIES		177
APPENDIX B EQUIPMENT AND INSTRUMENTATION		181
APPENDIX C EXPERIMENTAL TECHNIQUES		183

LIST OF TABLES

Table 3.1 Properties of Proteins that Affect their Interaction with Surfaces	41
Table 3.2 Properties of Surfaces that affect their interaction with Proteins	42
Table 5.1 Zeta-potentials (mV) of 400 nm silica particles at pH 4 and pH 10.....	83
Table 5.2 UV-Vis peak absorbance values at 215 nm for gelatin solutions.....	84
Table 5.3 Gelatin consumption by silica particles during layering process	84
Table 5.4 Roughness of PSS-coated polyelectrolyte thin films on glass substrates.....	101
Table 5.5 Roughness of fibronectin-coated polyelectrolyte thin films on glass substrates.....	107
Table 5.6 Probability of T-test of cell roundness and number of pseudopodia on different number of underlying polyelectrolyte architectures (m=n=15).	134
Table 5.7 Probability of paired T-test of cell roundness and number of pseudopodia on different coating materials (n=5).	135

LIST OF FIGURES

Figure 1.1 Schematic illustration of 3-D cell culture system.....	11
Figure 2.1 Illustration of collagen fiber	18
Figure 2.2 Molecular structure of gelatin	19
Figure 2.3 Illustration of elastin fiber	20
Figure 2.4 Three types of fibronectin modules.....	21
Figure 2.5 Molecular interactions of Fibronectin	22
Figure 2.6 Illustration of integrin function	23
Figure 3.1 Schematic layer-by-layer film assembly on a solid substrate	48
Figure 3.2 Schematic illustrations of the protein shell assembly on a latex sphere.....	49
Figure 3.3 Schematic illustration of photolithography	51
Figure 3.4 Schematic illustration of ICP etching.....	52
Figure 3.5 Schematic illustration of soft lithography	53
Figure 3.6 Schematic illustration of hot-embossing	54
Figure 3.7 Contact angle analysis	56
Figure 3.8 Principle of Scanning Electron Microscopy.....	57
Figure 3.9 Concept of Atomic Force Microscopy and the optical lever.....	58
Figure 3.10 SEM image of a QCM electrode	59

Figure 3.11 Schematic illustration of Zeta-Potential Measurement	61
Figure 3.12 UV-Vis spectrum of a sample species.....	63
Figure 3.13 Beer's Law Plot	63
Figure 3.14 Fluorescence spectra of Hoechst 33342	65
Figure 3.15 Fluorescence spectra of Alexa Fluor 488 phalloidin.....	65
Figure 3.16 Fluorescence spectra of FM 1-43	66
Figure 3.17 Jablonski diagram illustrating the processes involved in the creation of an excited electronic singlet state by optical absorption and subsequent emission of fluorescence.....	68
Figure 3.18 Excitation of a fluorophore at three different wavelengths (EX 1, EX 2, EX 3) does not change the emission profile but does produce variations in fluorescence emission intensity (EM 1, EM 2, EM 3) that correspond to the amplitude of the excitation spec	70
Figure 4.1 Fabrication of polyelectrolyte thin film patterns on planar base substrates ...	76
Figure 4.2 Mask layout of strip and square patterns.....	77
Figure 4.3 Schematic illustration of measurement of cell roundness	80
Figure 5.1 Beer's Law Plot of gelatin solution.....	84
Figure 5.2 QCM Measurements with two layering architectures.....	87
Figure 5.3 Fluorescence spectrum of gelatin-coated 400nm silica particles	88
Figure 5.4 Fluorescence spectrum of flat glass substrate with layering architecture of (PDDA/PSS) ₃ /(PDDA/FITC-Gelatin) _n	89
Figure 5.5 Zeta-potential measurement of silica particles with layering order of PDDA/PSS/FITC-Gelatin/PDDA/FITC-Gelatin.....	911

Figure 5.6 Contact angle measurements of (a) (PAH/PSS) ₈ ; (b) (FITC-PAH/PSS) ₈ on Nanostrip pretreated glass substrates	93
Figure 5.7 Contact angle measurement of polyelectrolyte multilayer thin films with architecture of PDDA/(PSS/FITC-PAH) ₂ /(gelatin/FITC-PAH) ₃ /gelatin on glass substrates	94
Figure 5.8 Contact angle measurement of (PAH/PSS) ₆ on plain PMMA substrate	96
Figure 5.9 Contact angle measurement of (PAH/PSS) ₆ on hot-embossed PMMA substrate	96
Figure 5.10 QCM measurements of (PDDA/PSS) ₃ /(PDDA/FN) ₃ /PDDA/(PSS/FN) ₆ at pH 7.7	98
Figure 5.11 QCM measurement of (PSS/FN) ₂ /PSS at pH 5.76 for overnight incubation for each layer	98
Figure 5.12 AFM images of (PAH/PSS) ₁₀ on glass substrate	100
Figure 5.13 AFM image of gelatin-coated surface with a layering architecture of (PAH/PSS) ₂₀ /PAH/gelatin on nanostrip treated glass substrate.....	102
Figure 5.14 AFM image of a single gelatin molecule on the surface of 20-bilayer polyelectrolyte thin films.....	103
Figure 5.15 AFM image of fibronectin-coated surface with a layering architecture of (PAH/PSS) ₅ /gelatin on nanostrip treated glass substrate.	105
Figure 5.16 AFM image of a single fibronectin molecule on the surface of 5-bilayer polyelectrolyte thin films.	106
Figure 5.17 Surface roughness of PSS- and fibronectin-coated thin films.....	107
Figure 5.18 (a) Optical image of photoresist pattern before LbL; (b) Fluorescence image of FITC-gelatin pattern following the LbL-LO process	109

Figure 5.19	Optical and fluorescence images of polyelectrolyte, fluorescent particles and FITC-gelatin patterns on glass substrates fabricated with LbL-LO technology.....	110
Figure 5.20	Fluorescence images of square patterns with size of 50 μ m x 50 μ m on glass cover slips before lift-off step.....	113
Figure 5.21	Fluorescence images of square patterns with size of 50 μ m x 50 μ m on glass cover slip after lift-off step.....	114
Figure 5.22	3-D AFM graph of gelatin-coated square pattern on glass substrate	115
Figure 5.23	2-D AFM graph and image analysis of gelatin-coated square pattern	116
Figure 5.24	Fluorescence images of fibronectin-coated polyelectrolyte thin film	117
Figure 5.25	3-D AFM graph of fibronectin-coated polyelectrolyte patterns on glass substrate.....	118
Figure 5.26	Fluorescent images of (PDDA/PSS) ₂ / (FITC-PLL/PSS) ₂ / FITC-PLL patterns on PMMA substrate. (a) strip; (b) square patterns.....	119
Figure 5.27	SEM images of 100 μ m channel patterns on silicon substrate.....	120
Figure 5.28	SEM images of 60 μ m channel patterns on (a, b) silicon; (c, d) PMMA....	120
Figure 5.29	SEM images of 60 μ m silicon channel pattern and square PR 1813 photo resist patterns aligned in the channels with (a) non-uniform coating; (b) uniform coating.....	122
Figure 5.30	Fluorescent images of 3-D microfluidic cell culture system on silicon ...	1233
Figure 5.31	Optical images of cells cultured on a plain glass surface and FITC-Gelatin coated surfaces of glass substrates.....	124
Figure 5.32	(a) Phase contrast; (b) Fluorescence image of RASMCs in 24-well cell culture plastic plates after being stained with FM 1-43 and Hoechst 33342	125

Figure 5.33 Fluorescence images of cells in 24-well cell culture plates after being stained with goat anti-mouse IgG fluorescein secondary antibody	126
Figure 5.34 Fluorescence images of cells with Hoechst 33342 and Alexa Fluor 488 phalloidin stain cultured on fibronectin-coated multilayer polyelectrolyte thin films.....	128
Figure 5.35 Fluorescence images of cells with Hoechst 33342 and goat anti-mouse IgG fluorescein conjugated secondary antibody stain cultured on fibronectin-coated multilayer polyelectrolyte thin films.....	128
Figure 5.36 Fluorescence images of cells cultured on gelatin-coated multilayer polyelectrolyte thin films with Hoechst 33342 and Alexa Fluor 488 phalloidin stain	130
Figure 5.37 Fluorescence images of cells cultured on gelatin-coated multilayer polyelectrolyte thin films with Hoechst 33342 and goat anti-mouse IgG fluorescein conjugated secondary antibody stain.....	130
Figure 5.38 Fluorescence images of cells cultured on multilayer polyelectrolyte thin films with PSS as outermost layer with Hoechst 33342 and Alexa Fluor 488 phalloidin stain	131
Figure 5.39 Fluorescence images of cells cultured on multilayer polyelectrolyte thin films with PSS as the outermost layer with Hoechst 33342 and goat anti-mouse IgG fluorescein conjugated secondary antibody stain	131
Figure 5.40 Roundness of smooth muscle cells on PSS-, fibronectin-, and gelatin-coated multilayer polyelectrolyte thin films.....	133
Figure 5.41 Number of pseudopodia of smooth muscle cells on PSS-, fibronectin-, and gelatin-coated multilayer polyelectrolyte thin films.....	133
Figure 5.42 Optical images of cells cultured on the polyelectrolyte patterns with a variety of LbL architectures	137

Figure 5.43 Initial attraction of SMCs to gelatin-coated patterns in 30 minutes after cell passage.....	139
Figure 5.44 Optical images of SMCs transferred onto two types of substrates after 3 hours	140
Figure 5.45 Optical images of SMCs cultured on two types of substrates after 15 hours	141
Figure 5.46 Time-dependent of degradation of PDDA-coated nonadhesive region. SMCs cultured on substrate with gelatin-coated adhesive square patterns and PDDA-coated nonadhesive region.....	143
Figure 5.47 Cell culture on FITC-gelatin patterned glass substrate	144
Figure 5.48 Fluorescence images of cells on gelatin-coated thin film patterned glass substrate after staining by Alexa Fluor 488 Phalloidin.	145
Figure 5.49 Optical images of cells on (a) fibronectin-coated; (b) gelatin-coated thin film patterns on PDDA-coated glass substrates after 12 hours of cell culture.	147
Figure 5.50 Optical images of cells on fibronectin-coated film patterns on PDDA-coated glass substrates after 24 hours culture.	147
Figure 5.51 Optical images of cells on fibronectin-coated thin film patterns on PDDA-coated glass substrates after 2 days culture.....	148
Figure 5.52 Fluorescence images of cells on fibronectin-coated thin film patterns on PDDA-coated glass substrates	149
Figure 5.53 Cells cultured on (a) plain; (b) gelatin-coated 60 μ m channeled PMMA substrates	150
Figure 5.54 Cellular nuclei stain of cells in 60 μ m silicon channeled substrate.....	151
Figure 5.55 F-actin stain of cells cultured in 60 μ m channeled silicon substrate with Alexa Fluor 488 phalloidin.....	152

LIST OF EQUATIONS

Equation 3-1 Sauerbrey's Equation	59
Equation 3-2 Beer's Law Equation	61

ACKNOWLEDGMENTS

I would like first to express my sincere gratitude to my chair advisor, Dr. Michael McShane, the constant sources of advice and support throughout my research and dissertation work at the Institute for Micromanufacturing, Louisiana Tech University. I learned much from Dr. McShane because of his cautious, conscientious, and strict pursuit toward science and research. Second, I want to thank my co-chair advisor, Dr. Tianhong Cui, for his care and help during my Ph.D. study from 1999 to 2003. Dr. McShane and Dr. Cui directed me with the most zealous instructions on research and study, but also presented me intense solicitudes on daily living. Moreover, both of them brought forward many precious ideas and opinions on the dissertation at the end, which will be engraved on my heart whenever and wherever I am.

I would next thank all my advisory committee members, Dr. David Mills, Dr. Yuri Lvov, and Dr. Steven Jones, for their generous instruction and assistance during my research work. Also, I would thank all the student members in BioMINDS lab and supporting staff at IjM for their cooperation and help.

Finally, and most importantly, I would express my deep gratitude to my husband, Jun Lu, and my parents. Without their support, I would not have completed my study to achieve the degree of Ph.D. in Engineering.

This project is supported by NSF/EPSCoR (Grant # 0092001) Foundation.

CHAPTER 1

INTRODUCTION

1.1 Overview

Tissue engineering is an emerging field that allows us to look into the future of medicine, one in which doctors might routinely repair or replace failing or aging body parts. The field is made possible by years of research into the mechanisms which control and regulate cell growth [1-33]. Using tissue engineering technology, it will one day be possible to regenerate or replace damaged tissues with laboratory-grown parts such as bone, cartilage, blood vessels, and skin.

Conventional cell culture studies are universally based on the immersion of a population of cells in a homogeneous fluid medium. Consequently, cell behavior such as cell growth and motility cannot be adequately reproduced; experiments that investigate a wide range of media formulations require large amounts of cells and cell culture surfaces, dauntingly tedious human labor, and/or expensive robotics. As research into understanding of the basic mechanisms of life expands down to the single-cell and molecular level, and the need for more complex cell culture studies arises, the conventional cell culture approach becomes problematic in investigating cell behavior at the micro-/nano-scale.

Tissue engineering research has been ongoing for several decades and significant progress has been made in designing scaffolds for the growth and development of artificial tissues [3,8,10]. These scaffolds also tend to be randomly oriented [2,6]. Since tissues are well organized and highly oriented *in vivo*, the random structure of most tissue engineering scaffolds proves a significant limitation. Current attempts at organized cell and tissue growth in complex tissues have been thwarted by the fact that cells *in vitro* do not respond in the same way that they do *in vivo*. Most cells grow in a random fashion that does not approximate the natural growth of tissues in the body. Work is in progress to develop polymer fabrication methods to address this problem [1,2,6,8,11,18], but there may be other approaches to solving the problem, including the use of microfabrication techniques.

In vivo, many cells are adherent to extracellular matrices (ECM), which have an extremely complex three-dimensional (3-D) topography in the micrometer to nanometer range. In addition, many studies indicate that micro- and nano-scale mechanical stresses generated by cell-matrix interactions have significant effects on cellular phenotypic behavior [8,14,16,18]. Recent advances in micro/nanofabrication techniques have also significantly impacted the field of tissue engineering by tightly controlling the dimension, depth and shapes of the structures, and the surface properties of the of fabricated substrates that serve as artificial ECM [8,18,26]. Therefore, micro/nanofabricated 3-D substrates *in vitro* with different biomaterials and microstructures to mimic *in vivo* extracellular matrices may provide a further insight for future research on tissue engineering.

1.2 Research Review

Complex tissues appear to develop by the use of cues of signals between cells that direct the growth and development of individual cells. The signals include soluble molecules transported by the medium in which the cells are growing, signal molecules that reside on the surfaces of cells and the extracellular matrix, physical forces, and surface topography.

As we know, the extracellular matrix (ECM) is the material found around cells. Most cells are charge-dependent, requiring adherence to a substrate to grow and present cellular phenotype [34-40]. The extracellular matrix is that scaffolding. ECM also controls and regulates cell function because ECM interacts with the surface of the cells. For the *in vitro* ECM, some important factors can regulate cell behavior, such as topography of the ECM structure to align cells and surface material of ECM to regulate cell attachment. Researchers have developed microfabrication and self-assembly monolayer (SAM) techniques in tissue engineering to investigate these factors in the *in vitro* ECM on cell behavior.

Cells play a major role in building and maintaining tissue functions in their innate environment. However, after cells are removed from their innate environment (the extracellular matrices) to the *in vitro* environment, they lose their *in vivo* normal behavior. Therefore, a principal objective of tissue engineering is to reach a fundamental understanding of the factors in the microenvironment surrounding cells, which can induce and affect the basic functions of cells. To date, some studies indicate that the interactions between cells and the extracellular matrices can modulate the behavior of cells. The ability to manipulate the microenvironment around cells will greatly help the researchers

in the medical and health fields. The material architectures that serve as scaffolds for cellular composites can be developed to either replace or support a damaged or diseased organ or as testing system for determining behavior of materials. Scaffolds as cell and tissue carriers are critical for determining cell behavior. 3-D substrates can provide optimal spatial and nutritional conditions for cell maintenance.

Cell culture is one of the most important aspects of tissue engineering. Recent strides have been made in the surface morphology area with the help of micromachining. Micromachining is basically a set of tools and techniques for fabrication of structures and devices on the nanometer to millimeter scale. Because most cells and cellular features are of the same scale, microfabrication technologies and microfabricated devices are ideal for study of cellular phenomena.

Microelectromechanical systems (MEMS) have been used for various biological applications encompassing implantable neural microelectrodes [67-69], microfluidic cell sorting or DNA separation [70-72], and controlling cell shape and function [54-57,73,74], etc. Tissue engineering may require that cells be placed in specific locations on a substrate, and the chemistry and topology of the surface to which the cell is attached are also extremely useful in understanding the influence of the cell-material interface on the behavior of cells.

Microfluidics and cell biology are two fields with much potential for interdisciplinary research. The match between the two fields is perfect from the standpoint of size, as microsystems and cells are both micrometers in size. Microfluidic cell culture systems can be made by using a set of microfabrication techniques, such as photolithography, soft lithography, and hot embossing [14-29,47-54]. Cell-material

compatibility is improving through surface modifications of chemical reaction, physical O₂ plasma, and electrostatic attraction [55-66].

There has been an increasing level of interest in technologies for creating micropatterned surfaces, which integrate biocompatible materials with cells or tissues [47-69]. To that end, researchers have developed technologies to pattern surfaces that can be used to control cell behavior and understand the cell-cell and cell-ECM interactions [14-39,47-69,73-81]. Equally important are the choices of materials, designed for both limiting growth in background or off-pattern regions as well as encouraging growth in the foreground or on-pattern region [82]. Many efforts have been made to develop *in vitro* cell culture systems with a proper control of microenvironment for understanding cell behavior and for engineering cell function [1-33,73-78].

Random and regular surfaces have been found to affect the spreading, proliferation, and differentiation of cells *in vitro*. Most of the studies on cell culture to date came from the two-dimensional culture system or systems with specific grooves and ridges, where cells can only make attachments on the bottom surface of the substrate [22-28]. These cells lack the important third dimension through which cells may attach to the sidewalls or steps with a larger surface area, and other useful geometries.

Both surface chemical properties and surface topography of cell culture substrates are the critical factors in determining cell behavior for *in vitro* tissue engineering applications [6-18,90-93]. Because the surface properties of a self-assembled film are different from those of the bulk substrate, surface modification procedures have been developed to control cell-material interactions based on the exposed chemical moieties. Proteins such as fibronectin, or peptides containing integrin-binding domains (e.g. RGD),

have often been used to increase the attachment of specific cells on a designed substrate in an *in vitro* environment [94-97]. While it is generally understood that the material of the outermost layer, which interacts with the cells growing on it, is the major mediating factor in determining the surface properties of these substrates, some evidence suggests that underlying material properties may play a significant role in determining cell adhesion [1]. Nanostructured polyelectrolyte multilayer thin films were used to investigate cell interactions *in vitro* and results indicate that the subsurface molecular architecture of the thin films may direct a particular multilayer combination to be either cell adhesive or cell resistant [1].

In addition, recent years have seen the development of microfabrication methods to pattern surface chemistry, including soft lithography and micro-contact printing, in an attempt to define features of *in vitro* cell culture scaffolds that will allow control over cell orientation [41,83,98,99], because all cells are well organized and oriented in their *in vivo* environment. Soft lithography is a low-cost technique to fabricate high aspect ratio structures on polydimethylsiloxane (PDMS) substrates: PDMS microstamps are commonly coated with biomaterials, such as protein, which are transferred by micro-contact printing to other surfaces [98]. However, micro-contact printing forms only a single layer of cell-adhesive patterns on the substrates per stamping step, and cannot control the thickness of the patterns, so it is limited in the ability to create surfaces with significant topographical features and cannot provide architectures with complex composition.

Electrostatic layer-by-layer (LbL) self-assembly technology provides an approach to fabricate ultrathin films on solid substrates, a promising method to precisely modify

the surface properties of cell culture scaffolds. Lvov *et al.* demonstrated production of multilayer thin films containing several protein species [43-46]. In this approach, each protein type is adsorbed on an oppositely charged layer of material and then coated by further opposite-charge polyelectrolyte layers before addition of another protein. Hammond *et al.* developed polymer microstructures for selective deposition of polyelectrolyte multilayer thin films using a combination of micro-contact printing and self-assembled monolayer (SAM) technologies [83]. However, with only micro-contact printing and SAM techniques, it is difficult to control the vertical dimension of the polyelectrolyte thin film patterns.

Currently, there is a tendency to fabricate the cell culture scaffolds from micro-scale to nanoscale [1,2,41-43,54]. Micromachining technology has enabled production of micropatterns with difficult geometry and different function freely. Meanwhile, the assembly of alternating layers of oppositely charged linear or branched polyions, nanoparticles and proteins is simple and provides the means to form 5- to 500-nm-thick films with monolayers of various substances growing in a preset sequence on any substrate [1,2,41-45,82-89]. The oppositely charged species are held together by strong ionic bonds, and they form long-lasting, uniform, and stable films. Taking advantage of layer-by-layer alternate adsorption [44-46] of “nanopolymers” combined with conventional lithography process, the properties of the extracellular matrix of *in vitro* cell culture systems can be changed [1,2]. The polyion layer-by-layer self-assembly is one of the fundamental methods used for the assembly of ultrathin films with various degrees of molecular order and stability. In short, both lithography and layer-by-layer self-assembly techniques are economical and amenable to scaling up fabrication. This contribution

benefits the research study on tissue engineering in single-cell and sub-cell level.

Combining photolithography, layer-by-layer self-assembly (LbL), and lift-off (LO) techniques allow a different approach to define lateral dimensions for the self-assembled films [100-104], which are constructed with nanoscale precision in vertical direction. Using this combination approach, surface topographical and chemical features can be patterned in a desired manner, and the adhesion and growth of cells can be controlled. This versatile hybrid fabrication method may provide a technology platform and lead to great benefits in areas that require high precision in material definition, such as biosensors, drug delivery, artificial organs, and other biomedical applications.

1.3 Research Need and Motivation

Using the microfabricated substrates, the surface topography—including the dimension, depth, and shapes of the structures—can be tightly controlled. Combining traditional micromachining technologies with electrostatic layer-by-layer self-assembly nanotechnology, various biocoating materials are also being tested to determine the effect of surface characteristics and the “cell adhesiveness” of the substrate on the cell behavior. Micro/nanofabricated substrates may also have application in improving biocompatibility of surfaces, preparing tissue “patches” for diseased organs, or developing improved cell culture methods that more closely approximate the environment of cells *in vivo*.

Some important questions in the area of BioMEMS applied to tissue engineering being addressed are as follows: what shape of structures will prove most effective in orienting and aligning cells? What type of materials will increase cell attachment, maximize cell densities, and maintain cell differentiation? So, what is the optimal

combination of a variety of parameters to improve cell function? To begin addressing these questions, different types of microstructures possessing a variety of surface properties are needed to assess the effect of these cell culture scaffolds on the behavior of cells in an *in vitro* environment.

Smooth muscle is the main component of critical tissues and organs in human body, such as in blood circulating, respiration, and digestive systems, etc., which are important for the life functions of a human being. We propose a project to modify the surface topography and surface properties of the *in vitro* cell culture scaffolds to study the attachment, growth, and alignment of smooth muscle cells. These substrates may provide a more biocompatible surface with specific microarchitectures upon which cells may exhibit enhanced cellular adhesion due to increased surface cytocompatibility. We assume that the microtopography can help provide directional growth for cells and can recreate tissue architecture at the cellular level in a reproducible fashion. The main emphasis of this work is to develop and test processes for high-precision surface engineering of materials for tissue culture with control over chemical and structural properties of the biomaterial interface. This project will allow identification of general properties that will allow a narrower focus in future work of tissue engineering.

The ultimate goal of this project is to develop a better understanding of the environmental conditions that direct muscle cell growth and alignment. The general significance of this project is: first, a 3-D *in vitro* culture system will be generated that more closely resembles the *in vivo* environment to direct smooth muscle cell response (orientation, density, and function). The potential benefit of such a system is enormous with applications in the field of tissue engineering. The second general significance is of

a therapeutic nature and involves the growth and development of functional replacement organs or tissues and the development of medical implants for repair of damaged or diseased tissue. If the cells are already highly oriented and aligned *in vitro* culture, they could potentially be used to patch the damaged tissues and encourage the regrowth of the tissue.

As an added benefit from this project, research in tissue engineering will promote the development of the biomaterial industry. This research project aims at a better understanding of the cell behavior *in vitro* by creating a biomimetic microenvironment. Biocompatibility is also an important issue in tissue engineering. The improvement in the biocompatibility of materials using microfabricated substrates will speed the evolution of artificial organs and tissues. Current cell culture systems often have problems with adhesion, proliferation and orientation of the cells. In general, engineering cellular behavior for tissue reconstruction has focused on the understanding of a number of critical cell functions mentioned above. This project is expected to drive an improved *in vitro* microenvironment for cell functions.

The main objectives of this project are

1. Investigate a combination of micromachining methods, including mask design, lithography, soft-lithography, hot-embossing, deposition and etching, to make microstructures on base substrates attractive for cell culture, such as silicon, glass, and PMMA.
2. Develop the layer-by-layer alternative adsorption for patterning microstructures with cell adhesive or repulsive polymeric biomaterials poly(diallyldimethylammonium chloride) (PDMA), poly(ethyleneimine) solution (PEI),

poly(allylamine hydrochloride) (PAH), poly(sodium 4-styrenesulfonate) (PSS), and poly-L-lysine hydrobromide (PLL)) and ECM proteins (gelatin and fibronectin).

3. Build 3-D micro/nanostructures with desired materials on planar and microstructured base substrates for microfluidic cell culture system. (see Figure 1.1)

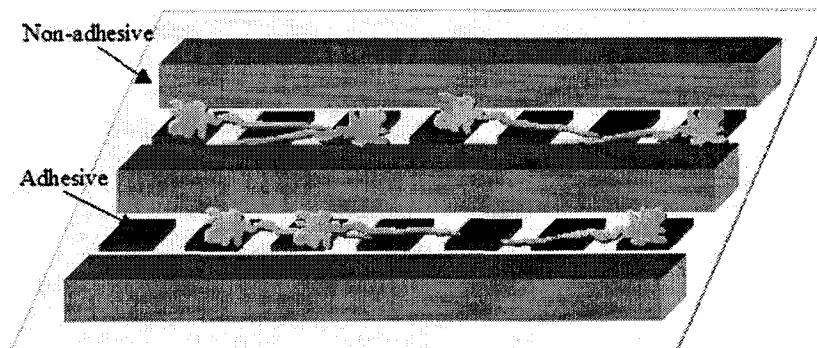


Figure 1.1 Schematic illustration of 3-D cell culture system

4. Observe and analyze cell behaviors, including attachment, proliferation, and alignment, in the designed cell culture systems to understand cell-ECM interactions *in vitro* microenvironment.

This dissertation describes the investigation of methods to achieve these objectives. Chapter 2 contains the detailed background of tissue engineering involving micro/nanoscale surface engineering including description of cellular interactions. Chapter 3 describes the experimental design and theories of materials and processes used to control surface chemistry and topography, common techniques in current use for patterning cells, etc. Chapter 4 introduces the experimental materials, instrumentation, and methods used in this project. Chapter 5 gives out the experimental results including

characterization of basic materials and techniques, fabricated cell culture scaffolds, and cell patterns on these engineered scaffolds. Chapter 6 summarizes the conclusion and contribution of this project to tissue engineering.

CHAPTER 2

BACKGROUND

2.1 Tissue Engineering

2.1.1 What is Tissue Engineering?

Tissue engineering is a rising interdisciplinary research area that applies the principles of biology and engineering to the development of viable substitutes that restore, maintain, or improve the function of human tissues or organs. It is a novel field based on a simple concept: start the substitute with building materials, shape it as needed, seed it with living cells, and incubate it with necessary nutrition. When the cells proliferate, they fill up the engineered scaffold and grow into a three-dimensional tissue. Once implanted in the body, the cells may recreate their intended tissue functions. For example, blood vessels would attach themselves to the new tissue, the biodegradable scaffold would dissolve, and the newly grown tissue would eventually blend in with its surroundings. However, tissue engineering is still in its early development although there is some promising progress in its field. Success will greatly depend upon the ability of scientists to figure out complex cellular interactions with cells, materials, and extracellular matrix, etc, then designing the appropriate scaffold with right materials, exact culture media, and cells.

Cells have been cultured, or grown, outside the body for many years; however, the possibility of growing complex, three-dimensional tissues is still a recent interest. The intricacies of this process require the input from many scientists in many research fields, including the problem-solving expertise of engineers.

Tissue engineering crosses a large number of medical and technical specialties. Cell biologists, molecular biologists, biomaterial engineers, computer-assisted designers, microscopic imaging specialists, robotics engineers, and developers of equipment such as bioreactors where tissues are grown and nurtured, are all involved in the process of tissue engineering. Tissue engineers in the United States and abroad have set out to grow virtually every type of human tissue—liver, bone, muscle, cartilage, blood vessels, heart muscles, nerves, pancreatic islets, and more. Commercially produced artificial skin is already available for use in treating patients with diabetic ulcers and burns. Many current medical therapies may be improved by tissue engineering with significant financial savings due to no need of finding a match donor. In standard organ transplantation, a mismatch of tissue types necessitates lifelong immunosuppression, with its attendant problems of graft rejection, drug therapy costs, and the potential for the development of certain types of cancer. Furthermore, there is always the potential for rejection of the tissue, and the surgery itself always carries some risk.

2.1.2 Tissue Engineering Approaches

Generally, three approaches in tissue engineering have been adopted for the creation of new tissue:

Design and grow human tissues outside the body for later implantation to repair or replace diseased tissues. For example, skin graft is used for treatment of burns [104-111].

Implantation of cell-containing or cell-free devices induces the regeneration of functional human tissues. Novel polymers are being created and assembled into three-dimensional configurations, to which cells attach and grow to reconstitute tissues. An example for this technique involves using biomaterial matrix to promote bone re-growth for periodontal disease [112-116].

The development of external or internal devices containing human tissues designed to replace the function of diseased internal tissues. This approach involves isolating cells from the body, using such techniques as stem cell therapy, placing them on or within structural matrices, and implanting the new system inside the body or using the system outside the body. Examples of this approach include repair of bone, muscle, tendon, and cartilage, as well as cell-lined vascular grafts and artificial liver [117-122].

2.1.3 Motivations of Tissue Engineering

Tissue engineering will have a great impact in several fields of medicine in the future. One important area of the impact is on clinical medicine. Tissue engineering products based on cell transplantation approaches are already available for clinical use. Regeneration of skin, bone, and blood vessels using delivery of recombinant growth factors will possibly be routine in the near future as well. Other engineered tissues also will be used in the different clinical applications in the future. A goal currently pursued in tissue engineering is the completion of engineered internal organs due to the urgent need for additional organs for transplantation. Tissue engineering will need to integrate even more basic biology and fundamental engineering to solve complex biological problems, though it is already an interdisciplinary field. A variety of engineering design elements, including biomechanics and mass transport, will be crucially important to the long-term

success of tissue engineering.

Tissue engineering will continue to provide novel experimental systems to investigate basic developmental, pathologic, and regenerative biological processes. Two-dimensional cell culture, the standard model system of today, apparently fails to mimic a number of critical features of normal tissues. Tissue engineering systems should allow one to precisely define the microenvironment in which tissues are growing and developing, such as cell types, extracellular matrix, and growth factors. Obviously, it will likely be invaluable to employ these systems in basic biological studies in the future. This role may even be more important than the direct clinical application of engineered tissues for the field, as it may lead to scientific advances on many fronts.

2.2 The Environment of Cells - Extracellular Matrix (ECM)

The extracellular matrix (ECM) is a complex structural entity surrounding and supporting cells found within mammalian tissues. Most types of cells must grow adherent to a substratum; i.e., they must have a scaffolding to which to attach. The extracellular matrix is the scaffolding to which cells adhere, and it also modulates the functions of cells. The ECM interacts with the surface of the cell. Some of the most striking interactions exist with the large glycoprotein, fibronectin. New mechanisms of cell adhesion are being found with considerable frequency, but all seem to involve cell-surface receptors for molecules found in the space surrounding the cell which in turn interact with molecules in the territorial matrix. Thus the matrix can exert a physical force on the cell and supply feedback undoubtedly of importance in controlling tissues shape.

The extracellular matrix is mainly made up of two classes of macromolecules: (1) The first class is called glycosaminoglycans (GAGs), which are polysaccharide chains. Members of this class are usually found to be covalently linked to protein in the form of proteoglycans. (2) The second class is made of fibrous proteins. There are two functional types of fibrous proteins: the mainly structural ones, like collagen and elastin, and the mainly adhesive ones, like fibronectin and laminin.

Members of both classes come in a great many shapes and sizes. The members of the glycosaminoglycans form a highly hydrated, gel-like substance in which the members of the fibrous proteins are embedded. Collagen fibers strengthen and help to organize the matrix while elastin fibres give it resilience. The adhesive proteins assist cells to attach to the ECM. For example, fibronectin promotes the attachment of fibroblasts and other cells to the matrix in connective tissues via the extracellular parts of some members of the integrin family (discussed below), while laminin promotes the attachment of epithelial cells to the basal lamina, again via the extracellular domains of some members of integrins.

2.2.1 Proteoglycans

Proteoglycans, such as mucoproteins, are formed of glycosaminoglycans covalently attached to the core proteins. They are found in all connective tissues and on the surfaces of many cell types. Proteoglycans are remarkable for their diversity. They have different protein cores and different numbers of GAGs with various lengths and compositions. GAGs are highly negatively charged, which is essential for their function. Many proteins may bind to proteoglycans. Also some proteoglycan types may easily self-aggregate through their core proteins and glycosaminoglycan chains due to the ionic

interactions.

2.2.2 Collagen

Life is a string of complex molecules: polymers. Nature's most abundant protein polymer is collagen. More than a third of the body's protein is collagen. Collagen acts as scaffolding for human bodies and controls cell shape and differentiation.

Collagen is the most important building block in the entire animal world. It is a type of fibrous protein. It is synthesized and secreted by the cells of the connective tissue. At least 20 types of collagen have been identified so far. Collagens are the most commonly occurring proteins in the human body and play a major role in the formation of ECM. Collagens are triple-helical structural proteins, which give the collagens the strength and stability central to the structure and support of the tissues in the body.

Figure 2.1 shows the illustration of collagen. Collagen is a triple helix formed by three extended protein chains that wrap around one another. Many rod-like collagen molecules are cross-linked together in the extracellular space to form unextendable collagen fibrils (top) that have the tensile strength of steel. The striping on the collagen fibril is caused by the regular repeating arrangement of the collagen molecules within the fibril.

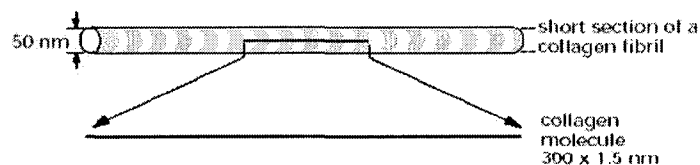


Figure 2.1 Illustration of collagen fiber

Gelatin, essentially denatured collagen, is isolated from animal skin and bones with very dilute acid. It contains a large number of glycine, proline and 4-hydroxyproline

residues. A typical structure is -Ala-Gly-Pro-Arg-Gly-Glu-4Hyp-Gly-Pro-. Figure 2.2 shows the molecular structure of gelatin.

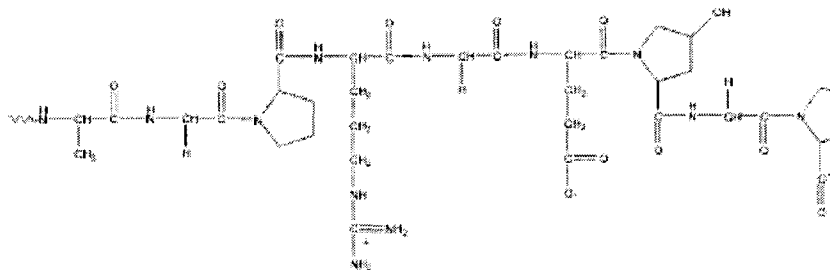


Figure 2.2 Molecular structure of gelatin

Gelatin consists of extended left-handed proline helix conformation in single or multi-stranded polypeptides, each containing between 300 - 4000 amino acids. Solutions undergo coil-helix transition followed by aggregation of the helices by the formation of collagen-like right-handed triple-helical proline/hydroxyproline-rich junction zones. Higher levels of these pyrrolidines result in stronger gels. Each of the three strands in the triple helix requires 25 residues to complete one turn; typically there would be between one and two turns per junction zone. Chemical cross-links can be introduced to alter the gel properties using transglutaminase to link lysine to glutamine residues

There are two types of gelatin, depending on whether the preparation involves an alkaline pretreatment, which converts asparagine and glutamine residues to their respective acids and results in higher viscosity. When the collagen is allowed to renature, then interchain bonds that form between collagen chains lead to the formation of a meshwork, which gives gelatin its characteristic gel appearance and is critical to its performance.

2.2.3 Elastin

Elastin is the major extracellular matrix protein in human body that provides elasticity to the tissues and organs. It is an important component of tissues that require elasticity to function, such as skin, blood vessels, ligaments, and lungs. Elastin functions in connective tissue in partnership with collagen, whereas collagen provides rigidity. Elastin polypeptide chains are cross-linked together to form rubberlike, elastic fibers. Each elastin molecule uncoils into a more extended conformation when the fiber is stretched and will recoil spontaneously as soon as the stretching force is relaxed, as illustrated in Figure 2.3.

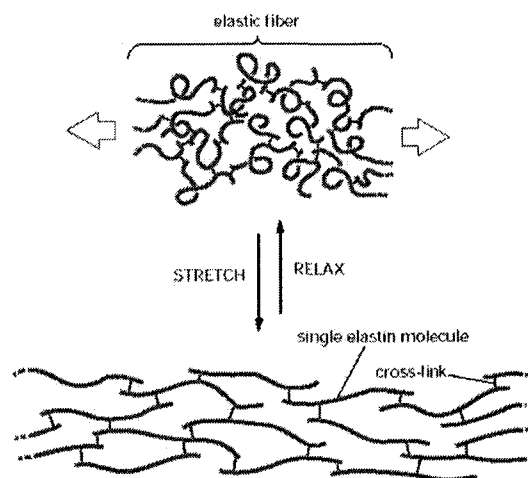


Figure 2.3 Illustration of elastin fiber

2.2.4 Fibronectin

The extracellular matrix also contains noncollagenous adhesive proteins which play critical roles in organizing the matrix and in enabling cells to attach to it. Fibronectin (FN) is a prototype cell adhesion protein, widely distributed in the tissues of all vertebrates and a potential ligand for most cell types. It is present as a polymeric fibrillar

network in the ECM and as soluble protomers in body fluids. Fibronectin comprises multiple domains, each with specific binding sites for other matrix macromolecules and for receptors on the surfaces of cells.

Fibronectin's structure is rod-like, composed of three different types of homologous, repeating modules, Types I, II, and III as shown in Figure 2.4. These modules, though all part of the same amino acid chain, can be envisioned as "beads on a string," each one joined to its neighbors by short linkers. Figure 2.5 illustrates the molecular interactions of fibronectin.

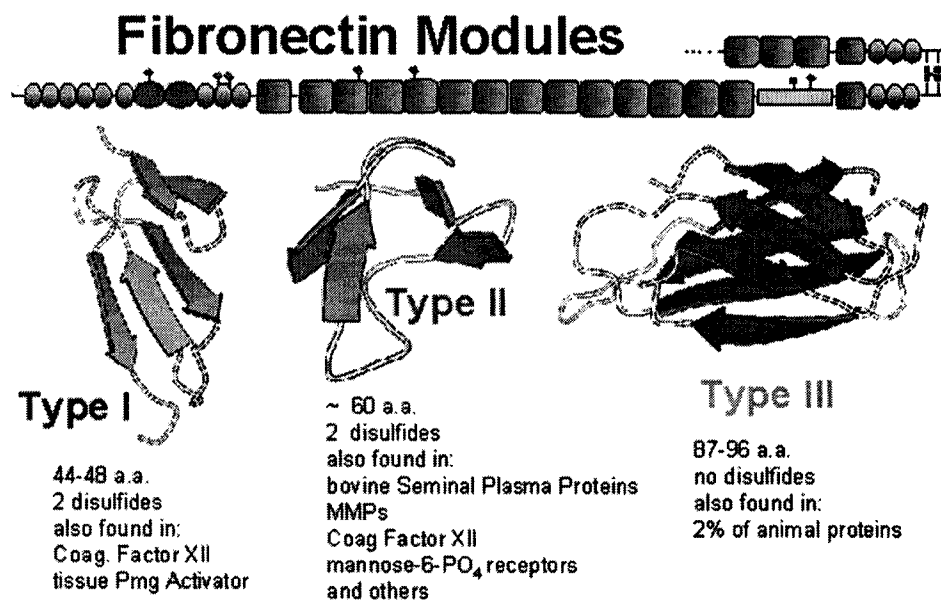


Figure 2.4 Three types of fibronectin modules

Fibronectin is involved in many cellular processes, including tissue repair, embryogenesis, blood clotting, and cell migration/adhesion. Sometimes FN serves as a general cell adhesion molecule by anchoring cells to collagen or proteoglycan substrates. Fibronectin also can serve to organize cellular interaction with the extracellular matrix by

binding to different components of the ECM and to membrane-bound FN receptors on cell surfaces.

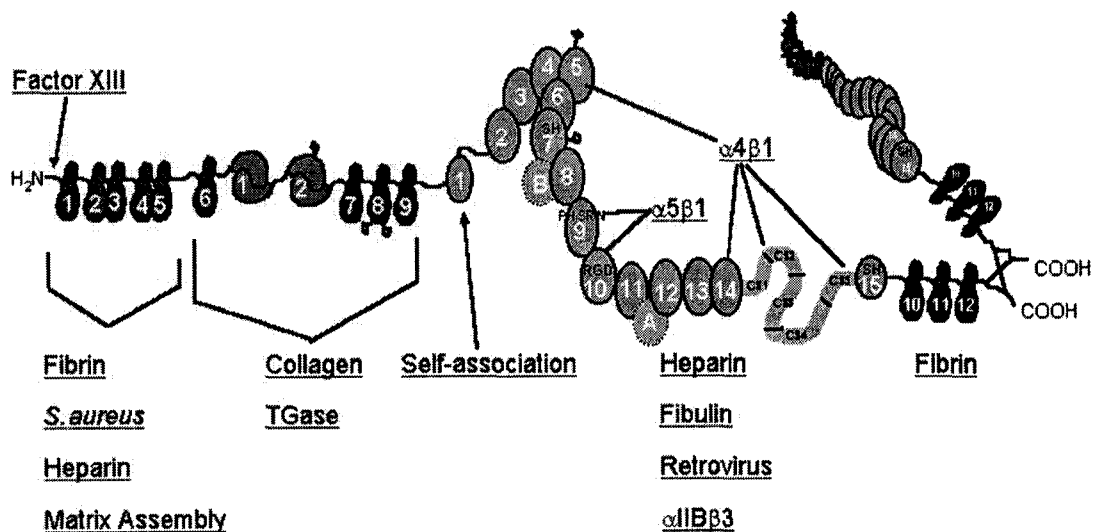


Figure 2.5 Molecular interactions of Fibronectin

2.2.5 Laminin

Laminins are a large family of glycoproteins distributed ubiquitously within basement membranes. They have key roles in development, differentiation and migration due to their ability to interact with cells via cell-surface receptors including integrins and type IV collagen.

2.3 Integrins

The main receptors on animal cells for binding and responding to most extracellular matrix proteins are the integrins. Many matrix proteins in vertebrates are recognized by multiple integrins.

Integrins are receptor proteins which are of crucial importance to engage cells

with their environment as the main means that cells both bind to and respond to the ECM.

Figure 2.6 shows the illustration of integrin function.

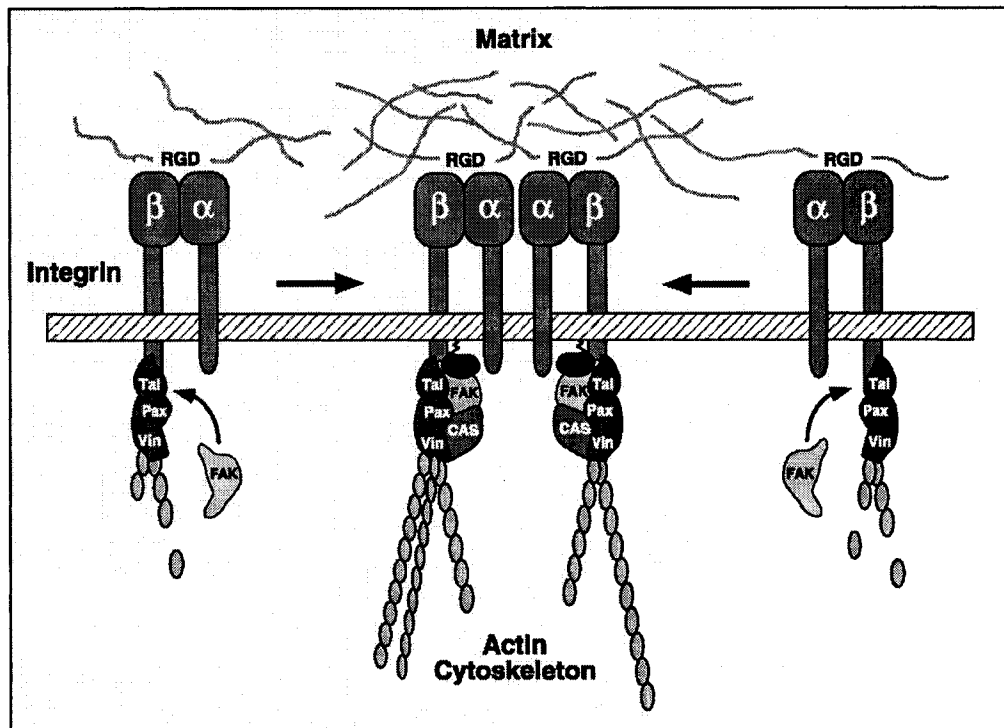


Figure 2.6 Illustration of integrin function
(Giancotti & Ruoslahti, Science 285: 1029, 1999)

Integrins are transmembrane binding glycoproteins that usually bind cells to matrix but also may bind cells to cells. Integrins are part of a large family of cell adhesion receptors which regulate cell-extracellular matrix and cell-cell interactions. They allow the cytoskeleton and ECM to communicate across the plasma membrane. The extracellular domains bind to components of the extracellular matrix (ECM), usually through recognition of an RGD tripeptide as first identified in fibronectin. This bond triggers changes in the cytoplasmic domains, altering their interaction with cytoskeletal and/or other proteins that regulate cell adhesion, growth and migration. At the same time, signals generated inside the cell can alter the activation state of some integrins, affecting

their affinity for their extracellular ligands. Thus, integrins are able to signal across the membrane in both directions, inside-out and outside-in. The binding of integrins to ligands is dependent on extracellular divalent cations, such as calcium or magnesium.

2.4 Cellular Interactions

Tissue function is modulated by an intricate architecture of cells and biomolecules on a micro-scale. Cells play an extremely important role in tissue functions in their innate microenvironment. Understanding all aspects of cellular interactions is essential to development of reliable technological system requiring reproducible performance of cells and tissues.

2.4.1 Cell-Cell Interaction

In tissues, cells can bind to other cells either by the binding of cell membrane proteins to structures on other cells or by forming highly organized cell-cell junctional structures. Cell-cell interactions are the means by which cells can communicate, transfer information, develop spatial awareness and coordinate their differentiation. The strength of a particular cell-cell interaction depends on the mixture of adhesion molecules, their concentrations, their cytoskeletal linkages, and their distributions on the cell surface. Proper cell-cell interaction is essential to normal organ development [75].

Kosaka *et al.* examined the effects of peripheral blood mononuclear cells (PBMCs) on endometrial epithelial cell function [123]. Functional changes in endometrial epithelial cells induced by PBMCs suggest possible regulation of endometrial receptivity by immune cells. It has also been shown that mast cells enhance fibroblast-mediated

contraction of collagen lattices via direct cell–cell contact [124]. Montes *et al.* demonstrated calcium responses elicited in human T-cells and dendritic cells by cell–cell interaction and soluble ligands [125]. Armour *et al.* studied P19 embryonal carcinoma cells and suggested that the cell–cell contact achieved in aggregates results in the induction of an activity that increases accessibility of the myoD transcription factor to muscle-specific genes in chromatin [126].

2.4.2 Cell-ECM Interaction

Cell-extracellular matrix (ECM) interaction is important for adhesion, migration, proliferation, and differentiation in cells [11-29,54-59,139]. Plasma membrane proteins and proteoglycans mediate cell-ECM recognition [127-132]. This cell-ECM interaction is mediated by integrins [133-138], a family of cell adhesion receptors. Integrins establish a mechanical link not only between the membrane and the ECM substrate but also between the ECM and the cytoskeleton. Moreover, integrins aggregate in organized structures termed focal contacts [140-145]. Cell-ECM junctions can be observed in cultured cells as focal adhesions. Cell-ECM interactions can also regulate gene expression at the transcriptional level [146-148].

It has been found that differentiation of skeletal tissues such as bone, ligament and cartilage is regulated by complex interaction between genetic and epigenetic factors, as that stretching activates gene expression of $\beta 1$ integrin and FAK and inhibits chondrogenesis through cell-ECM interactions of chondroprogenitor cells [149]. The interaction of cells with the extracellular matrix at the interface of an implant determines the biology of cells and tissues. Lange *et al.* proved that cell-extracellular matrix interaction and physico-chemical characteristics of titanium surfaces depend on the

roughness of the material [139].

2.5 Cellular Behavior

The function of an organ is defined by its constituent differentiated cells. In an adult, the processes of cell growth, differentiation, and cell death are tightly linked to provide a steady state of tissue function while ensuring that there are sufficient cells will replenish the tissue. During development, these processes are also firmly controlled to ensure that organs develop in the right proportions and at the correct spatial and temporal point.

The interaction of cells with their extracellular matrix generates a complex series of signaling events which serve to regulate several aspects of cell behavior, including adhesion, growth, differentiation, and motility. These are discussed in more detail below due to the relevance to the substrate/surface engineering topic of this thesis.

2.5.1 Cell Adhesion / Attachment

Cell adhesion, either of cells to cells, or of cells to other objects, is a very important phenomenon for a variety of investigations. Adhesion and changes in adhesion form an essential feature of the normal developmental processes of animals. They are also often the features of pathogenesis of disease and play a critical role for the replacement and repair of tissues.

Most mammalian cells are adherent. They must attach to and spread on an underlying matrix in order to carry out normal metabolism, proliferation and differentiation. The biological matrix that serves this role comprises a collection of

insoluble proteins and glycoaminoglycans collectively referred to as the ECM [150,151]. In addition to maintaining the organization and mechanical properties of tissue, the ECM presents many peptide and carbohydrate ligands recognized by cellular receptors. These receptor–ligand interactions are critical to maintaining cell function and enabling cells to respond appropriately to their environments. The primary function of ECM is to mediate the adhesion of cells [6,14,21,26,62-66,94-967,131,137,152]. Without adhesion, most cells initiate a program of apoptosis that results in their death, while the loss of adhesion-related signal transduction pathways leads to the growth and spreading of cancerous tumors [153,154]. The study of these and many other interactions between a cell and its matrix is an active area of research in cell biology.

2.5.2 Cell Alignment / Orientation

Tissues are well organized and highly oriented *in vivo*, and cells are well controlled by their innate extracellular matrix. Biomimetic strategies can be employed to promote directional outgrowth of cells *in vitro* by using a synergistic combination of physical, chemical, and cellular cues. Microgrooved substrates promoted cell alignment as well as outgrowth; cells have been found to orient even on shallower grooves and exhibit continued alignment even as the grooves degrade [22,24,25,28,29,32,155].

Many types of cells, when grown on the surface of a cyclically stretched substrate, align away from the stretch direction [156-159]. It has been suggested that the fibroblasts are more responsive to stretch because of their more highly developed actin cytoskeleton [157]. Wang *et al.* demonstrated that the orientation of cells affects the organization of the collagenous matrix produced by the cells, which also suggested that orienting cells along the longitudinal direction of healing ligaments and tendons may lead to the

production of aligned collagenous matrix that more closely represents the uninjured state [160]. It has been reported that osteoblasts and fibroblast-like cells in contact with a ground biomaterial surface spread in the direction of the surface structures. These aligned cells provide more favorable adhesion behavior than spherically shaped cells. The oriented cells had a higher density of focal contacts when in contact with the edges of the grooves, and they showed a better organization of the cytoskeleton and stronger actin fibres [161].

2.5.3 Cell Migration / Mobility

Cell migration is a main component of normal tissue function. It is a crucial process for every type of living organism. Cells in the body will often move from place to place to complete their functions. Cell migration can be modulated *in vivo* and *in vitro* by altering the expression of adhesion molecules, so it depends on the proper balance between assembly and disassembly of focal adhesions. Focal contacts facilitate attachment of the cell to the substratum and allow cells to exert tension on the substratum, which is necessary for cell migration along the substratum [162,163]. Cell migration plays an important role in both normal physiology and disease. The process of cell migration involves a dynamic interaction between the cell and the extracellular environment and is essential in such things as wound repair and cell differentiation [164,165]. Such cell migration for most animal cell types is based on the actin cytoskeleton. Control of cell migration is important for success in tissue engineering.

2.5.4 Cell Growth / Spreading / Proliferation

The extent of cell spreading modulates cell growth and function. Tight control of cell proliferation is required to ensure normal tissue patterning and prevent cancer

formation. The importance of cell binding to the extracellular matrix and associated changes in cell shape and cytoskeletal tension to the spatial control of cell-cycle progression has been revealed [166-169]. Cell proliferation is controlled by growth factors that bind to receptors on the cell surface; those, in turn, connect to signaling molecules that convey messages from receptors to the nucleus. There, transcription factors bind to DNA, turning on or off the production of proteins that cause cells to continue dividing.

2.5.5 Cell Differentiation

Cell behavior is controlled by a network of signals derived from growth and differentiation factors as well as from the local cellular environment. These signals are interpreted by appropriate receptors and converted into intracellular pathways that modulate transcriptional or post-transcriptional events. Multicellular organization in animals depends on cooperative behavior of the cells making up the organism. Differentiation gives rise to populations of cells, which specialize in specific functions, such as muscles, neurons, and epithelia.

2.6 *In vitro* Cell Culture Scaffolds

In most cell types, certain biochemical signals essential for cell growth, function, and survival are triggered by integrins upon attachment; without attachment, the cell undergoes apoptosis [153,154,170,171]. Since many cell types secrete ECM, an artificial substrate may support cell adhesion even if it is not initially coated with an ECM protein. Success in creating cellular micropatterns thus rests on the ability to control the size,

geometry, and chemical nature of the adherent layer of *in vitro* cell culture scaffolds.

2.6.1 Biomaterials

Biomaterials are substances used in the creation of a medical device or other implanted therapeutic product. Collagen is frequently used as a biomaterial due to its ability to persist in the body long enough to carry out its specific role without developing a foreign body response that could lead to the premature rejection or overall failure of the biomaterial. A biomaterial is a natural or synthetic material that replaces part of a living system or to function in intimate contact with living tissue.

Traditionally, biomaterials encompass synthetic alternatives to the native materials found in the body. A central limitation in the performance of traditional materials used in the medical device, biotechnological, and pharmaceutical industries is their inability to integrate with biological systems through either a molecular or cellular pathway, thus leading to unfavorable outcomes and device failure. The design and synthesis of materials that circumvent their passive behavior in complex mammalian cells is the focus of the work of today's tissue engineering.

2.6.2 Biocompatibility

The degree to which a device avoids the foreign body response is a measure of its biocompatibility. An improvement in the biocompatibility of materials for traditional device-based therapies could be considered a step in the right direction; however, recent advances in biotechnology and tissue engineering make possible a major leap forward in the function and compatibility of the devices. The ability to regulate cell behavior at a biomaterial interface requires strict control over the material's surface properties and an

ability to impart to the material a defined biological activity.

The biocompatibility of implants and the growth of cells in culture depend on the fact that most cells prefer to exist on some kind of extracellular support, to which they bind through a wide variety of specific adhesion receptors on the cell surface. The mechanisms by which the surface properties of biomaterials control cell behavior via the adhesion receptors and attachment factors are being studied extensively.

2.7 Surface Modification

The hydrophobicity and the poor cytocompatibility of many substrate materials lead to the inefficiency of the scaffold in constructing a friendly interface with living cells. It is the surface of a biomaterial that first comes into contact with a living system; hence, the initial response of cells to the biomaterial mostly depends on the surface properties. Therefore, surface modification of base substrates is necessary to control cytocompatibility.

A stable connection between the biomaterial surface and the surrounding tissue is one of the most important prerequisites for the long-term success of implants. Therefore, a strong adhesion of the cells on the biomaterial surface is required. Beside the surface composition, the surface topography influences the properties of the adherent cells. The quality of the connection between the cell and the biomaterial is determined by the dimensions of the surface topography.

Surface microfabrication technologies have been recently used to control cell behavior to *in vitro* environment. The variations in surface topography, surface properties, such as hydrophilicity or hydrophobicity, surface charge, surface proteins, involving

various type of biomolecules and growth factors have been investigated to regulate cell functions such as attachment, alignment, and differentiation [14-39,47-69,73-81,152-171].

2.7.1 Modification of Surface Topography

Topographic modulation is one of the most important aspects to control cell or tissue response to engineered extracellular matrix. Fitton *et al.* has reported the impact of the 3-D surfaces that result from pores in the material upon migration of the intact epithelial tissue *in vitro* [57]. Lee *et al.* cultured fibroblasts *in vitro* on a range of porous polycarbonate membranes with well-defined surface topography and wettability gradients [58]. It was observed that the cells adhered and showed greater proliferation more on the hydrophilic positions of the membrane surfaces than on the more hydrophobic ones, regardless of micropore size. It was also observed that cell adhesion and growth decreased gradually with increasing micropore size of the membrane surfaces.

Kooten *et al.* investigated the interaction of human fibroblasts with silicone grooved surfaces using cell cycle analysis *in vitro* [59]. Cells proliferated on the fibronectin-preadsorbed silicone, as demonstrated by increased coverage and occurrence of subpopulations in the S and G2/M phase of the cell cycle. Cell cycle analysis proved to be a sensitive screening method for proliferation on the silicone surfaces.

In addition to polymeric materials, titanium microtextured surfaces were also used for the investigation of cellular responses and suggested that material-specific properties do not influence the orientational effect of the surface texture on the observed rat dermal fibroblast (RDF) cellular behavior. The proliferation rate of the RDFs, however, seemed to be much higher on titanium than on silicone rubber substrata [189].

2.7.2 Modification of Surface Properties

Surface hydrophobicity or electric charge of polymer substrates strongly influences cell adhesion. As early in 1990's, Matsuda's group reported the development of micropatterning technology for cultured cells by precise surface regional modification via photochemical fixation of phenyl azido-derivatized polymers on polymer surface [60,190]. The photochemical fixation of these photoreactive polymers consisted of three steps: coating of a photoreactive polymer on a material surface; ultraviolet irradiation through a photomask; and removal of nonreacted polymer by a solvent. Dontha *et al.* also presented a method to generate biotin/avidin/enzyme nanostructures with maskless photolithography by modifying micrometer-sized domains of a carbon surface to allow derivatization to attach redox enzymes with biotin/avidin technology [61]. DeFife *et al.* examined the surface effect of electric charges of surface polymers. A photomask was placed over different regions to generate micropatterned surfaces with graft polymer stripes of three distinct ionic characters [62]. Nonionic polyacrylamide greatly inhibited adhesion and induced clumping of the few monocytes that did not adhere. On the other hand, the group of Ingber and Whitesides demonstrated that attachment of cells to surfaces could be confined by patterning the formation of SAMs using micro-contact printing into regions that promote or resist adsorption of protein [191-193].

Micropattern immobilization of various proteins has been performed by many researchers. Among the proteins, cell adhesion proteins, such as collagen, elastin, fibrillin, fibronectin, and laminin, were immobilized to regulate cell attachment. Growth factor proteins are also becoming extremely valuable tools in the attempts to understand the mechanisms that modulate cellular activities.

Fromherz *et al.* immobilized laminin by irradiation with UV light through a mask. This treatment denatured laminin in the exposed regions and the resultant surface inhibited neural cell attachment and neurite outgrowth [194]. Patterned immobilization of active peptides to regulate cell adhesion has also been carried out by several researchers [195-197]. Blawas and Reichert recently reviewed the current technology available for patterning proteins [198]. Consideration was also given to some major issues affecting protein patterning, including non-specific binding, protein pattern uniformity, and measurement techniques. In another paper, Ravi *et al.* reviewed the patterning of proteins and cells using non-photolithographic microfabrication technology [199]. This review described techniques for patterning the properties and structures of surfaces at the molecular level, and using these patterns to control both the adsorption of proteins to these surfaces and the attachment of cells to them. Lance *et al.* reported a new method for constructing controlled interfaces between cells and synthetic supported lipid bilayer membranes [200].

McFarland *et al.* examined the mechanism of attachment of human bone derived cells (HBDC) to surfaces with patterned surface chemistry *in vitro* [201]. Photolithography was used to generate alternate domains of N-(2-aminoethyl)-3-aminopropyl-triethoxysilane (EDS) and dimethyldichlorosilane (DMS). It was found that HBDC were localized preferentially to the EDS region of the pattern. Using serum specifically depleted of adhesive glycoproteins, this spatial organization was found to be mediated by adsorption of vitronectin from serum onto the EDS domains. In contrast, fibronectin could not adsorb in the face of competition from other serum components. Immunostaining revealed that both vitronectin and fibronectin could not adsorb to EDS

and DMS regions when coated from pure solution. In this situation, each protein was able to mediate cell adhesion across a range of surface densities. Cell spreading was constrained on the EDS domains as indicated by cell morphology and the lack of integrin receptor clustering and focal adhesion formation.

2.8 Layer-by-Layer Self-Assembly

Self-assembly of polyelectrolytes has developed into a viable alternative to Langmuir-Blodgett technique, spin-coating, in-situ polymerization and other methods of preparation of organic and hybrid nanostructures. Polyelectrolyte multilayer deposition is a simple strategy to assemble uniform, highly interpenetrated ultrathin films with one molecular layer at a time from the repetitive, alternate adsorption of polyelectrolytes from dilute solution [44-46]. Such an approach offers unprecedented nanoscale control over thin film architecture and properties, including film thickness, composition, conformation, degree of interchain ionic bonding, roughness, and wettability [172]. The resulting thin films can deposit on the substrates of any type, size, or shape. Furthermore, a variety of materials, including biological compounds [173,174], conducting polymers [175-177], dyes [178-180], metal nanoparticles [181,182] can be used to form the multilayer ultrathin films with layer-by-layer self-assembly. The layer-by-layer deposition is particularly attractive for its exceptional simplicity. A trade-off for the ease of preparation is structural imperfection. As compared with LB films, the polyelectrolyte films produced by this method are substantially less ordered. Nevertheless, they may find numerous application as very interesting composite materials. Both organic-inorganic super lattices [183,184], protein assemblies [44,45,87,185], new optical, and electronic

coatings [186,187] can be constructed on their basis and may be readily incorporated into the multilayer thin films [188].

In summary, this chapter introduced the background for this research project, from the biological concepts to engineering capability. Researchers have known more and more how the human body is organized and how it works as a functional system *in vivo* with cellular and molecular biological analysis approaches. And also using microfabrication and monolayer self-assembly techniques, much work has been done to understand how cells and tissues function in an *in vitro* environment. However, most of current studies in tissue engineering still emphasize on fibroblast, endothelial, and neural cells with fibronectin and other cell adhesive proteins. In this work, first of all, a combined microfabrication and nanopatterning technique was investigated for the fabrication of engineered cell culture scaffolds with different materials and different architectures. Secondly, smooth muscle cells were cultured to test the fabricated *in vitro* cell culture scaffolds and gelatin was considered as a cell adhesive protein for smooth muscle cells. This work may give out a understanding of how smooth muscle cells behave in the *in vitro* environment and further contribute to the research work on artificial muscle tissues in the field of tissue engineering.

CHAPTER 3

EXPERIMENTAL DESIGN AND THEORIES

Cells are essential ingredients for building and maintaining tissue functions. However, after cells are removed from their innate environment and placed in an *in vitro* environment, they typically lose some of their normal *in vivo* behavior. A principal objective of tissue engineering is to reach a fundamental understanding of the factors in the microenvironment surrounding cells, which can induce and affect the basic functions of cells. In this work, surface topography, surface chemistries, and physical architecture of engineered cell culture scaffolds were varied to assess their role as important factors to control the attachment, growth, and alignment of cells for their normal function.

3.1 General Design

The main purpose of this project is to investigate and develop the technologies to fabricate cell culture scaffolds and control cell behavior in the *in vitro* environment. Using electrostatic layer-by-layer self-assembly (LbL) and layer-by-layer lift-off (LbL-LO) techniques, the dimensions, shapes, and depths of the micro/nanostructures, as well as the surface properties with different materials and properties of the underlying architectures can be precisely controlled. The general design of the experiments is to fabricate the scaffolds with these two techniques. Meanwhile, the materials being used

and the scaffolds fabricated are characterized by appropriate equipments and instruments. Finally, rat aortic smooth muscle cells are cultured to test the cell responses to these engineered cell culture scaffolds.

In the following sections, the theories on materials, fabrication methods, and characterization methods will be described.

3.2 Biomaterials

“Biomaterials” is a term used to indicate a material that constitutes part of medical implants, extracorporeal devices, and disposables that have been used in medicine, surgery, dentistry, and veterinary medicine as well as in every aspect of patient health care. The National Institutes of Health Consensus Development Conference defined a biomaterial as “any substance (other than a drug) or combination of substances, synthetic or natural in origin, which can be used for any period of time, as a whole or as a part of a system which treats, augments, or replaces any tissue, organ, or function of the body” [202, 203].

3.2.1 Polymeric Materials and Surface Treatment

Synthetic materials currently used for biomedical applications include metals and alloys, polymers, and ceramics. Because the structures of these materials differ, they have different properties and, therefore, different uses in the body. Polymers are the most widely used materials in biomedical applications. They also are used in drug delivery systems, in diagnostic aids, and as a scaffolding material for tissue engineering applications.

Polymers are organic materials consisting of large macromolecules composed of many repeating units. These long molecules are covalently bonded chains of atoms. Unless they are cross-linked, the macromolecules interact with one another by weak secondary bonds, hydrogen and van der Waals bonds, and by entanglement. Because of the covalent nature of interatomic bonding within the molecules, the electrons are localized, and consequently polymers tend to be poor thermal and electric conductors. The mechanical and thermal behavior of polymers is influenced by several factors, including the composition of the backbone and side groups, the structure of the chains, and the molecular weight of the molecules. The polymeric surfaces can be modified by chemical and physical approaches.

Recently, plasma gas discharge and corona treatment with reactive groups introduced on the polymeric surfaces have emerged as other ways to modify biomaterial surfaces. Hydrophobic coatings composed of silicon- and fluorine-containing polymeric materials as well as polyurethanes have been studied because of the relatively accepted clinical performances of polyurethane polymers in cardiovascular implants and devices. Polymeric fluorocarbon coatings deposited from a tetrafluoroethylene gas discharge have been found to greatly enhance resistance to both acute thrombotic occlusion and embolization in small-diameter grafts. Hydrophilic coatings have also been popular because of their low interfacial tension in biologic environments. Hydrogels as well as various combinations of hydrophilic and hydrophobic monomers have been studied on the premise that there will be an optimum polar-dispersion force ratio, which could be matched to that on the surfaces of the most passivating proteins. The reasoning behind this method is that the passive surface would induce less clot formation. Polyethylene

oxide coated surfaces have been found to resist protein adsorption and cell adhesion and have therefore been proposed as potential “blood compatible” coatings.

3.2.2 Protein-Surface Interactions

The behavior of proteins at surfaces plays a vital role in determining the nature of the tissue-implant interface [203]. Adsorbed proteins affect blood coagulation, complement activation, and bacterial and cell adhesion. Furthermore, adsorbed proteins can influence biomaterial surface properties and degradation. The behavior of the adsorption and desorption of blood proteins or adhesion and proliferation of different types of mammalian cells on polymeric materials depend on the surface characteristics such as wettability (contact angle), hydrophilicity-hydrophobicity ratio, bulk chemistry, surface charge and charge distribution, surface roughness, and rigidity.

The properties of both protein and the surface, with which the biomolecule is interacting, influence interfacial behavior. The properties of proteins that influence surface activity are related to the primary structure of the protein, meaning that the sequence of amino acids affects protein-surface interactions. Larger molecules are likely to interact with surfaces because they are able to contact the surface at more sites. However, size is not the sole determinant. Because of their hydrophilicity, charged amino acids are generally located on the outside of proteins and are readily available to interact with surfaces. Consequently, the charge, as well as the distribution of charge on the protein surface, can greatly influence protein adsorption. As with size, however, charge is not the only determinant. Interestingly, proteins often show greater surface activity near their isoelectric point. Properties related to unfolding of the proteins also affect adsorption. Unfolding of a protein is likely to expose more sites for protein-surface

contact. Less stable proteins or those with less intramolecular cross-linking and disulfide bonding are likely to unfold more of faster.

Table 3.1 Properties of Proteins that Affect their Interaction with Surfaces

Properties		Effect
Size		Larger molecules can have more sites of contact with the surface
Charge		Molecules near their isoelectric point generally adsorb more readily and opposite charge to surface by electrostatic adsorption
Structure	Stability	Less stable proteins, such as those with less intramolecular cross-linking, can unfold to a greater extent and form more contact points with the surface
	Unfolding rate	Molecules that rapidly unfold can form contacts with the surface more quickly

The properties of biomaterial surfaces that influence interaction with proteins are similar to the characteristics that determine the adsorption behavior of proteins. Substrates with more topographical features will expose more surface area for possible interaction with proteins. For example, surfaces with grooves or pores have greater surface area compared with smooth surfaces. The surface chemical composition will determine which functional species are available for interaction with biomolecules. A variety of functional species, such as amino, carbonyl, carboxyl, and aromatic groups, can be present on the surface of polymeric biomaterials. Depending on which species are exposed, biomolecules will have different affinities for the surface. For example, hydrophobic surfaces tend to bind more protein as well as binding it more strongly. On a microscopic scale, biomaterial surfaces can be inhomogeneous.

Patches, or domains, of different functionality can exist on biomaterial surface, and these patches can interact differently with biomolecules. Depending on the chemical

species present within the various domains, proteins will have different affinities for the patches. The surface potential influences the structure and composition of the electrolyte solution adjacent to the biomaterial. The combined effects of water, molecules, and net surface potential will determine whether interaction with biomolecules is enhanced or hindered.

Table 3.2 Properties of Surfaces that affect their interaction with Proteins

Properties	Effect
Topography	Greater texture exposes more surface area for interaction with proteins
Composition	Chemical makeup of a surface will determine the types of intermolecular forces governing interaction with proteins
Hydrophobicity	Hydrophobic surfaces tend to bind more protein
Heterogeneity	Nonuniformity of surface characteristics results in domains that can interact differently proteins
Potential	Surface potential will influence the distribution of ions in solution and interaction with proteins

3.3 Layer-by-Layer Self-Assembly and Hydrophobic Interactions

3.3.1 Gibbs Free Energy of Film Formation

The layer-by-layer (LbL) adsorption of polyelectrolytes and other compounds is considered to be the result of electrostatic attraction between ionic side-groups of a polymer backbone to oppositely charged groups located on the surface of a substrate. The energy of electrostatic attraction, transformation of ionic atmosphere and the hydration shell around a polyelectrolyte chain during the self-assembly were estimated on the basis of available theoretical and experimental data for aqueous polyelectrolyte solutions. The analysis revealed that both ionic and hydrophobic interactions must be taken into account

when considering LbL multilayer formation [204].

3.3.2 Energy Model

Layer-by-layer self-assembly can be regarded as a process of adsorption of positively charged polyelectrolyte on a layer of negatively charged polyelectrolyte present on a substrate.

A hydrated ion can be represented as a charged core and a layer of partially immobilized water molecules around it (hydration shell). The number of H₂O units bound in the hydration layer can vary from 1 to 14, depending on the charge and the diameter of an ion. Outside the hydration shell, electrostatically attracted oppositely charged ions form an ionic atmosphere. Their concentration reaches a maximum at the border of the shell and quickly falls down to zero as the distance to the central ion increases.

The energy of ionic atmosphere and conformation of polyelectrolyte strongly depend on ionic strength. The thermodynamics of electrostatic interactions between polyelectrolytes in water at low concentration can be described quite well using Poisson-Boltzmann formalism. The contribution of the ionic atmosphere restructuring to Gibbs free energy directly depends on the energy of ionic atmosphere. Upon adsorption to a substrate, a cylindrical ionic cloud around polyelectrolyte transforms into a collective double electric layer of a charged plane. The lower limit of the Gibbs energy associated with this restructuring can be assumed the charged plane to be composed of polyelectrolyte molecules that lost the ionic atmosphere only on one hemisphere adjacent to the substrate. The other half of the ionic atmosphere facing the solution is retained.

Adsorption of positively charged polyelectrolyte onto negatively charged polyelectrolyte is analogous to the transfer of ions from an aqueous medium into an

organic one. The environment in polyelectrolyte complexes is quite hydrophobic. The energy required to replace solvent molecules in the solvation shell can be estimated from the free energy of ion transfer from water to a solvent of an appropriate polarity.

Covalent bonds between the monomer units do not allow the charged side groups of the polyelectrolyte to attain a minimum energy conformation achievable for regular supporting electrolyte. Most of the counterions around polyelectrolytes are concentrated within a few nanometers around the polyelectrolyte chain. In all layer-by-layer self-assembled structures, including multilayers of proteins and nanoparticles, the thickness of a single polymer layer was determined to be 2-5 nm. This thickness enables consideration of the radial distribution of charges around positively charged polyelectrolyte, of buffer salt ions in solution and that of ionic side group around positively charged polyelectrolyte molecule surrounded by negatively charged polyelectrolyte as qualitatively similar.

The entropy change for LbL self-assembly includes the contributions from: (1) the release of ions from the solvation shell; (2) the reorientation of water previously oriented by charged headgroups of polyelectrolyte; (3) the destruction of a shell of water molecules around hydrophobic parts of polyelectrolyte; (4) the loss of mobility of polyelectrolyte chains. Entropy contributions (1) and (2) have been taken into consideration when energy of the ionic atmosphere and energy of the hydration shell were estimated. Entropy (3) is accounted in the hydrophobic interactions.

3.3.3 Correlation with Experimental Data

Many proteins, for example myoglobin or lysozyme, readily form multilayers on oppositely charged polymers, such as poly(sodium 4-styrenesulfonate) (PSS). When negatively charged PSS is replaced with negatively charged aluminosilicate sheets

(montmorillonite), the formation of multilayers does not occur. Protein-alumosilicates complexes are not “cemented” by short-range charge-independent interactions due to a quite hydrophilic surface of alumosilicates. The loose electrostatic aggregates between alumosilicate and protein can be easily destroyed during the subsequent rinsing with water. Conversely, strong hydrophobic forces present in protein-polyelectrolyte multilayers make these complexes exceptionally stable.

The significance of hydrophobic forces can be also seen in recent results on LbL self-assembly of cationic and anionic dyes on poly(diallyldimethylammonium chloride) (PDDA), PSS, and poly(ethyleneimine) (PEI). It was observed that large dye molecules have a greater tendency to self-assemble than smaller ones. A dye molecule must have properly balanced hydrophilic and hydrophobic properties in order to self-assemble. If a molecule is too hydrophilic; i.e., if it is small and highly charged, it will not form a thermodynamically stable complex with polyelectrolyte.

It was demonstrated that strong electrostatic attraction of opposite charges located on a substrate and on a molecule to be assembled does not guarantee the formation of multilayers. Along with pure electrostatic forces, hydrophobic interactions, restructuring of the solvation shell, and the ionic atmosphere have been considered. Short-range hydrophobic forces can be identified as one of the important factors determining the ability of a compound to self-assemble via LbL technique. They should be considered as a main driving force of layer-by-layer adsorption. The preparation of LbL films of proteins, alumosilicates, dyes, polymers and nanoparticles confirm significance of hydrophobic interactions.

3.4 Electrostatic Layer-by-Layer Self-Assembly

Electrostatic layer-by-layer self-assembly is now employed in the fabrication of ultrathin films from charged polyions (polymers), dyes, nanoparticles, proteins and other supramolecular species. The main idea of this method consists in the resaturation of polyion adsorption, which results in the alternation of the terminal charge after each layer is deposited. This idea also implies that there are no major restrictions on the choice of polyelectrolytes. It is possible to design composite polymeric films in the range of 5 to 1000nm, with a definite knowledge of their composition.

A precleaned negatively charged substrate with any shape and size is incubated in a dilute solution of a positive charged polyelectrolyte, generally for a time optimized for the adsorption of a single monolayer with several nanometers thickness. The adsorption time also depends on the species of polyions or protein and concentration of salt. The substrate then is rinsed and dried. The next step is the immersion of the polycation-covered substrate into a dilute dispersion of negatively charged polyelectrolytes or other charged species, also for a time optimized for the adsorption of a monolayer. Then it is rinsed and dried. These operations complete to form a desired bilayer polyelectrolyte film on the substrate. Linear polycation-polyanion multilayers can be assembled and repeated by similar means. Different polyions, nanoparticles, proteins may be assembled in a preplanned order in a single film.

The forces between the oppositely charged layers govern the spontaneous layer-by-layer self-assembly of ultrathin films. These forces are primarily electrostatic and covalent in nature, but they can also involve hydrogen bonding, hydrophobic and other types of interaction. The properties of the self-assembled multilayers depend on the

choice of building blocks used and their rational organization and integration along the axis perpendicular to the substrate.

3.4.1 Polyanion / Polycation Alternate Assembly

The principle of alternate adsorption for film formation was first invented for charged colloidal particles and proteins in the pioneering work of Iler [45]. Later, a related method for film assembly by means of alternate adsorption of linear polycations and polyanions was introduced. In Figure 3.1, the assembly scheme is presented. A solid substrate with a negatively charged planar surface is immersed in the solution containing the cationic polyelectrolyte, and a layer of polycation is adsorbed. Because the adsorption is carried out at a relatively high concentration of polyelectrolytes, a number of ionic groups remains exposed at the interface with the solution, and thus the surface charge is effectively reversed. The reversed surface charge prevents further polyion adsorption. After rinsing in pure water the substrate is immersed in the solution containing the anionic polyelectrolyte. Again a layer is adsorbed, but now the original surface charge is restored. By repeating both steps, alternating multilayer assemblies are obtained with precisely the same layer thickness. Naturally, polyions have to be used at pH levels that provide a high degree of ionization.

Figure 3.1 summarizes the two modes of alternate adsorption assembly as applied to the following pairs: linear polycation/polyanion, and charged protein/linear polyion.

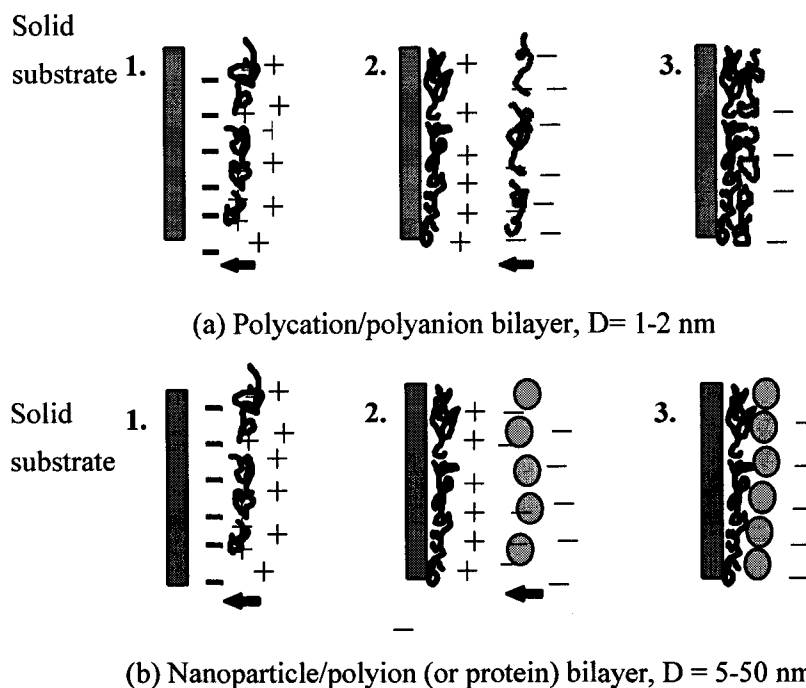


Figure 3.1 Schematic layer-by-layer film assembly on a solid substrate

3.4.2 Multilayer Microencapsulation of Microspheres

In most cases, polyion film formation on a flat solid support has been discussed because this formation provides better possibilities for studying the multilayer structure with standard analytical methods. However, the assembly process elaborated for a solid support may be transferred for an assembly onto porous carriers (e.g., chromatographic carriers, membranes, porous beads, and fibers) or onto the surface of charged particles with diameters of 0.5 - 5 microns (such as charged polystyrene microspheres). The assembly of organized polyion shells on latex is promising for the creation of complex catalytic particles. In the process, one adds the polycation solution to a suspension of the negative latex. After adsorption saturation is reached, one has to separate the latex from the polycation solution (usually by centrifugation or filtration), and then expose the latex to the polyanion solution, shown in Figure 3.2.

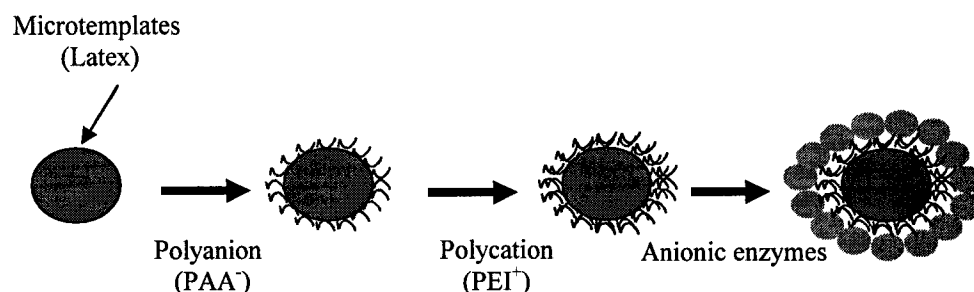


Figure 3.2 Schematic illustrations of the protein shell assembly on a latex sphere

Protein microcapsules or living cells may be covered by a shell of several polyion layers. By alternate treatment with poly (ethylenimine) (PEI) and polyacrylic acid (PAA) solutions at pH 6.5, the multilayer shell of (PEI/PAA)₈ was formed onto 0.5-mm diameter acidic phosphatase/alginate beads.

3.4.3 Standard Assembly Procedure

- Take aqueous solutions of polyion, nanoparticles, or protein at a concentration of 1-3 mg/mL, and adjust the pH value in such a way that the components are oppositely charged.
- Take a substrate carrying a surface (e.g., solid plates or polymer films covered by a layer of cationic poly(ethylenimine), which may be readily attached to many surfaces).
- Carry out alternate immersion of the substrate in the component's solutions for 10 min with 1-min intermediate DI water rinsing.
- Optionally dry the sample using nitrogen flow.

Polyions predominately used in the Assembly include poly(ethylenimine) (PEI), poly(dimethyldiallylammonium chloride) (PDDA), poly(allylamine) (PAH), poly-l-lysine

(PLL), poly(styrenesulfonate) (PSS), polyacrylic acid (PAA), gelatin, etc. The purpose of using LbL is to modify the surface properties with different materials

3.5 Principles of Microfabrication

Generally, there are several ways to fabricate the micro/nanostructures on base substrates, such as silicon, glass, PDMS and PMMA. First of all, photolithography is the most widely used technique to fabricate photoresist microstructures (PR 1813 and SU-8) on the base substrates; secondly, inductively coupled plasma (ICP) etching is very useful to achieve high aspect ratio structures on silicon wafer; thirdly, using the high aspect ratio SU-8 photoresist or silicon patterns, the microstructures can be reversed onto PDMS substrate by soft lithography; fourthly, hot-embossing can be employed to transfer the high aspect ratio micropatterns from silicon wafer to PMMS substrate. Combining these microfabrication techniques and layer-by-layer self-assembly above, the desired micro/nanostructures will be mainly fabricated on optically clear base substrates to achieve cell-specific patterns by surface modification.

3.5.1 Photolithography and Inductively Coupled Plasma Etching

Photolithography is the basic technique used to define the pattern of microstructures with photoresists and UV light. The technique is essentially the same as that used in the semiconductor microelectronics industry, as shown in Figure 3.3. In this figure, two types of photoresist can be used in photolithography process: one is positive photoresist which can be removed by specific developer after exposed to UV light; the other is negative photoresist which will be crosslinked after exposed to UV light, while

the unexposed negative photoresist can be removed by developer. Coupling with ICP etching, photolithography is very useful to make high aspect ratio structures with vertical sidewalls, as shown in Figure 3.4.

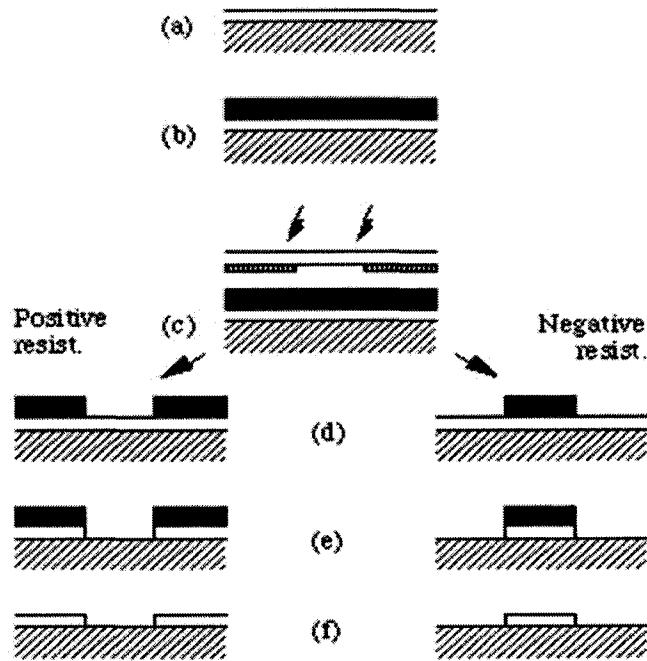


Figure 3.3 Schematic illustration of photolithography

Positive photo resist PR 1813 (Shiply), one of the S1800 Series Photo Resists, is used mostly in our clean room. Microposit S1800 Series Photo Resists are positive photoresist systems engineered to satisfy the microelectronics industry's requirements for the fabrication of advanced IC devices. The system has been engineered using a toxicologically safer alternative casting solvent to the ethylene glycol derived ether acetates. The dyed photoresist versions are recommended to minimize notching and maintain line width control when processing on highly reflective substrates.

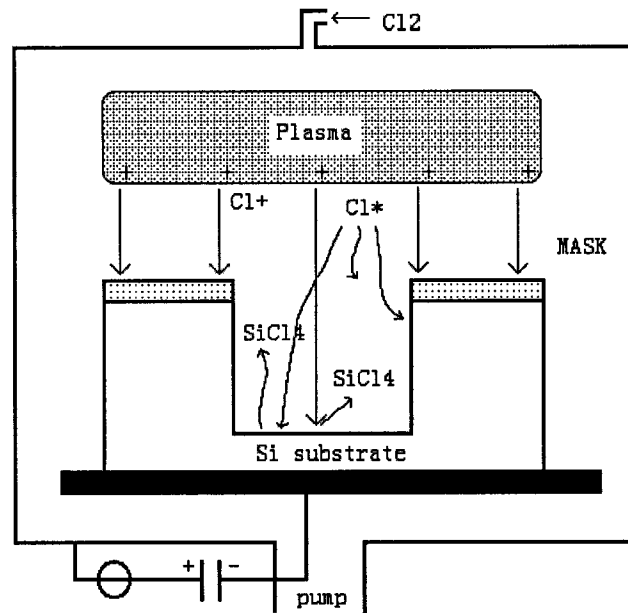


Figure 3.4 Schematic illustration of ICP etching

SU-8 (MicroChem, Inc.) is a negative, epoxy-type, near-UV photoresist based on EPON SU-8 epoxy resin (from Shell Chemical) that has been originally developed, and patented (US Patent No. 4882245) by IBM. This photoresist can be as thick as 2 mm, and aspect ratio >20 has been demonstrated with standard contact lithography equipment. These astounding results are due to the low optical absorption in the UV range which only limits the thickness to 2 mm for the 365nm-wavelength where the photo-resist is the most sensitive (i.e., for this thickness 100% absorption occurs). Of course, LIGA still yield better results for thick structures and high aspect ratios, but low-cost application will undoubtedly benefit from this resist that is well suited for acting as a mold for electroplating because of its relatively high thermal stability ($T_g > 200^\circ\text{C}$ for the cross-linked resist).

3.5.2 Soft Lithography

Soft lithography represents an alternative set of techniques for fabricating micro- and nanostructures. For low-cost high aspect ratio fabrication, the LIGA-like process is available with an epoxy-based resist, SU-8, with the compensation of lower resolution and aspect ratio. Polydimethylsiloxane (PDMS) elastomer replication has been utilized mostly in bioMEMS with patterned SU-8 or silicon master as mold inserts. Figure 3.5 shows the schematic soft lithography process.

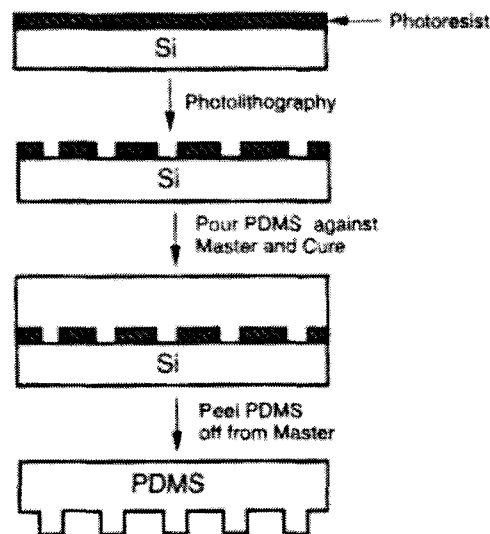


Figure 3.5 Schematic illustration of soft lithography

PDMS is durable, optically transparent, and inexpensive. Using SU-8 and silicon patterns obtained by photolithography and ICP etching, PDMS microstructures and microchannels were fabricated using a molding procedure. By reversing the columnar SU-8 and silicon patterns, we obtained microstructures and microchannels with the same shape and spacing given for the SU-8 and silicon substrates in PDMS. The PDMS (Sylgard 184, Dow Corning, Midland, MI) used was supplied as two-part liquid component kit comprised of a base and a curing agent. The liquid components were

thoroughly mixed in the ratio of 1 part curing agent to 10 silicone elastomer. The molding process was performed with the assistance of a vacuum pump to insure a quality reproduction of the SU-8 and silicon microstructures and microchannels. The PDMS film was then peeled from the SU-8 and silicon substrates to obtain the reversed PDMS substrate.

3.5.3 Hot-Embossing

Hot embossing is the process to press a mold into a pre-fabricated semi-finished plastic product that is located on a substrate under vacuum. The process takes place at a temperature that ensures sufficient flow ability of the plastic materials. After the mold insert, the plastic material is cooled down to a temperature which provides for sufficient strength. So the microstructured plastic material can be demolded.

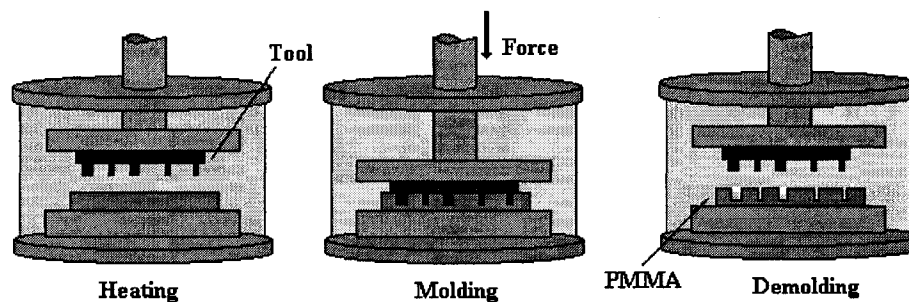


Figure 3.6 Schematic illustration of hot-embossing

As shown in Figure 3.6, in a hot embossing process, the poly(methyl methacrylate) (PMMA) sheet is placed on the substrate holder right below the tool. The substrate holder is on the lower part of the chamber. After the chamber is evacuated down below 1mTorr, the tool and PMMA are heated above the glass transition temperature of the PMMA separately. For most thermoplastic materials this temperature is in the range of 120°C ~ 180°C. Then the tool is embossed into the PMMA under a controlled force for a while.

Still applying the embossing force, the tool and PMMA are cooled down just below the glass transition temperature. The molding tool is then demolded from PMMA.

3.6 Physical Surface Characterization

Biomaterials interact with the body through their surface. Consequently, the properties of the outermost layers of a material are critically important in determining both biological responses to implants and material responses to the physiological environment. Changes in surface characteristics during exposure to the hostile physiological environment further modify biological responses.

Surface analytical techniques provide information about the outermost one to ten atomic layers of a material. Characterization of a material's surface properties is needed to relate important surface characteristics to biological responses. Chemical, topographic, mechanical, and electrical properties may all affect how proteins and cells interact with a material. Therefore, comprehensive characterization of a surface requires several pieces of information. Thorough surface characterization requires the use of multiple analytical methods.

3.6.1 Contact Angle Analysis

Contact angle, θ , is a quantitative measure of the wetting of a solid by a liquid. When a drop of liquid is placed on a surface, it will spread to reach a force equilibrium, in which the sum of the interfacial tensions in the plane of the surface is zero. It is defined geometrically as the angle formed by a liquid at the three phase boundary where a liquid, gas and solid intersect as shown in Figure 3.7 below:

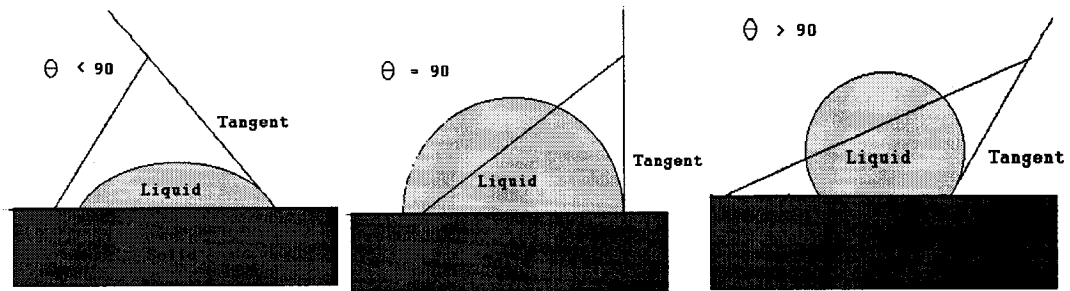


Figure 3.7 Contact angle analysis assesses the ability of a liquid to spread on a surface

The contact angle is an inverse measure of the ability of a particular liquid to “wet” the surface. If the liquid is water, a smaller θ indicates a hydrophilic surface, on which water spreads to a greater extent; a larger θ indicates a hydrophobic surface, on which water beads up. Thus, it can be seen from this figure that low values of θ indicate that the liquid spreads, or wets well, while high values indicate poor wetting. If the angle θ is less than 90, the liquid is said to wet the solid. If it is greater than 90, it is said to be non-wetting. A zero contact angle represents complete wetting.

3.6.2 Scanning Electron Microscopy (SEM)

SEM is an instrument that produces a largely magnified image by using electrons instead of light to form an image. Figure 3.8 shows the principle of SEM, in which incident electron beam emits X-rays, Auger electrons, primary backscattered electrons, and secondary electrons.

A beam of electrons is produced at the top of the microscope by an electron gun. The electron beam follows a vertical path through the microscope, which is held within a vacuum. The beam travels through electromagnetic fields and lenses, which focus the beam down toward the sample. Once the beam hits the sample, electrons and X-rays are

ejected from the sample. Detectors collect these X-rays, backscattered electrons, and secondary electrons and convert them into a signal sent to a screen similar to a television screen, which produces the final image.

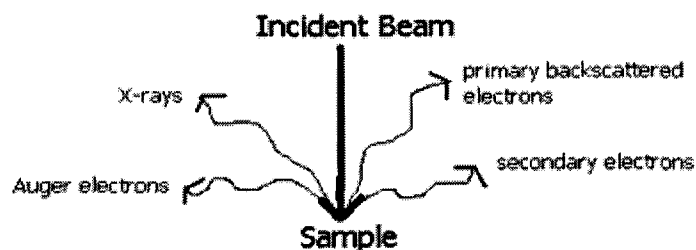


Figure 3.8 Principle of Scanning Electron Microscopy

3.6.3 Atomic Force Microscopy (AFM)

The atomic force microscope is one of about two dozen types of scanned-proximity probe microscopes. All of these microscopes work by measuring a local property—such as height, optical absorption, or magnetism—with a probe or "tip" placed very close to the sample. The small probe-sample separation (on the order of the instrument's resolution) makes it possible to take measurements over a small area. To acquire an image the microscope raster-scans the probe over the sample while measuring the local property in question.

Figure 3.9 shows the concept of AFM and optical lever. AFM operates by measuring attractive or repulsive forces between a tip and the sample. In its repulsive "contact" mode, the instrument lightly touches a tip at the end of a leaf spring or "cantilever" to the sample. As a raster-scan drags the tip over the sample, some sort of detection apparatus measures the vertical deflection of the cantilever, which indicates the local sample height. Thus, in contact mode the AFM measures hard-sphere repulsion forces between the tip and sample.

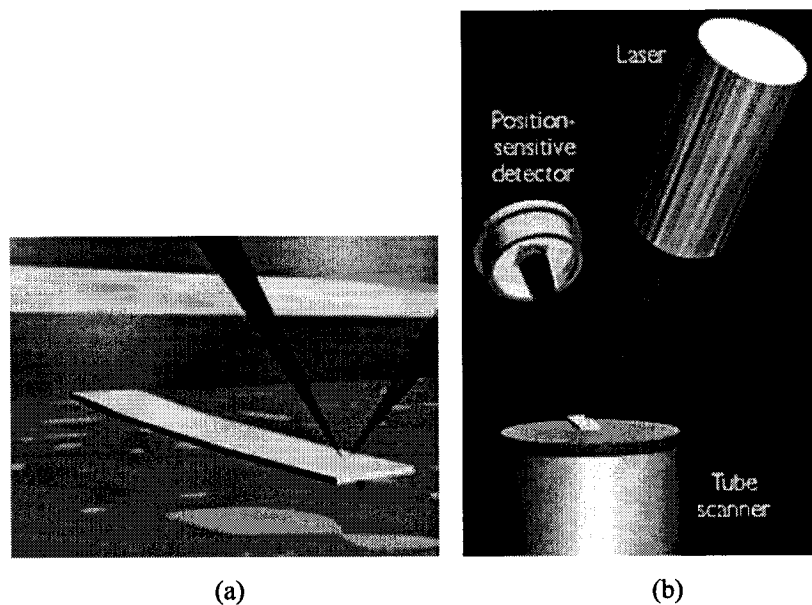


Figure 3.9 Concept of Atomic Force Microscopy and the optical lever

(a) a cantilever touching a sample; (b) the optical lever.

In principle, AFM resembles the record player as well as the stylus profilometer. However, AFM incorporates a number of refinements that enable it to achieve atomic-scale resolution. Also, because AFM is based on interaction between the tip and sample, as well as surface topography, local properties, such as stiffness and friction, can be determined.

3.7 Material Characterization

3.7.1 Quartz Crystal Microbalance (QCM)

The quartz crystal microbalance (QCM) is an ultra-sensitive weighing device. It consists of a piezoelectric quartz crystal, often in the form of a disk, which is sandwiched between a pair of evaporated electrodes. Figure 3.10 is a SEM image of a QCM electrode.

When these are connected to an electronic oscillator, the crystal can be made to oscillate in a very stable manner at its resonant frequency, due to the piezoelectric effect. If a thin, rigid film is deposited evenly over one or both of the electrode surfaces in such a way that it does not slip on the surface, the resonant frequency decreases proportionally to the mass of the film. By measuring the resonant frequency, surface mass density well below 1 ng/cm^2 can be gauged.

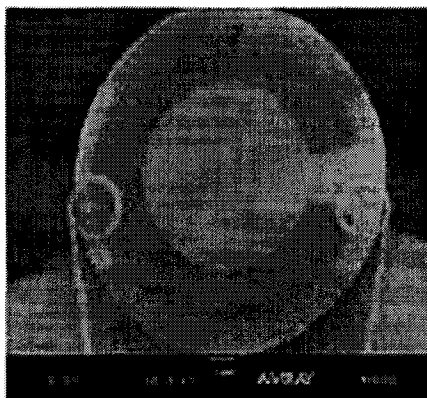


Figure 3.10 SEM image of a QCM electrode

Quartz crystal microbalance monitoring of multilayer growth is often the first stage in elaboration of an assembly procedure. The frequency shift with adsorption cycles gives the adsorbed mass at every assembly step. A linear film mass increase with the number of assembly steps indicated a successful procedure.

The mass of material coated on substrate may be determined by QCM method. The amount of deposition, Δm , was measured by detection the frequency decrease of QCM, ΔF , by using Sauerbrey's equation:

$$-\Delta F = \frac{2F_0^2}{A\sqrt{\rho_q u_q}} \Delta M \quad \text{Equation 3-1}$$

where F_0 is the natural frequency of QCM, A is the area of the electrode, Pq is the density of the quartz, and Uq is the shear modulus.

The thickness and mechanical properties of deposited film can be affected by (1) pH value; (2) Ionic strength; (3) Surfactant of the solution.

The following relationship is obtained between adsorbed mass M (g) and frequency shift ΔF (Hz) by taking into account the characteristics of the 9 MHz quartz resonators used: $\Delta F = -1.83 \times 10^8 M/A$, where $A = 0.16 \pm 0.01 \text{ cm}^2$ is the surface area of the resonator; and $\Delta M \text{ (ng)} = -0.87 \Delta F \text{ (Hz)}$. One finds that 1 Hz change in ΔF corresponds to 0.87 ng, and the thickness of a film may be calculated from its mass. The adsorbed film thickness at both faces of the electrodes (d) is obtainable from the density of the protein / polyion film (ca 1.3 g/cm^3) and the real film area: $d(\text{nm}) = -(0.016 \pm 0.02) \Delta F \text{ (Hz)}$. The scanning electron microscopy data from a number of protein / polyion and linear polycation / polyanion film cross-sections permitted us to confirm the validity of this equation. Another powerful method for polyion film characterization was small-angle X-ray and neutron reflectivity.

3.7.2 Zeta-potential Analysis

A charged particle suspended in an electrolytic solution attracts ions of opposite charge to those at its surface, where they form the Stern layer. To maintain the electrical balance of the suspending fluid, ions of opposite charge are attracted to the Stern layer. The potential at the surface of that part of this diffuse double-layer of ions that can move with the particle when subjected to a voltage gradient is the zeta potential. This potential measured is very much dependent upon the ionic concentration, pH, viscosity, and dielectric constant of the solution being analyzed.

Charged particles in a liquid suspension can be made to move by applying an electric field to the liquid through two electrodes as shown in Figure 3.11. By alternating the charge between the electrodes, the particles move back and forth between the electrodes at a velocity relative to their surface charge and the electrode potential. This velocity can be determined by measuring the doppler shift of laser light scattered off of the moving particles.

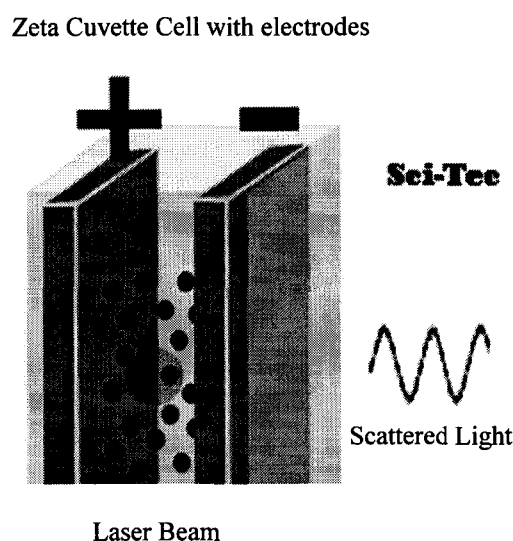


Figure 3.11 Schematic illustration of Zeta-Potential Measurement

3.7.3 Beer's Law – Concentration and Absorbance

Beer's Law states that the absorbance, $A(\lambda)$, of a species at a particular wavelength of electromagnetic radiation, w , is proportional to the concentration, c , of the absorbing species and to the length of the path, L , of the electromagnetic radiation through the sample containing the absorbing species. This can be written in the form:

$$A(\lambda) = e(\lambda) L c \quad \text{Equation 3-2}$$

The proportionality constant $e(w)$ is called the absorptivity of the species at the

wavelength, λ .

The way in which $\epsilon(\lambda)$ depends on wavelength defines the spectrum of the substance in question. Most substances show a maximum in $\epsilon(\lambda)$ over a sufficiently broad wavelength range. The wavelength at that maximum value is called the analytical wavelength of the substance. Normally, Beer's law is applied at the analytical wavelength of a given material. The sensitivity to concentration differences should be largest at that wavelength.

The experimental procedure for using Beer's Law to measure concentrations generally involves the following:

- Determine the analytical wavelength of the substance whose concentration is desired, λ_{anal}
- Prepare a series of samples of known concentration of the substance.
- Measure the absorbance of each of the solutions of known concentration at the analytical wavelength, see Figure 3.12.
- Plot the values of the absorbance as a function of the concentration as shown in Figure 3.13.
- Verify that, within experimental error, the absorbance is a linear function of the concentration.

If linearity is confirmed, determine the slope of the best straight line through the experimental points in the absorbance vs. concentration plot. Call this the Beer's Law slope. The Beer's law slope has the value $\epsilon(\lambda_{\text{anal}}) l$, where l is the path length through the sample.

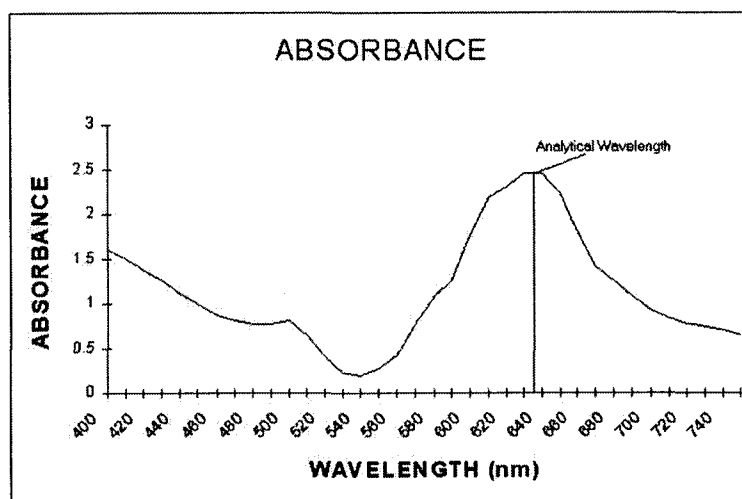


Figure 3.12 UV-Vis spectrum of a sample species

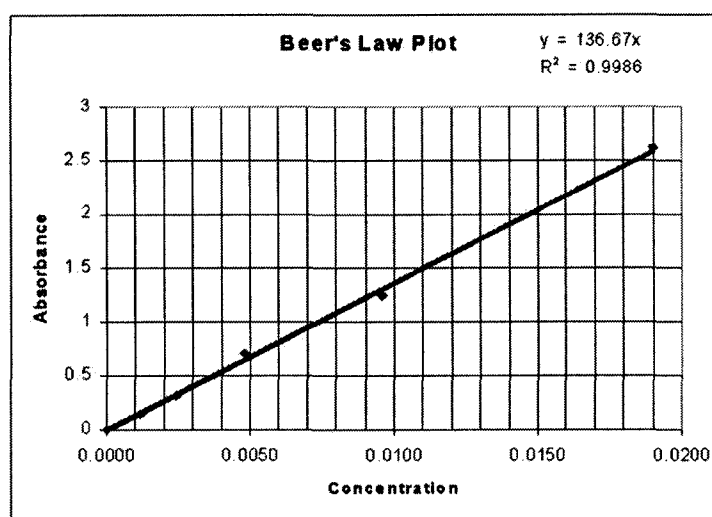


Figure 3.13 Beer's Law Plot

If the same experimental arrangement (same spectrometer, same cell) will be used for subsequent absorbance measurements, the value of the slope can be used to determine the concentration corresponding to a given absorbance by samples of unknown concentration.

If a different experimental arrangement will be used (e.g., a different cell), the

Beer's Law slope will need to be adjusted by the path length through the cell used in the Beer's Law determination. This slope will provide the value of the absorptivity, $\epsilon(\lambda_{\text{anal}})$, which should be characteristic only of the substance and the wavelength, and independent of the experimental arrangement used to determine it.

3.8 Biological characterization

3.8.1 Staining Cells

Several fluorescent probes can be used to analyze the viability, alignment, and focal adhesion of smooth muscle cells (SMCs) [210,211]. These fluorescent probes bind to the specific protein in the cells directly or indirectly via chemical reaction (positively charged dyes) or biological binding (fluorescent conjugated secondary antibody).

3.8.1.1 Hoechst 33242 / Propidium Iodide Nuclei Stain

The bisbenzimidazole dye, Hoechst 33342, is cell membrane-permeant, minor groove-binding DNA stains that fluoresce bright blue upon binding to DNA. Hoechst 33342 is quite soluble in water (up to 2% solutions can be prepared) and relatively nontoxic. This Hoechst dye, excited with the UV spectral lines of the argon-ion laser and by most conventional fluorescence excitation sources, exhibits relatively large Stokes shifts (excitation/emission maxima $\sim 350/460$ nm), shown in Figure 3.14, making them suitable for multicolor labeling experiments. Propidium iodide is a membrane impermeant dye that also binds to nucleic acids and is viewed with the TRITC filter cube. Cells with intact membranes, live cells, will not stain with propidium iodide.

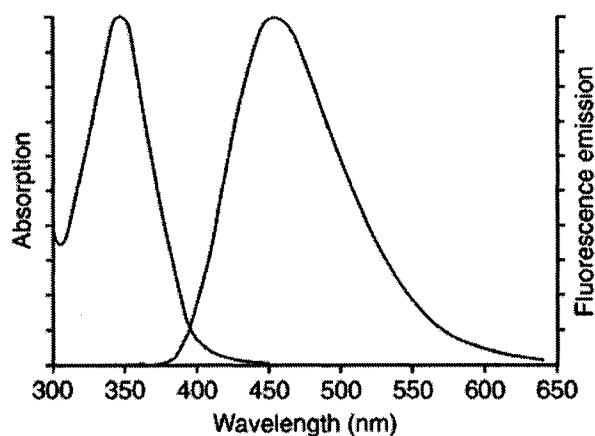


Figure 3.14 Fluorescence spectra of Hoechst 33342

3.8.1.2 Phalloidin F-actin Stain

The cytoskeleton is an essential component of a cell's structure and one of the easiest to label with fluorescent reagents. Numerous fluorescent and biotinylated derivatives of phalloidin and phalloidin can be used for selectively labeling F-actin. Alexa Fluor dye-labeled phalloidins are now the preferred F-actin stains for most applications across the full spectral range.

Figure 3.15 shows the fluorescence spectra of Alexa Fluor 488 phalloidin.

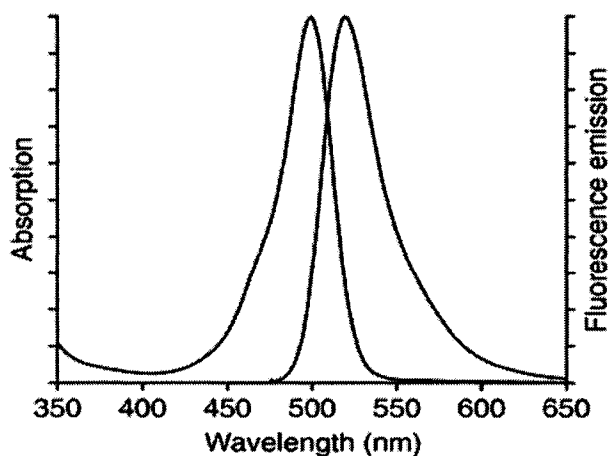


Figure 3.15 Fluorescence spectra of Alexa Fluor 488 phalloidin

The Alexa Fluor phalloidin conjugates provide researchers with fluorescent probes that are superior in brightness and photostability to all other spectrally similar conjugates tested. Alexa Fluor 488 phalloidin has maximum excitation and emission wavelengths of 495/518 nm and can be visualized with a FITC filter.

3.8.1.3 Plasma Membrane Stain

FM 1-43 and FM 4-64, offered by Molecular Probe, are easily applied to cells, where they bind rapidly and reversibly to the plasma membrane with strong fluorescence enhancement. All these probes have large Stokes shifts and can be excited by the argon-ion laser, see Figure 3.16. FM 1-43 is efficiently excited with standard fluorescein optical filters, but poorly excited with standard tetramethylrhodamine optical filters. Membranes labeled with FM 4-64 exhibit long-wavelength red fluorescence that can be distinguished from the green fluorescence of FM 1-43 staining with the proper optical filter sets, thus permitting two-color observation of membrane recycling in real time.

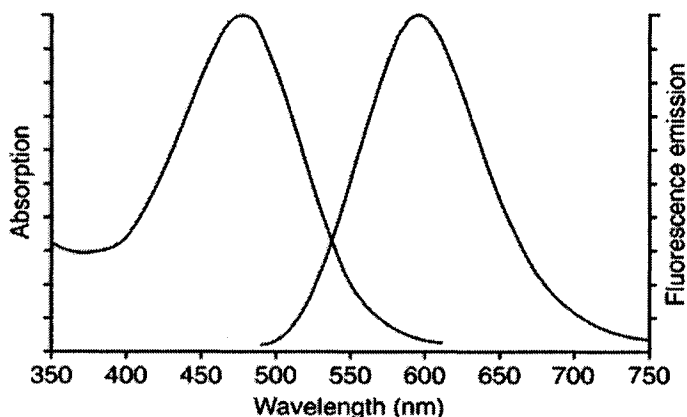


Figure 3.16 Fluorescence spectra of FM 1-43

3.8.1.4 Indirect Immunohistochemistry Stain

Adhesion between a cell and its surrounding extracellular matrix controls

complex biological processes such as development, wound healing, immune response, and tissue function and is therefore a central theme in the design of bioactive surfaces and biomaterials that successfully interface with the body. Cell attachment to the ECM is primarily mediated by integrins, a widely expressed family of cell surface adhesion receptors. In addition to anchoring cells, integrins transmit signals that direct cell migration, proliferation, and differentiation. After binding to ECM proteins, integrins cluster together form focal adhesions—complexes of intracellular signaling and structural proteins. These specialized sites of attachment provide not only a structural link between the internal actin cytoskeleton and the ECM but also function as a locus of signal transduction activity that ultimately governs cellular response. Numerous proteins have been identified in focal adhesions, some of which play a predominantly structural role (e.g., actinin, talin, vinculin) while others are involved in signal transduction pathways (e.g., focal adhesion kinase, paxillin).

Vinculin is an attachment protein involved in the indirect binding of intracellular actin filaments to extracellular fibronectin. It is widely distributed in tissues and expressed where smooth muscle actin and fibroblasts attach to the extracellular matrix. Vinculin has been found in all adherent junctions. Anti-Vinculin (Clone VLN01) recognizes the ~130 (vinculin) and ~150 (meta-vinculin) proteins and is commonly used to label vinculin. Using fluorescein goat anti-mouse IgG1 to bind anti-Vinculin allow investigating the focal adhesions of cells, and may be used to assess cell response to the engineered *in vitro* cell culture scaffolds.

3.8.2 Principle of Fluorescence

Fluorescent probes enable researchers to detect particular components of complex

biomolecular assemblies, including live cells, with exquisite sensitivity and selectivity. The purpose of this introduction is to briefly outline fluorescence techniques for newcomers to the field [210].

Fluorescence is the result of a three-stage process that occurs in certain molecules (generally polyaromatic hydrocarbons or heterocycles) called fluorophores or fluorescent dyes. A fluorescent probe is a fluorophore designed to localize within a specific region of a biological specimen or to respond to a specific stimulus. The process responsible for the fluorescence of fluorescent probes and other fluorophores is illustrated by the simple electronic-state diagram (Jablonski diagram) in Figure 3.17.

The entire fluorescence process is cyclical. Unless the fluorophore is irreversibly destroyed in the excited state (an important phenomenon known as photobleaching, see below), the same fluorophore can be repeatedly excited and detected. The fact that a single fluorophore can generate many thousands of detectable photons is fundamental to the high sensitivity of fluorescence detection techniques.

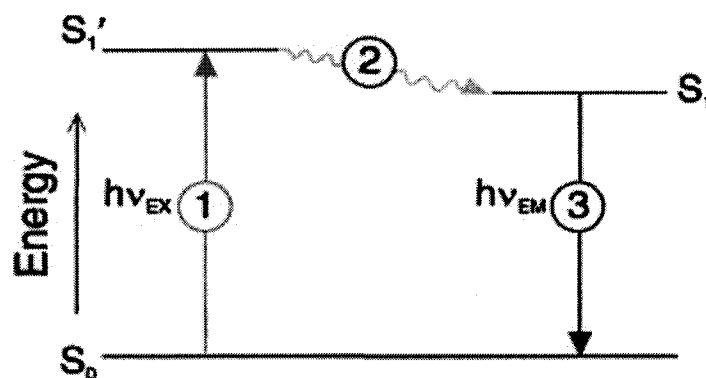


Figure 3.17 Jablonski diagram illustrating the processes involved in the creation of an excited electronic singlet state by optical absorption and subsequent emission of fluorescence

For polyatomic molecules in solution, the discrete electronic transitions represented by $h\nu_{EX}$ and $h\nu_{EM}$ in Figure 3.17 are replaced by rather broad energy spectra

called the fluorescence excitation spectrum and fluorescence emission spectrum, respectively. The bandwidths of these spectra are parameters of particular importance for applications in which two or more different fluorophores are simultaneously detected (see below). With few exceptions, the fluorescence excitation spectrum of a single fluorophore species in dilute solution is identical to its absorption spectrum. Under the same conditions, the fluorescence emission spectrum is independent of the excitation wavelength, due to the partial dissipation of excitation energy during the excited-state lifetime. The emission intensity is proportional to the amplitude of the fluorescence excitation spectrum at the excitation wavelength as shown in Figure 3.18.

Fluorophores currently used as fluorescent probes offer sufficient permutations of wavelength range, Stokes shift and spectral bandwidth to meet requirements imposed by instrumentation, while allowing flexibility in the design of multicolor labeling experiments. The fluorescence output of a given dye depends on the efficiency with which it absorbs and emits photons, and its ability to undergo repeated excitation/emission cycles. Absorption and emission efficiencies are most usefully quantified in terms of the molar extinction coefficient (ϵ) for absorption and the quantum yield (QY) for fluorescence. Both are constants under specific environmental conditions. The value of ϵ is specified at a single wavelength (usually the absorption maximum), whereas QY is a measure of the total photon emission over the entire fluorescence spectral profile.

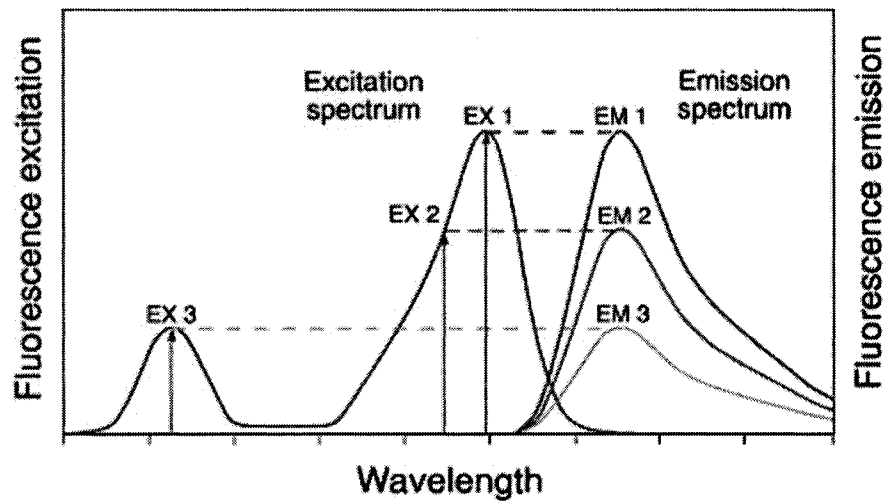


Figure 3.18 Excitation of a fluorophore at three different wavelengths (EX 1, EX 2, EX 3) does not change the emission profile but does produce variations in fluorescence emission intensity (EM 1, EM 2, EM 3) that correspond to the amplitude of the excitation spec

In summary, this chapter described the engineering design and experimental theories that are necessary to be employed to investigate the fabrication and cell culture technologies. Many engineering and biological techniques will be involved in this project to study behavior and response of smooth muscle cells to the engineered cell culture scaffolds.

CHAPTER 4

MATERIALS AND METHODS

4.1 Materials and Instrumentation

All the materials, chemicals, fluorescent dyes, medium, serum, and proteins used in this work are commercial products. For detailed information about the inventory of these materials being used, please refer to Appendix A. Appendix A includes product name, product number, vendor, etc. Other supplies, such as sterile pipettes, tissue culture dishes and flasks, centrifuge tubes, etc., were purchased from Fisher Scientific and VWR International Inc.

In general, polyion solutions, including poly(diallyldimethylammonium chloride) (PDDA), poly(ethyleneimine) solution (PEI), poly(allylamine hydrochloride) (PAH), and poly(sodium 4-styrenesulfonate) (PSS) were dissolved in pH 6.2 deionized (DI) water at a concentration of 2 mg/ml with 0.5 M potassium chloride (KCl). Gelatin and Poly-L-lysine hydrobromide (PLL) were dissolved at 2 mg/mL in Phosphate Buffered Saline (PBS). Fibronectin and ribonuclease were dissolved at 100 μ g/mL in PBS. Triton X-100 and bovine serum Albumin (BSA) were made at varying concentration as needed, refer to Appendix C.2 for cell staining.

All the fabrication, metrology, inspection equipment and instrumentation used in this project are also commercial products, Appendix B contains detailed information.

4.2 Techniques and Methods

4.2.1 Conjugate Solution Preparation

In the fabrication process, fluorescent dyes were integrated into the engineered cell culture scaffolds in LbL self-assembly step. Ru(bpy) is an oxygen sensitive fluorophore and FITC is a pH-sensitive fluorophore; these dyes were used as contrast agents to observe patterning behavior of charged materials. However, since both oxygen concentration and pH value are critical factors for *in vitro* cell culture systems, inclusion of these materials also opens a perspective for continuous monitoring the change on oxygen concentration and pH value in cell culture media to allow better understanding of *in vitro* cell culture conditions for future research work. Using a standard labeling procedure, gelatin was conjugated with FITC to form FITC-gelatin. Separate batches of PAH were labeled with FITC and Ru(bpy) in pH 9 NaHCO₃ buffer as will be described below.

PAH, PLL, and gelatin were conjugated with a fluorescent dye, Fluorescein isothiocyanate isomer I (FITC) or Bis(2,2'-bipyridine)-4'-methyl-4-carboxybipyridine-ruthenium N-succinimidyl ester-bis (hexafluorophosphate (Ru(bpy)₂(mcbpy-O-Su-ester)(PF₆)₂) to facilitate inspection of nanoscale patterns comprising polyion/protein films. ITC, the isothiocyanate group of FITC can react with the NH₂ (amino group) of PAH to form conjugate of FITC-PAH.

The following procedure was used for making FITC-PAH: 0.1 M sodium bicarbonate (NaHCO₃) buffer was prepared and adjusted to pH 9 by HCl and KOH. Next, 60 mg PAH was dissolved in 1 mL 0.1M NaHCO₃ buffer and 0.25mg FITC was dissolved in 100 μ L N,N-Dimethylformamide (DMF). FITC solution was added into

PAH solution and stirred at room temperature for 1 hour. Then, FITC-PAH conjugation was precipitated in 30 mL acetone and centrifuged at 3000 rpm for 5 minutes. After removing the supernatant, the remaining FITC-PAH conjugate solid was resuspended and dissolved in 30 mL pH 7 tris buffer. FITC-PLL was made in a similar way, but 5mg PLL was dissolved in 1 mL 0.1M NaHCO₃ buffer in place of the PAH.

A protein-labeling procedure for tagging gelatin with FITC was adopted from the guidelines provided by Molecular Probes and Sigma-Aldrich. According to these procedure, 0.1 M sodium bicarbonate buffer was prepared and adjusted to pH 9. Next, 20 mg of gelatin was dissolved in 2 mL of 0.1 M NaHCO₃ buffer. Then, 0.2 mg FITC powder was dissolved in 200 μ L DMF. While stirring the gelatin solution slowly, the FITC solution was added. The reaction was incubated at room temperature with continuous stirring for 1 hour. Finally, the conjugate was separated from unreacted labeling reagent with an Amersham Pharmacia Biotech PD-10 desalting column.

4.2.2 Electrostatic Layer-by-Layer Self-Assembly

Electrostatic layer-by-layer self-assembly can be applied to almost any solid planar substrate or particle surface. It is very useful to modify the surface properties with different materials being used.

4.2.2.1 Assembling Gelatin/fibronectin/polyelectrolyte on Glass/silicon Substrate

The deposition of nanocomposite polymer/protein films was achieved using electrostatic self-assembly. The standard layering process was as follows: individual aqueous solutions of polyion and protein at concentrations of 2 mg/mL were prepared and adjusted to the appropriate pH, which varied depending on the purposes of the

experiments. For each case, a glass or silicon substrate was pretreated with incubation in Nanostrip solution at 70°C for about one hour to introduce negative surface charges such that the initial layering step can be readily started. The substrate was alternately immersed in polyion solutions for 10 minutes or protein solution for 20 minutes, respectively, with an intermediate water rinse for 1 minute in all cases. For some experiments, such as Quartz Crystal Microbalance (QCM) analysis, it was necessary to perform a drying step (fluxing with nitrogen) to arrive at an accurate measurement. The removal of water trapped in the film adsorbed on the electrode helped avoid the fluctuation of mass by evaporation during measurement. Using this standard layer-by-layer self-assembly method, the properties of polyelectrolyte and protein materials can be characterized by QCM, Zeta-potential analyzer, UV-Vis, and fluorescence spectroscopy.

4.2.2.2 Coating Gelatin/polyelectrolyte Thin Films on Nanoparticles

The self-assembly properties of FITC-gelatin were studied to assess the conditions under which multilayer films containing this molecule could be formed. To determine the charge properties of the labeled protein using measurements of zeta potential, nanoparticles were coated with alternating layers of polyions and proteins. PDDA, PSS and gelatin were dissolved in pH 4.0 or pH 10.0 tris buffers, and pH 6.2 DI water, at a concentration of 2 mg/mL. The selection of pH 4.0 and 10.0 tris buffers was to test the charge polarities of gelatin at pH values away from its isoelectric point (4.8-5.1). Next, 400 nm silica particles were coated with PDDA/PSS and PDDA/gelatin through a process of alternate exposure, centrifugation, and water rinsing. During the layering process, the particles were immersed in PDDA, PSS, and gelatin solution for 20 minutes

per layer, and rinsed with pH 4 or pH 10 tris buffers, or DI water, twice before Zeta-potential measurement. In addition, the UV-Vis spectra of the original gelatin solution and gelatin solution remaining were measured after layering silica particles.

To further confirm the charge polarity of FITC-gelatin, 400 nm silica particles coated with FITC-gelatin were scanned by fluorescence spectroscopy. In one case, the silica particles were assembled with films of PDDA/PSS/FITC-gelatin, and in a second case, particles were coated with PDDA/FITC-gelatin. In both cases, PDDA and PSS were dissolved in pH 6.2 DI water at a concentration of 2 mg/mL; FITC-gelatin was made in pH 9 NaHCO₃ buffer at a concentration of 10mg/mL. Using the same PDDA, PSS, and FITC-gelatin solutions, silica particles were coated in the order of PDDA/PSS/FITC-gelatin/PDDA/FITC-gelatin for later zeta-potential measurement.

4.2.2.3 Underlying Architecture Studies with Different Surface Coatings

Multilayers polyelectrolyte thin films of (PAH/PSS)_n were deposited on the planar glass substrates with standard LbL procedure, where n=1, 2, 5, 10, 20. Then, gelatin and fibronectin were coated on the surfaces of the polyelectrolyte films. The overall 2-D cell culture scaffolds include: (1) (PAH/PSS)_n; (2) (PAH/PSS)_n + fibronectin; (3) (PAH/PSS)_n + PAH/gelatin. These scaffolds were used to study the effect of surface materials and underlying architectures on the cell landing and cell adhesion.

4.2.3 Layer-by-Layer & Lift-Off (LbL-LO)

Combing traditional photolithography and electrostatic layer-by-layer self-assembly technologies, a novel so-called layer-by-layer lift-off technique has been proposed to fabricate multilayer ultra thin film patterns.

4.2.3.1 Fabrication of Thin Film Patterns on Planar Base Substrate

Figure 4.1 shows the schematic fabrication process of polyelectrolyte thin film patterns on the planar base substrate.

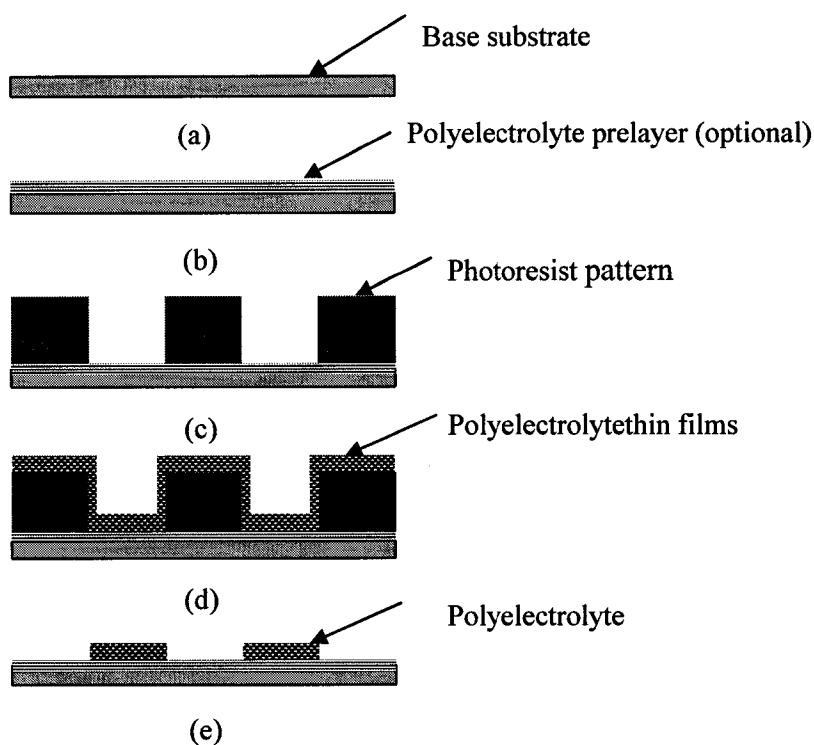


Figure 4.1 Fabrication of polyelectrolyte thin film patterns on planar base substrates

This figure also gives the basic idea of LbL-LO technology. The first two steps are general photolithography (refer to Appendix C.1 for the detail photolithography procedure): after pretreatment, optional step of first LbL is performed to modify the surface properties of base substrate; then, the base substrate is spin coated with positive photoresist PR 1813, which is subject to exposure of UV light later on; the resist patterns are achieved after development. The next step is to apply LbL self-assembly and form multilayer polyelectrolyte thin films on the surface of the resist patterns and exposed area of base substrate. Finally, in the so-called lift-off step, resist patterns are removed in

acetone or developer solvent and only the multilayer polyelectrolyte thin film patterns are left on the base substrate.

4.2.3.2 Comparison of Patterned Substrates

Figure 4.2 contains the strip and square patterns with feature size of 50, 60, 70, 80, 100, and 120 μm , which are marked with I to III. All the patterns have equal spacing as the width of the strip and size of the square in each block.

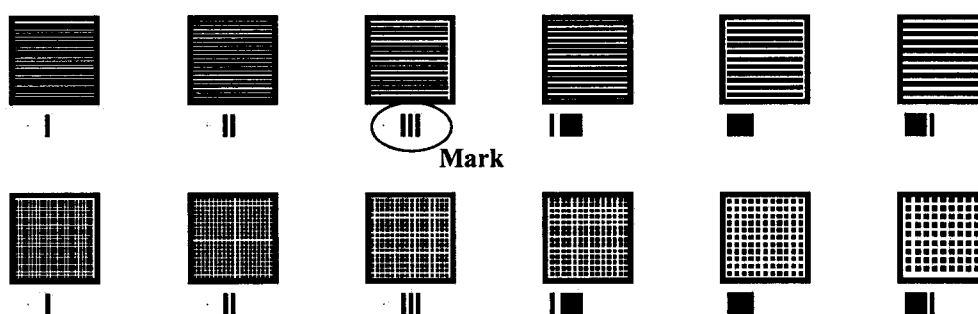


Figure 4.2 Mask layout of strip and square patterns.

Using LbL-LO technique, multiplayer thin film patterns with different surface materials and underlying architectures were fabricated on glass substrates. In this work, most of the patterns have underlying architectures of (FITC-PAH/PSS) $_n$, where $n=3-5$, with surface materials of gelatin, FITC-gelatin, fibronectin, PDDA, PAH, PEI, and PSS. In chapter 5, individual layering architecture will be described as part of the fabrication results. Then, smooth muscle cells were cultured on these fabricated patterns to study cell adhesion and alignment.

4.2.4 Monolayer Cell Culture

To investigate the cell behavior in a specific *in vitro* cell culture system,

monolayer cell culture was applied in the experiments. All cells cultured to test the designed cell culture scaffolds were rat aortic smooth muscle cells (RASM cells). RPMI 1640 complete cell culture medium contains 10% Fetal Bovine Serum (FBS) and 1% 100X antibiotic/antimycotic (ABAM) was used in all experiments.

Cell culture scaffolds were sterilized in ethanol or 1X ABAM solution for 2 hours before transfer to cell culture dishes containing RPMI 1640 complete cell culture medium. RASMCs were seeded into six-well dishes, at approximately 6×10^4 cells/ml with 2.5 ml of total media volume per well and one group of microstructured polyelectrolyte thin film patterns on a piece of glass substrate within each individual well. After cell passage, culture dishes holding scaffolds with cells were placed in a CO₂ incubator, set at 37 °C, containing 5% CO₂ and 95% air. RPMI 1640 complete cell culture media was changed every other day over the course of the culture. Cell behavior was observed and images of cell cultures were taken with the epifluorescence microscope (Nikon ECLIPSE TS100-F) and the digital camera (Nikon COOLPIX 995) connected to the microscope for a period of up to two weeks for each culture system.

4.2.5 Cell Staining

Hoechst 33342: After two to four days in culture, RPMI medium was removed from the culture dishes and RASM cells were subjected to two five-minute washes in PBS. After washing, cells were subsequently treated with a 1:1000 Hoechst 33242 stock solution in PBS for 20 minutes at 37°C in the dark and a 1:500 dilution of propidium iodide stock solution in PBS for 10 minutes at 37°C in the dark. After staining, cells were rinsed with PBS, inverted into separate culture dishes and viewed using an inverted epifluorescent microscope.

Phalloidin: RASM cells were fixed in 4% paraformaldehyde in PBS for 20 minutes for phalloidin staining following removal of media and a preliminary wash as stated above. Cells were subsequently subjected to a four-minute treatment of Triton-X 100 detergent for permeabilization. Staining was done for 20 minutes in the dark at 37°C with a 1:40 working solution of phalloidin stock solution in PBS. After staining, cells were rinsed with PBS, inverted into culture dishes and observed.

FM 1-43: RASM cells were stain in a 1:50 working solution of FM 1-43 stock solution in PBS for 2 minutes at 37°C in the dark and then fixed in 4% paraformaldehyde in PBS for 15 minutes following removal of media and a preliminary wash as stated above. After fixation, cells were rinsed with PBS, inverted into culture dishes and inspected.

Anti-mouse IgG: After removing RPMI medium from the culture dishes, RASM cells were rinsed with PBS and fixed with 4% paraformaldehyde in PBS for 10 minutes. Cells were subsequently treated with Triton-X 100 detergent for permeabilization, 8% BSA as block agent. Then, RASM cells were incubated with 10µg/ml anti-Vinculin in 1% BSA in PBS for 1 hour at room temperature and stained with a 1:100 dilution of goat anti-mouse IgG fluorescein conjugated secondary antibody in 1% BSA in PBS for 1 hour at room temperature. After the rinse step, cells were inverted into culture dishes and taken images for data analysis.

The above cell-staining techniques using individual probes can be combined, such as to stain both F-actin and nuclei of the cells. Appendix C.2. contains the detailed cell staining protocols.

4.2.6 Cell Density Counting

One general approach to measure the cell density in suspension is using 4% trypan blue solution and a hemocytometer mainly for control of seeding densities. Appendix C.3 contains a detailed protocol. Another way to count cell numbers on a specific area of engineered cell culture substrate is described below. The basic process involves collecting microscopic images and determining cell numbers by literally counting cells.

RASM cells cultured on the plain flat glass surface and on the FITC-gelatin coated surface were observed daily for 2 days using an inverted phase contrast microscope. Observations were documented using a Nikon digital camera. Cell numbers were determined manually in each optical image taken for the same area of image field.

4.2.7 Measurement of Cell Roundness and Number of Pseudopodia

The roundness of cells is defined as the ratio of cell width by cell length, as shown in Figure 4.3.

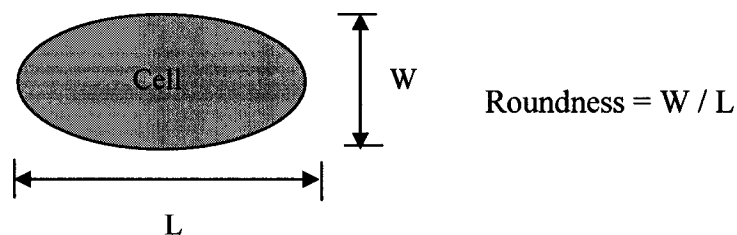


Figure 4.3 Schematic illustration of measurement of cell roundness

The roundness and number of pseudopodia were measured for the cells cultured on the PSS-, gelatin-, and fibronectin-coated polyelectrolyte thin films with different layer of underlying architectures to study the attachment of cells.

4.2.8 Statistical Analysis

A Student's t-Test was used for parameter estimation and hypothesis testing in order to draw a statistical conclusion from the cell culture experiments. If a statistical calculation result showed $P < 0.05$, then the hypothesis that there was a significant difference between the categories was considered proven correct, which indicated that smooth muscle cells preferred to grow on gelatin-coated surface compared to plain glass surface; cells had better attachment on gelatin- and fibronectin-coated surfaces than PSS-coated surfaces; cell attachment increased with increasing the number of polyelectrolyte underlying architectures.

CHAPTER 5

RESULTS AND DISCUSSION

In this chapter, the results of studies using the layer-by-layer self-assembly technique applied to the fabrication of cell culture scaffolds. The characterization of and fabricated nanofilm patterns and cell patterns are described and analyzed.

5.1 Basic Studies on Layer-by-Layer Assembled Thin Films

5.1.1 Zeta-potential and UV-Vis Measurements of Gelatin at Different pH Values

For LbL self-assembly, pH is one of the most important parameters during the fabrication, as it affects the efficiency of layering process. Therefore, it is necessary to perform the basic studies on the LbL process for any newly selected material such that appropriate assembly architectures may be defined.

5.1.1.1 Zeta-potential Measurement of Gelatin-coated Particles

The generic deposition of polyelectrolytes on micro/nanoparticles was described in the previous Material and Method section. Table 5.1 contains the zeta-potential measurement results for silica particles before and after coating with films of different outermost layers at pH 4 and pH 10.

These data demonstrate that pH significantly affects the surface potential of silica particles layered with different coating materials. Gelatin has an isoelectric point of 4.8-5.1 (Great Lakes Gelatin), resulting in varying charge polarities and densities when placed in a solution with pH different from its isoelectric point.

Table 5.1 Zeta-potentials (mV) of 400 nm silica particles at pH 4 and pH 10

Architecture of silica particles with coating material	pH=4	pH=10
Plain silica particles	-46.52	-57.71
Silica/PDDA	24.97	16.29
Silica/PDDA/Gelatin	8.25	-5.63

From the table, it is clear that the measured potentials of gelatin in pH 4 tris buffer were positive, while the potentials of gelatin in pH 10 tris buffer were negative. All of these data match expected values – the carboxylate-modified silica particles maintain negative charge, which shows slight increase with pH; the PDDA coat layer shared a decreasing positive charge as pH increases; and gelatin exhibited a reversed polarity from positive to negative as pH rose above the isoelectric point. If we know the zeta-potential of gelatin at different pH lower or higher than its isoelectric point, the layering architecture can be determined to form multilayer polyelectrolyte/gelatin thin films with positively charged PDDA or PAH when gelatin is dissolved in pH 7.4 PBS.

5.1.1.2 UV-Vis Measurement of Gelatin-coated Silica Particles

Again, one should refer to material and method section that describes the method of layering nanoparticles. According to UV-Vis spectra of gelatin solutions, the analytical wavelength is around 215 nm. Figure 5.1 contains a Beer's law plot for gelatin

at 215 nm, and Table 5.2 contains peak absorbance values (~215 nm) for gelatin solutions before and after layering silica particles with two different layering architectures. Based on Figure 5.1 and the data in Table 5.2 the adsorption of gelatin on plain silica particle and PDDA-coated silica particles at pH 4 and pH 10 was calculated, as shown in Table 5.3.

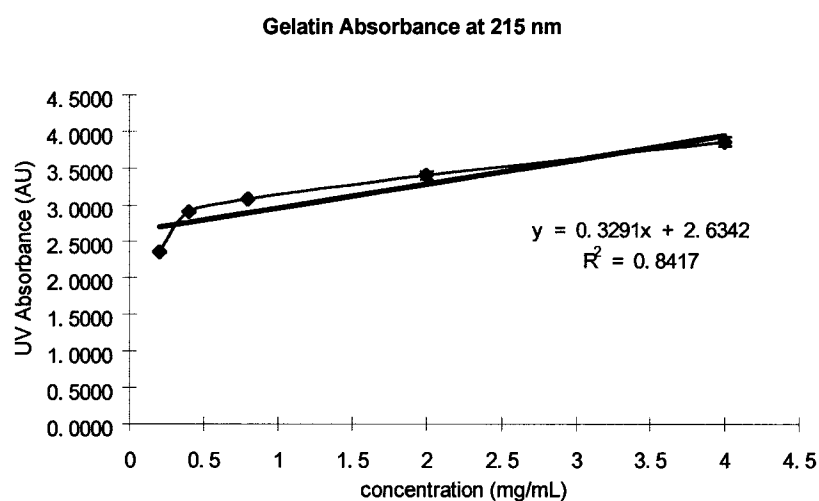


Figure 5.1 Beer's Law Plot of gelatin solution

Table 5.2 UV-Vis peak absorbance values at 215 nm for gelatin solutions

Laying Architecture	pH=4	pH=10
Original Gelatin B Solution	3.098	2.446
Gelatin solution after layering plain silica particles	2.968	2.321
Gelatin solution after layering PDDA coated silica particles	3.004	2.296

Table 5.3 Gelatin consumption by silica particles during layering process

	pH=4	pH=10
Plain silica particles	0.3951 mg/mL	0.3798 mg/mL
PDDA coated silica particles	0.2857 mg/mL	0.4558 mg/mL

The data in Table 5.2 and 5.3 directly indicate the consumption of gelatin after layering silica particles and allow estimation of mass adsorbed to surface with Beer's Law in each case. As indicated by the zeta-potential measurements, plain silica particles are negatively charged and PDDA is positively charged at pH 7.6, both exhibit the same charge polarities but some shift in charge densities at pH 4 and pH 10. The data in Table 5.3 show that more gelatin is adsorbed by plain silica particles than PDDA-coated particles at pH 4. Conversely, more gelatin is adsorbed by PDDA-coated particles than plain silica particles at pH 10. It can be understood from these data that gelatin is positively charged at pH 4 and negatively charged at pH 10, which agrees with the isoelectric point of gelatin as given by the manufacturer and the above zeta-potential measurements. Furthermore, it can also be inferred that there exists an additional attractive force of significant magnitude between gelatin and other materials since gelatin is adsorbed on both positively and negatively charged particles. Thus, spontaneous adsorption of gelatin despite electrostatic repulsion was observed from the UV-Vis spectra of original gelatin solutions compared to gelatin solutions after layering the silica particles at pH 4 and pH 10.

These data demonstrate the adsorption of gelatin on silica particles during the suspension process, regardless of surface charge and pH. However, appropriate layering order would be selected for a better deposition efficiency to form multilayer polyelectrolyte/gelatin thin films according to the pH of gelatin solution.

5.1.2 QCM, Fluorescence Spectra, and Zeta-potential Measurements of FITC-gelatin

FITC, a fluorescent dye with pH sensitive properties, was used to allow ease of

visualization of the gelatin in nanofilms. FITC also served as a model for other fluorescent probes, which can be conjugated to polyions or proteins assembled into multilayer films to be used as *in situ* indicators. Thus, a fluorescent tag may provide a label for analyzing structures as well as a probe for future sensing of cell culture conditions in an *in vitro* microenvironment. QCM, zeta-potential, and fluorescence spectroscopy measurements were performed after labeling gelatin with FITC to study the charge properties of the FITC-gelatin conjugate.

The main purpose to measure the properties of FITC-gelatin is to investigate if there is any difference between plain gelatin and conjugated FITC-gelatin and if they can be used interchangeably. It is expected that either of them may be used in the fabrication of cell culture scaffolds without any change for the chemistry properties of the engineered scaffolds, so, it will be facilitated for the inspection of fabrication result via different measuring instruments.

5.1.2.1 QCM Measurement of FITC-gelatin

The QCM measurements are shown in Figure 5.2. It was evident that FITC-gelatin could be alternately adsorbed onto the electrode with PDDA, as shown in Figure 5.2 (a). This result was anticipated, as the amine-labeling process was expected to reduce the number of positively-charged residues available on the protein. In contrast, FITC-gelatin could not be efficiently deposited and form multiplayer films with PSS when it was dissolved in pH 6.1 DI water, as shown in Figure 5.2 (b). It is known that PDDA, a strong polyelectrolyte, is always positively charged regardless of pH while PSS, which has isoelectric point of 1, is highly negatively charged in DI water. Thus, the QCM measurements confirm that FITC-gelatin is negatively charged at pH 6.2. This is what is

expected to be as same as plain gelatin, which is negative charge when pH is higher than its isoelectric point.

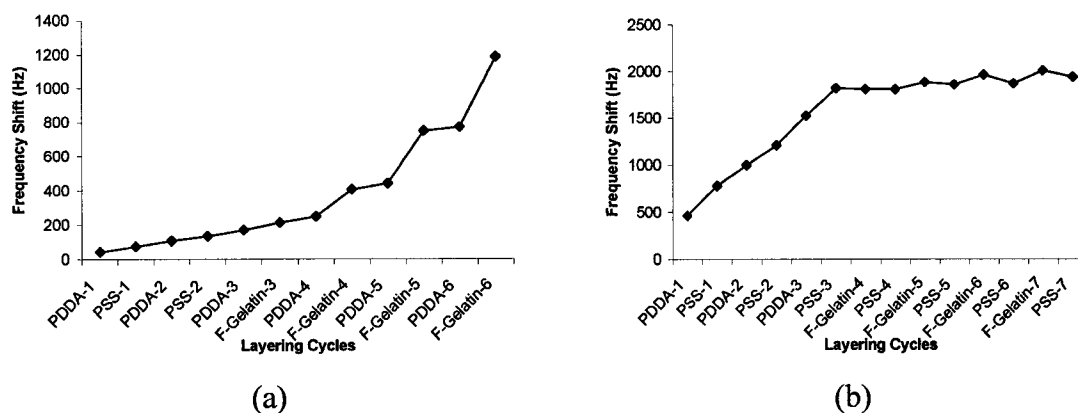


Figure 5.2 QCM Measurements with two layering architectures.

(a) (PDDA/PSS)₂/(PDDA/FITC-gelatin)₄; (b) (PDDA/PSS)₃/(FITC-gelatin/PSS)₄

It has been demonstrated by some researchers that ionic strength affects the thickness of polyelectrolyte films during the layering process [45], and the same observation can be seen here. In both methods, the precursor layering steps were taken as (PDDA/PSS)_n, and the frequency shift had an approximately linear increase. Refer to the Sauerbrey's equation in chapter 3, the thickness of the multilayer polyelectrolyte and FITC-gelatin thin films can be calculated. However, the frequency shift was about 500 Hz (~11 nm in thickness) per bilayer in method with 0.5M NaCl added, an increase of ~500% than that obtained without salt (only 100 Hz, ~2.2 nm per bilayer), which agrees with our previous results. So, adjusting the ionic strength may control the thickness of the layering films for the fabrication of cell culture scaffolds.

5.1.2.2 Fluorescence Spectra of FITC-gelatin on Silica Particles

The fluorescence spectra of 400 nm silica particles in solution shown in Figure

5.3 were collected immediately after the layering and rinsing process, which may also be referred to the experiment procedure described in chapter 4.

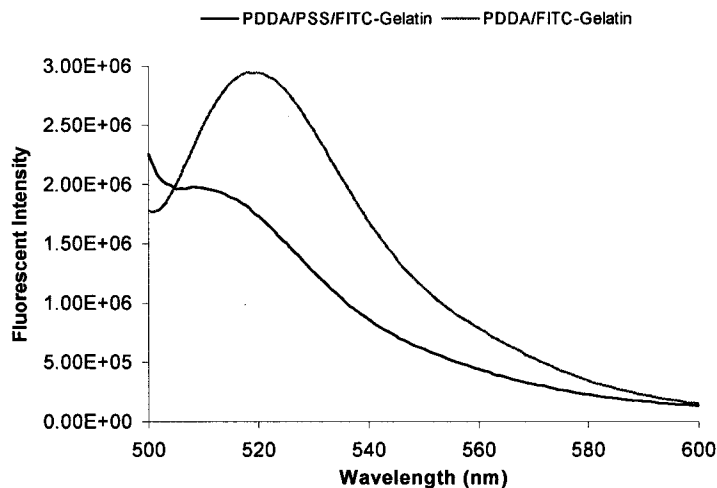


Figure 5.3 Fluorescence spectrum of gelatin-coated 400nm silica particles

In Figure 5.3, it can be observed that there is a very weak fluorescence emission peak, barely above the profile due to scattering, for silica particles layered with the order of PDDA/PSS/FITC-gelatin. In contrast, using the same concentration of particle suspension, the fluorescence emission peak of silica particles with PDDA/FITC-gelatin layering order is much stronger. It is important to note that spectra of supernatant obtained from these same samples did not show any fluorescence after thoroughly rinsed by DI water, suggesting that all fluorescence in these data does in fact arise from FITC-gelatin immobilized on particle templates. These data support the findings from QCM and zeta potential measurement experiments that FITC-gelatin is negatively charged. Thus, FITC-gelatin is more strongly attracted to adhere with positively-charged PDDA than negatively-charged PSS. However, in absence of electrostatic attraction—in fact, in the presence of repulsive forces—there remains spontaneous attractive force between

gelatin and PSS.

Again, these data also strongly suggest that it would be a better choice to alternately deposit FITC-gelatin with positive charged polyelectrolytes to form multilayer thin films during the fabrication process.

5.1.2.3 Fluorescence Spectra of FITC-gelatin on Glass Slides

The fluorescence spectra of the planar glass substrate layered with FITC-gelatin, shown in Figure 5.4, were taken after adsorbing FITC-gelatin onto the plain glass slide. There was a stronger emission peak after layering four layers of FITC-gelatin than only one layer of FITC-gelatin, as expected. The fluorescence intensity is stronger as more layers of FITC-gelatin are applied to the substrate, indicating that multilayers of FITC-gelatin film are formed on the glass substrate.

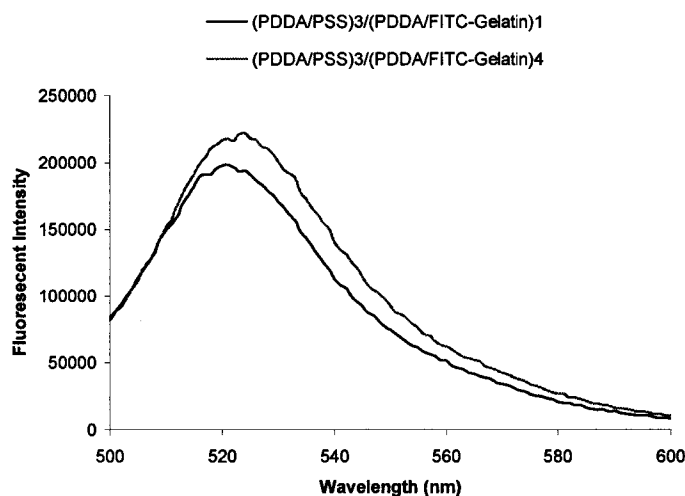


Figure 5.4 Fluorescence spectrum of flat glass substrate with layering architecture of $(\text{PDDA/PSS})_3/(\text{PDDA/FITC-Gelatin})_n$.

It is important to note that, because the layer-by-layer self-assembly process is

time consuming, it is often advantageous to limit the number of layers employed. For surface property investigations of cell culture purposes, it is likely unnecessary to apply many layers of FITC-gelatin on the surface of a planar substrate, as long as the outermost layer is uniformly assembled with FITC-gelatin. However, for 3-D patterned cell culture scaffolds, micropatterned with nanoscale vertical dimensions, the thickness of the patterns, which may affect the behavior of cells, must be considered as the surface roughness may be varied with the increasing of the thickness of the polyelectrolyte thin films.

It has been reported that by manipulating the pH or ionic strength conditions of multilayer assembly, which in turn dictate the molecular architecture of the thin films, one may direct a single multiplayer combination to be either cell adhesive or cell resistant [22]. Therefore, it is assumed that the surface roughness and the molecular architecture of gelatin multilayer films may also affect the cell attachment. The study on layering architecture of gelatin and cell attachment will be described in the later sections in this chapter.

5.1.2.4 Zeta-potential measurement of coated silica particles with FITC-gelatin

The zeta-potential measurements of FITC-gelatin are shown in Figure 5.5. From this figure, it can be observed that the surface charge changed from a positive value due to PDDA to a negative value for PSS. After assembling FITC-gelatin on the PSS coated particles, the zeta-potential was kept negative, although the value of negative potential changed slightly. UV-Vis and fluorescence measurements confirmed that FITC-gelatin remained in solution, showing that the protein was not completely consumed. The

particles were then exposed to PDDA solution, and the zeta-potential of FITC-gelatin coated particles was returned to positive. FITC-gelatin was then layered on the PDDA-coated particles, and the zeta-potential became negative again. These experiments further demonstrate that FITC-gelatin is negatively charged at pH 9, which is consistent with the results from QCM measurements and fluorescence spectra.

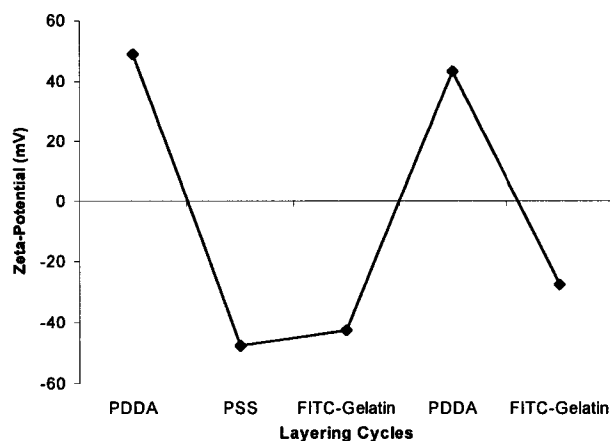


Figure 5.5 Zeta-potential measurement of silica particles with layering order of PDDA/PSS/FITC-Gelatin/PDDA/FITC-Gelatin.

Based on the measurement results of gelatin and FITC-gelatin, it can be inferred that there is no much difference of the charge property between plain gelatin and conjugated FITC-gelatin. Thus, plain gelatin and FITC-gelatin may be employed interchangeably for fabrication and inspection convenience.

5.1.3 Contact Angle Measurements of Multilayer Polyelectrolyte Thin Films

Contact angle (CA) is a quantitative measure of the wetting of a solid by a liquid. The CA is directly related to the surface energy of the materials. As noted previously, hydrophilicity/hydrophobicity is one of the important factors to be considered for cell attachment when designing an *in vitro* cell culture system. Using layer-by-layer self-

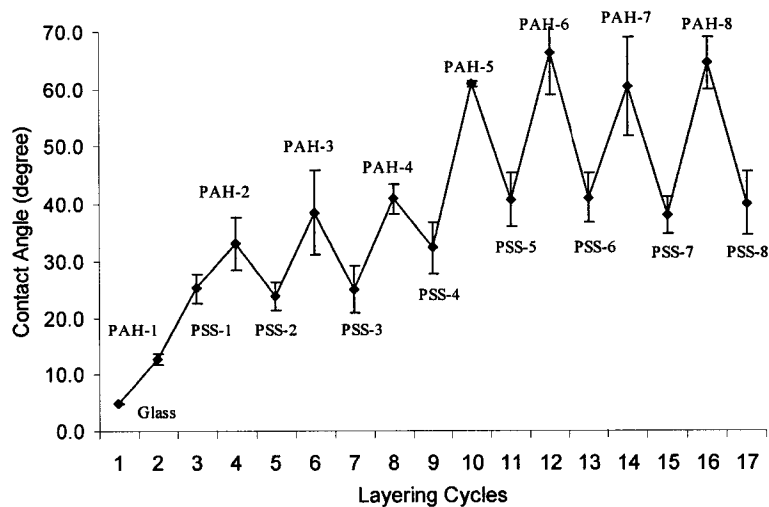
assembly technology described in above, polyelectrolytes and gelatin thin films were deposited on the planar glass substrates.

5.1.3.1 Compare Contact Angles of PAH and FITC-PAH on Glass Substrate

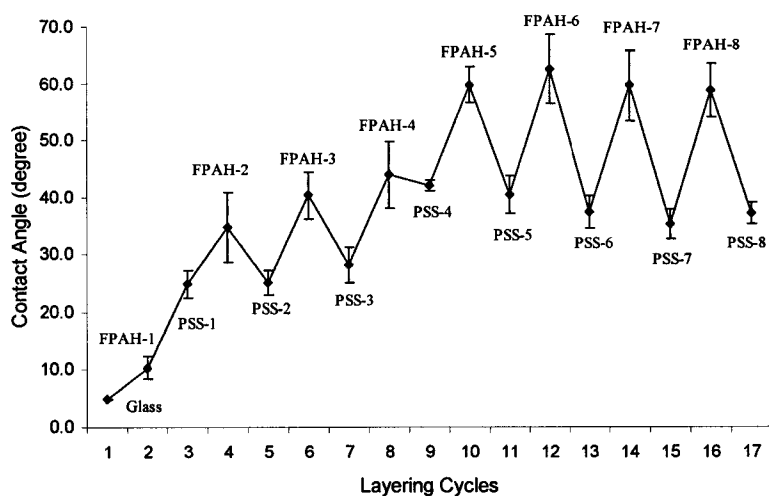
Since polymer and protein components were labeled with fluorescent dyes to assist in pattern inspection in later fabrication of three-dimensional cell culture scaffolds, it was necessary to examine if the conjugated polymer would make the surface properties different from those of original polymer molecules, as what has been done for gelatin and FITC-gelatin with zeta-potential and fluorescence spectra.

Figure 5.6 shows the contact angle measurements of (PAH/PSS)₈ and (FITC-PAH/PSS)₈ on Nanostrip pretreated glass substrates. From the two graphs in Figure 5.6, it is evident that the trends of contact angles of surface polymer films with PAH and FITC-PAH are similar when both alternately deposit with PSS. One can see that the surface hydrophilicity is affected greatly by the underlying films and bulk substrate in the first few layers. The ultrathin films do not significantly modify CA at small layer numbers. However, after several layers, the CA oscillates up and down according to the properties of the surface material, the average CA becomes relatively consistent; thus, the hydrophobicity of the outmost layer is only affected by that of the previous layers.

In comparing Figure 5.6 (a) and (b), it appears that there is little difference in CA for the polymer properties after conjugation with fluorescent dyes. It is very important for keeping the properties of surface material consistent whether or not conjugating the polyelectrolyte with fluorescent dyes as conjugated polyelectrolytes are very useful for the pattern recognition for fabrication of cell culture scaffolds



(a)



(b)

Figure 5.6 Contact angle measurements of
 (a) (PAH/PSS)₈; (b) (FITC-PAH/PSS)₈ on Nanostrip pretreated glass substrates

5.1.3.2 Contact Angles of FITC-gelatin on Glass Substrate

Gelatin is expected to have different surface properties from polymer molecules for cell attachment. The CA of gelatin-coated multilayer films was measured. As described

material and method section in chapter 4, gelatin were deposited on the planar glass substrates with a layering architecture of PDDA/(PSS/FITC-PAH)₂/(gelatin/FITC-PAH)₄/gelatin after NanoStrip pretreatment in this measurement.

Figure 5.7 contains the CA measurement results with a series of layers of polyelectrolyte thin films. The control sample surface after nanoStrip pretreatment has the smallest contact angle, with almost complete wetting. Contact angle of PSS-coated surface is around 14 to 17 for different number of layers. Contact angles of FITC-PAH coated surface range from 30 to 40 when alternately layered with PSS, which match the values obtained in the previous experiment in Figure 5.6. The CA jumped to between 40 and 50 when FITC-PAH was alternately deposited with gelatin. It is apparent that gelatin-coated surface had a larger contact angle, around 50 to 60.

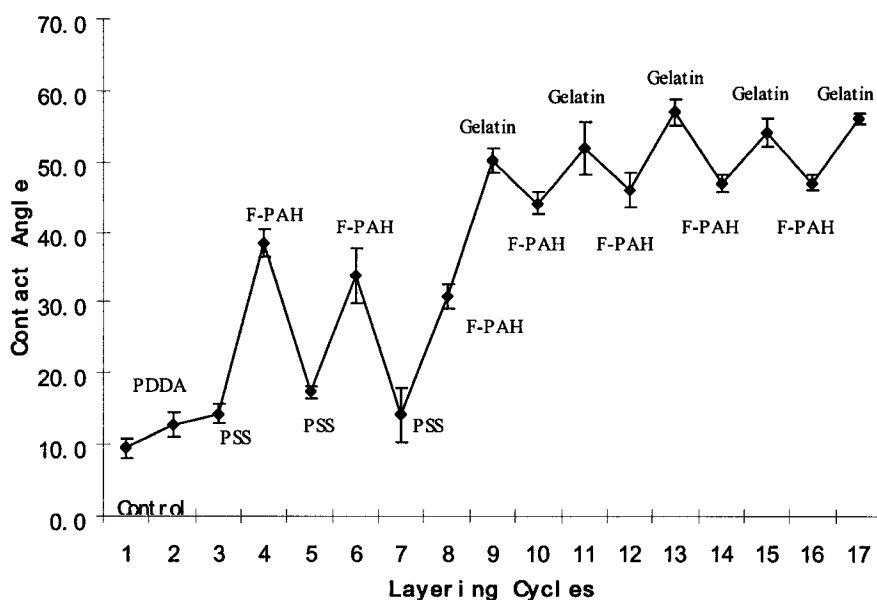


Figure 5.7 Contact angle measurement of polyelectrolyte multilayer thin films with architecture of PDDA/(PSS/FITC-PAH)₂/(gelatin/FITC-PAH)₃/gelatin on glass substrates

Although there is no known direct relationship between hydrophobicity and cytotoxicity of materials, surface hydrophobicity is critical to cell attachment and

growth. Figure 5.7 also indicates that the surface wetting property of the material on the outermost layer is affected by the underlying materials of the multilayer thin films. It can be seen from the CA of FITC-PAH that its CA is different when layered with PSS or gelatin as its underlying film. This idea obtained from CA measurement may probably be extended to other aspects, such as surface charge polarity and density, when performing multilayer self-assembly process with different materials. However, it is necessary to be further explored in the future material studies. Meanwhile, information on the surface stability of electrolyte thin films deposited with layer-by-layer self-assembly technology is also present in Figure 5.7. The contact angles of the same surface polyelectrolyte film with different number of deposition layers are very consistent. It is critical to make the surface properties standard when studying cell responses to various biomaterials used in engineered cell culture systems.

5.1.3.3 Contact Angles of Polyelectrolyte Thin Films on PMMA Substrates

As mentioned above, the properties of underlying bulk substrates may affect the surface hydrophobicity of the polymer thin films greatly. Plain glass substrates are highly hydrophilic after acid treatment, but plain PMMA substrates are generally hydrophobic in nature. Figure 5.8 contains contact angle measurements of multilayer polyelectrolyte thin films on PMMA plain substrate.

This figure proves the previous findings by contact angle measurements of multilayer polyelectrolyte thin films on glass substrate that the surface hydrophobicity of the first a few layers of polymer thin films is largely influenced by the properties of both bulk substrate and the polymer material itself. More layers of the polyelectrolyte thin

films, the more consistency of the surface properties to the nature of the deposited polymer material.

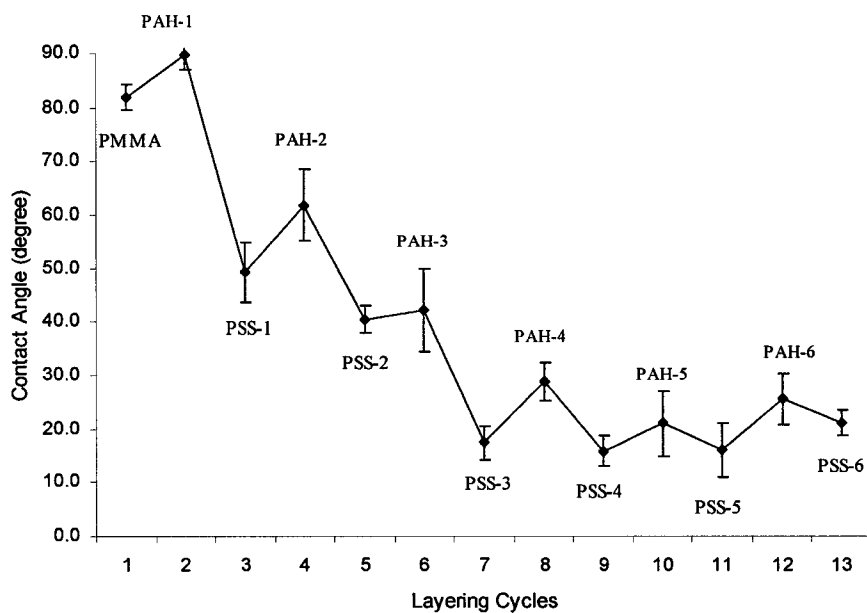


Figure 5.8 Contact angle measurement of (PAH/PSS)₆ on plain PMMA substrate

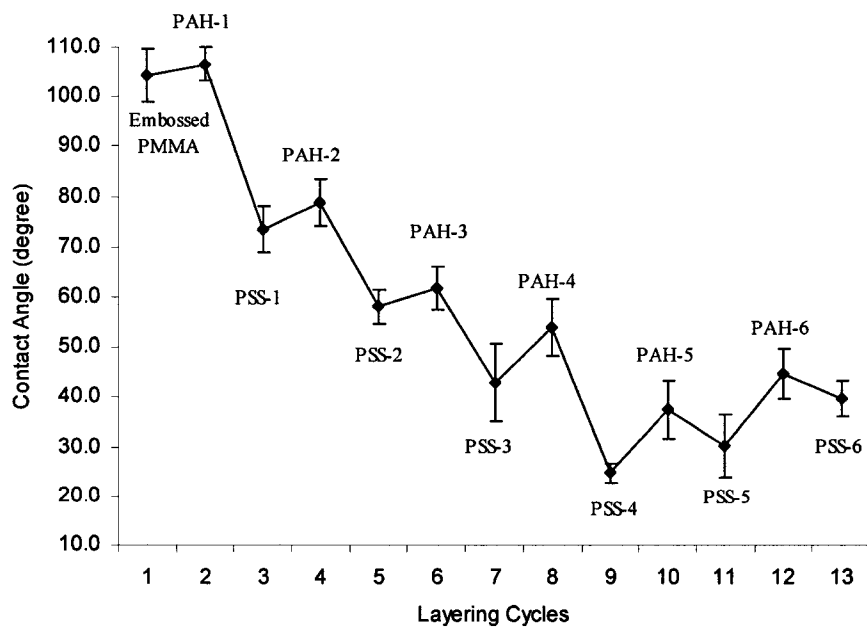


Figure 5.9 Contact angle measurement of (PAH/PSS)₆ on hot-embossed PMMA substrate

It was also found that the final contact angles of polymer thin films were determined by the initial contact angle of base substrate. Figure 5.9 contains the contact angle of multilayer of (PAH/PSS)₆ on hot-embossed PMMA substrate. Compare Figure 5.9 to Figure 5.8, it can be seen that these two figures have the similar trends of contact angles, while the amplitudes of contact angles on hot-embossed PMMA substrate are approximately 20 degree larger than those on plain PMMA substrate due to the difference of initial natures of bulk PMMA and hot-embossed PMMA substrates.

5.1.4 QCM Measurement of Fibronectin

Although it is known that every protein has an isoelectric point, the isoelectric point of fibronectin was not found during a careful search of the literature and consultation with vendors. QCM measurements were performed to study the charge property of fibronectin, using a similar procedure as for gelatin.

Figure 5.10 shows QCM measurement of fibronectin with an architecture of (PDDA/PSS)₃/(PDDA/FN)₃/PDDA/(PSS/FN)₆ at pH 7.7 using a generic layering procedure. In this layering process, the QCM silver electrode was incubated in polymer solution for 10 minutes and fibronectin solution for 20 minutes for each individual layer. In this figure, it seems that fibronectin can be alternately deposited with PSS instead of PDDA, but the increase of frequency shift is too small to be believable as LbL process compared to previous QCM measurements of PDDA and FITC-gelatin. Although QCM measurements were repeated several times at different pH, as low as 5.76 and 2.0, a satisfactory increment in mass deposition either with PSS or PDDA was not achieved.

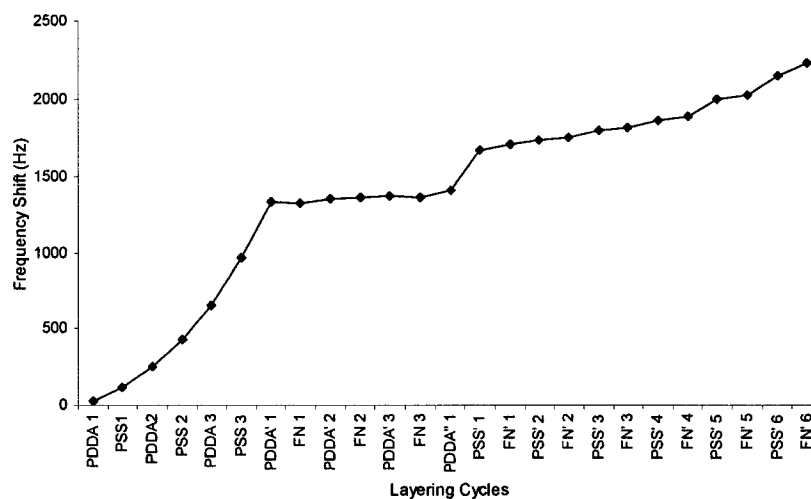


Figure 5.10 QCM measurements of $(\text{PDDA}/\text{PSS})_3/(\text{PDDA}/\text{FN})_3/\text{PDDA}/(\text{PSS}/\text{FN})_6$ at pH 7.7

It was then considered that the adsorption saturation time of deposition from protein solution may be much longer than that for polymer solution. Therefore, an additional QCM measurement was performed, wherein the silver electrode was incubated in fibronectin solution overnight (around 10-12 hours) for each layer.

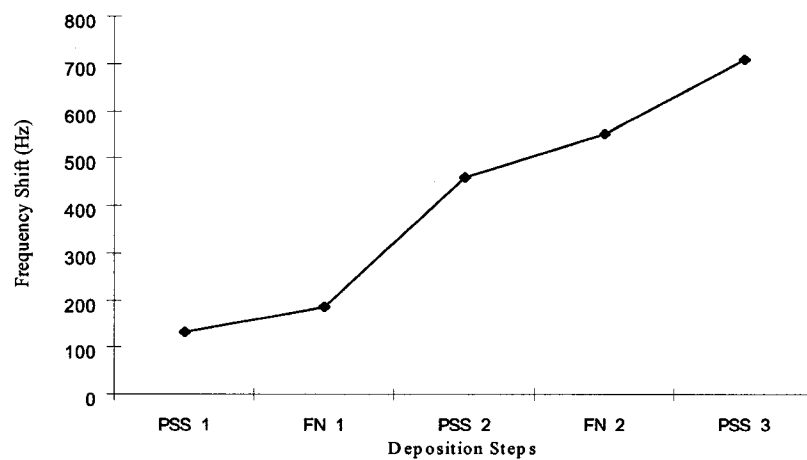


Figure 5.11 QCM measurement of $(\text{PSS}/\text{FN})_2/\text{PSS}$ at pH 5.76 for overnight incubation for each layer

Figure 5.11 shows the more typical increase of frequency shift, which seems to

indicate that fibronectin has been adsorbed on PSS-coated surface. However, as it is known that most proteins can self-adsorb on almost all the solid surfaces, it is hard to say whether the principal force of the adsorption between fibronectin and PSS is electrostatic or some other attractive force. Therefore, the charge polarity of fibronectin can not be sufficiently demonstrated. Meanwhile, a parallel QCM measurement was also performed to alternately incubate the electrode in fibronectin and PDDA solutions, the expected increment of frequency shift was not achieved in the deposition of PDDA layer. At this point, it is believed that it would have a better fibronectin coating on PSS-coated surface than on PDDA-coated surface.

In addition, in terms of predeposition of cell-adhesive materials, it is not acceptable to incubate the substrates overnight for each layer in LbL process due to the extended time required. Although LbL process was not proven to be applicable for fibronectin, Figure 5.11 does indicate that fibronectin can deposit on PSS-coated surface if only one layer of fibronectin is applied as the outmost layer of the fabricated substrate. This finding is sufficient to allow the contribution of scaffold production using fibronectin as the surface material to study cell attachment. As mentioned previously, the surface roughness of same material may significantly vary with different layers of underlying multilayer polyelectrolyte thin films. The surface roughness of fibronectin with different layers of underlying PAH/PSS thin films measured by atomic force microscopy (AFM) is described in the following section.

5.1.5 Atomic Force Microscopy (AFM) Scan of Polyelectrolyte and Protein Thin Films

AFM measurements were performed to investigate the surface roughness of

multilayer polyelectrolyte thin films with different architectures and different surface material component. It has been reported that the attachment, activity, and proliferation of human endothelia cells on the poly(L-lactic acid) (PLLA) membranes assembled with three or five-bilayers of PSS/chitosan with chitosan as the outermost layer are better than those with one bilayer of PSS/chitosan or the control PLLA. The cells also show morphology of an elongated shape with abundant cytoplasm [2]. Therefore, it is expected that the both surface material and surface roughness affect the behavior of smooth muscle cell in an *in vitro* cell culture systems in this work.

5.1.5.1 AFM Images of Polyelectrolyte Thin Films

AFM scans were taken for polyelectrolyte thin films deposited on nanostrip pretreated glass substrates with different bilayers of (PAH/PSS)_n, where n = 2, 5, 10 20. Figure 5.12 contains the representative AFM images of 10-bilayers of polyelectrolyte thin films with PSS as the outermost layer. These images show that the PSS-coated surface is relatively smooth with roughness values of 10-20 nm. The data in Table 5.4 also suggest that the roughness increases with increasing the number of layers of polymer thin films.

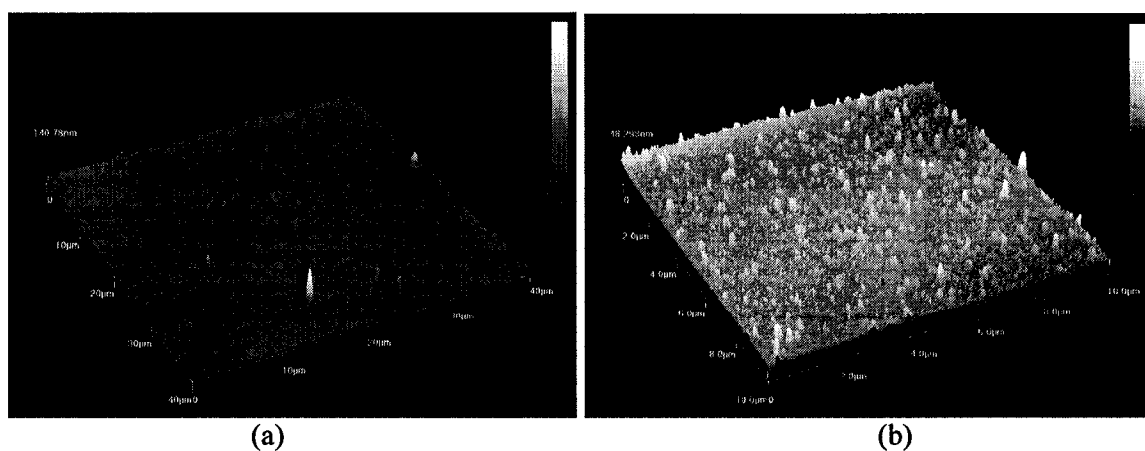


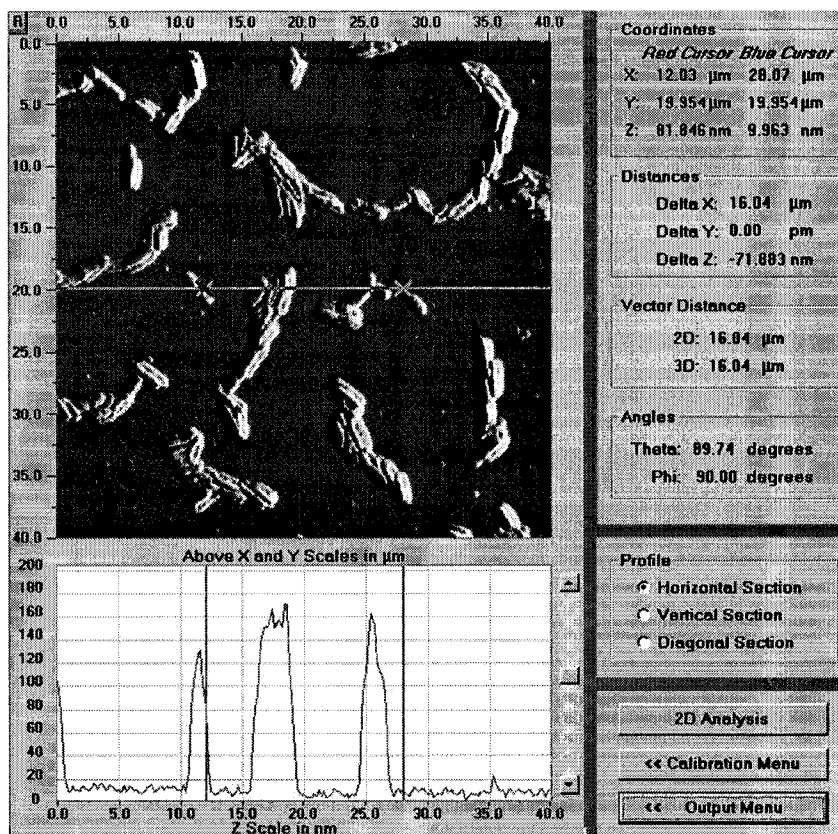
Figure 5.12 AFM images of (PAH/PSS)₁₀ on glass substrate
(a) 40 μm x 40 μm; (b) 10 μm x 10 μm

Table 5.4 Roughness of PSS-coated polyelectrolyte thin films on glass substrates.

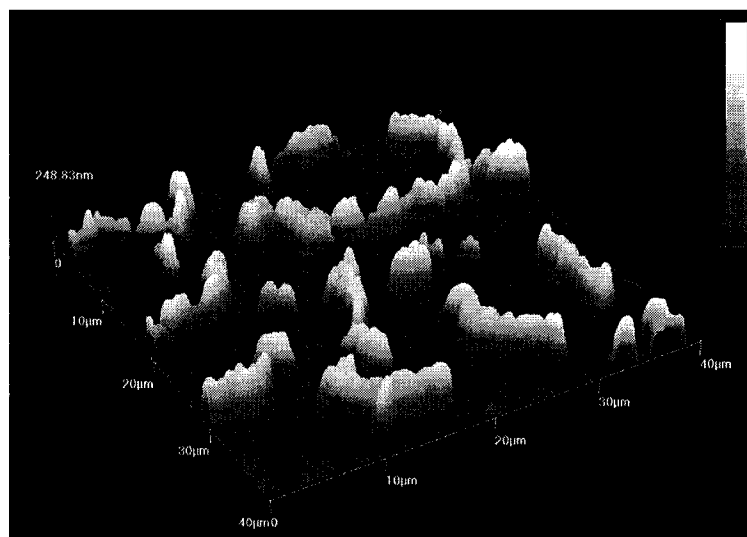
# of Bilayers	Layering Architecture	Roughness (nm)	
		Average	SD
20	(PAH/PSS) ₂₀	20.31	3.01
10	(PAH/PSS) ₁₀	13.21	0.73
5	(PAH/PSS) ₅	11.21	0.58
2	(PAH/PSS) ₂	9.64	1.69

5.1.5.2 AFM Images of Gelatin-coated Polyelectrolyte Thin Films

Based on the previous study of the charge property of gelatin, gelatin was deposited on the polymer surface using LbL technique as described in chapter 4. Figure 5.13 shows the representative 2-D and 3-D AFM images of gelatin-coated 20-bilayers of polyelectrolyte thin films, respectively. As seen in these two images, gelatin molecules did not uniformly cover the entire surface of polyelectrolyte thin films, while it is unclear why this behavior was observed, a possible explanation is the repulsive force of strong negatively charged gelatin molecule clusters. In this case, the AFM measurement of average roughness can not reflect the real surface roughness due to the non-uniform coating of gelatin. Figure 5.14 shows the AFM images of a single gelatin molecule. From these images, the size of a single adsorbed gelatin molecule was estimated at 1 μm in wide, 2 μm long, and 160 nm tall, assuming little is embedded in the underlying polyelectrolyte films.

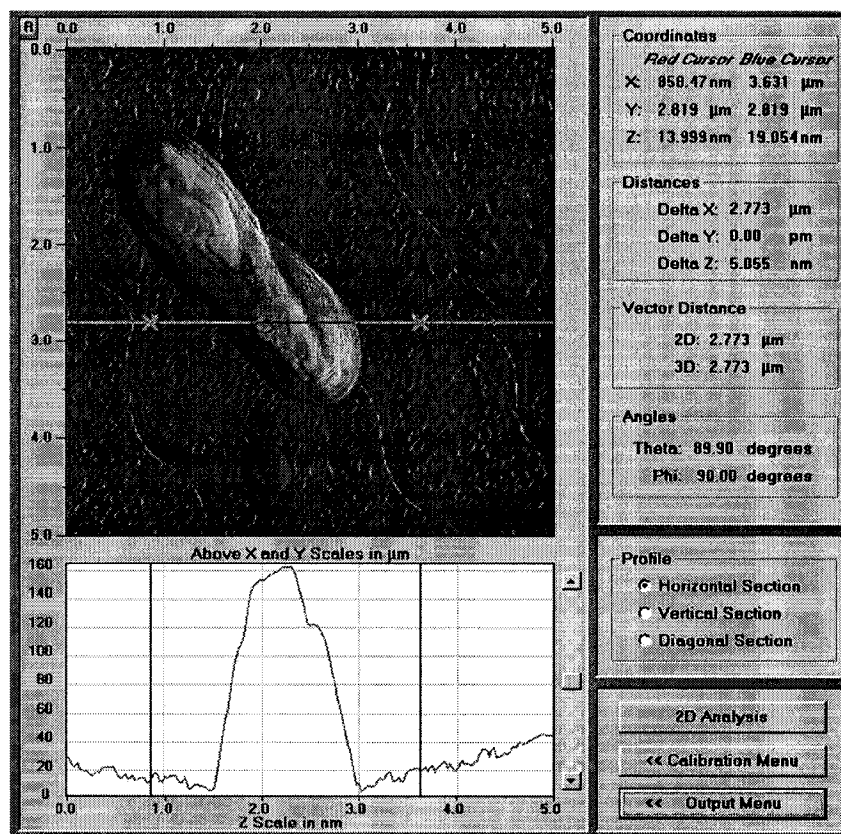


(a)

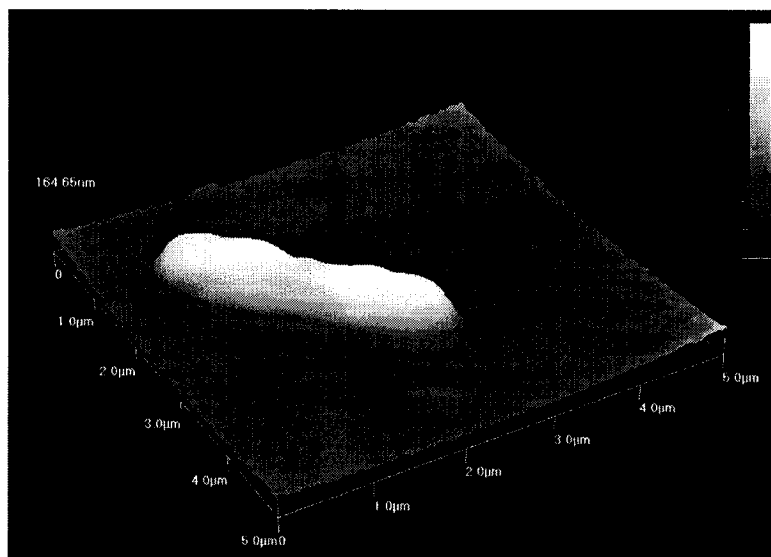


(b)

Figure 5.13 AFM image of gelatin-coated surface with a layering architecture of $(\text{PAH/PSS})_{20}/\text{PAH}/\text{gelatin}$ on nanostrip treated glass substrate. (a) 2-D; (b) 3-D.



(a)



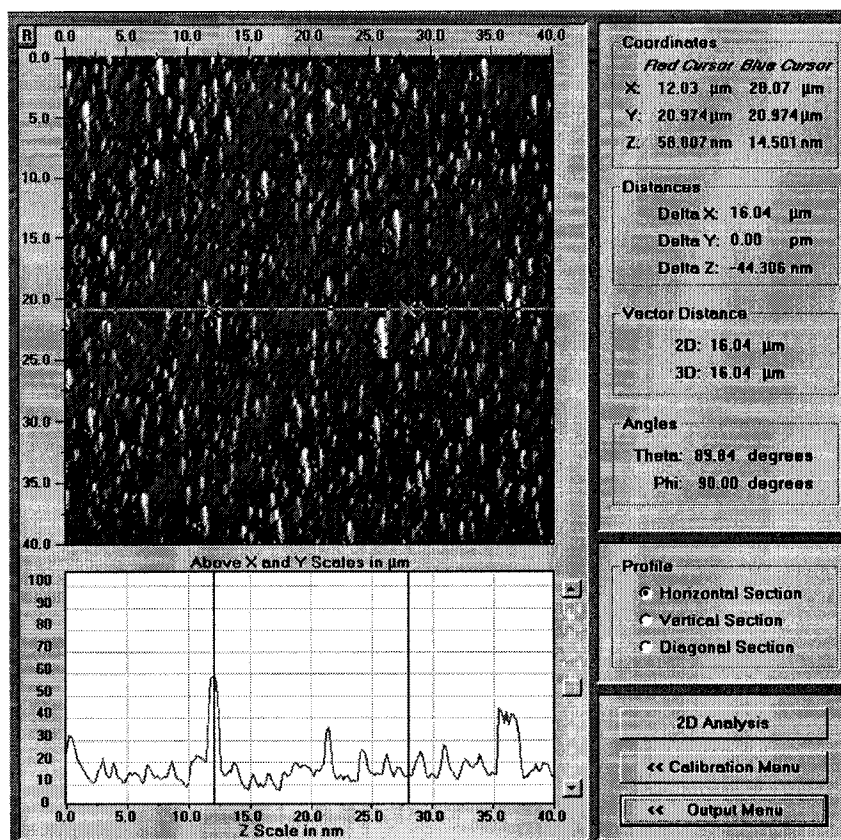
(b)

Figure 5.14 AFM image of a single gelatin molecule on the surface of 20-bilayer polyelectrolyte thin films. (a) 2-D; (b) 3-D.

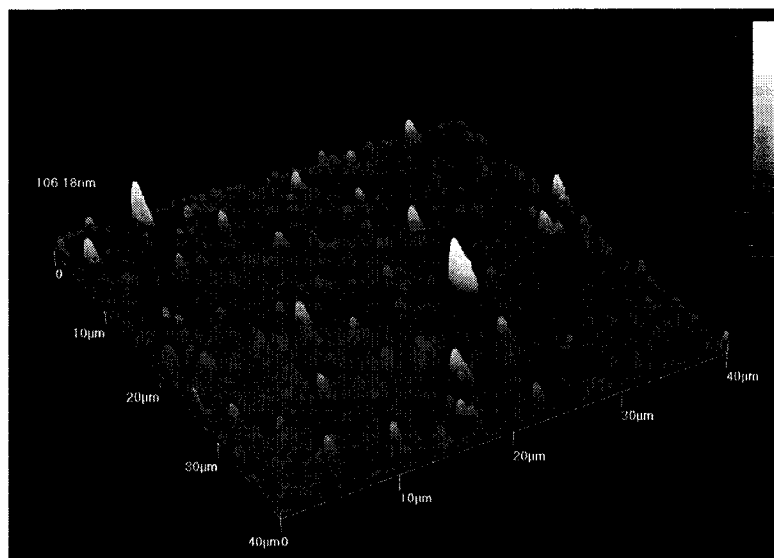
5.1.5.3 AFM Images of Fibronectin-coated Polyelectrolyte Thin Films

As shown previously, fibronectin can be adsorbed on PSS-coated surface by incubation in protein solution for overnight. Figure 5.15 contains the representative 2-D and 3-D AFM images of fibronectin-coated 5-bilayer polyelectrolyte thin films on glass substrate with $40\mu\text{m} \times 40\mu\text{m}$ scan area. These two images indicate that, unlike gelatin, fibronectin molecules cover the entire surface of the polyelectrolyte thin films. Also, similar to what was found for PSS/PAH multilayers, the roughness of fibronectin-coated surface increases with increasing of the number of bilayers of polyelectrolyte thin films (Table 5.5). Compared with the data in Table 5.4, the fibronectin-coated surface is around 30% rougher than PSS-coated surface for the same layering architecture. The roughness difference is a possible factor to affect cell response to the surface, but also the protein material, fibronectin and gelatin, may be more important for the influence of cell-material interactions

Similar to what is shown in Figure 5.14 for gelatin, Figure 5.16 shows AFM images of a single adsorbed fibronectin molecule. From these images, the size of a single fibronectin molecule was approximately estimated with $1\ \mu\text{m}$ in width, $3.5\ \mu\text{m}$ in length, and $60\ \text{nm}$ in height. AFM image of the single fibronectin molecule gives a top view how it looks like, which is essential for later inspection of fibronectin-coated polyelectrolyte patterns on the substrate after lift-off process in the fabrication of 3-D cell culture scaffolds.

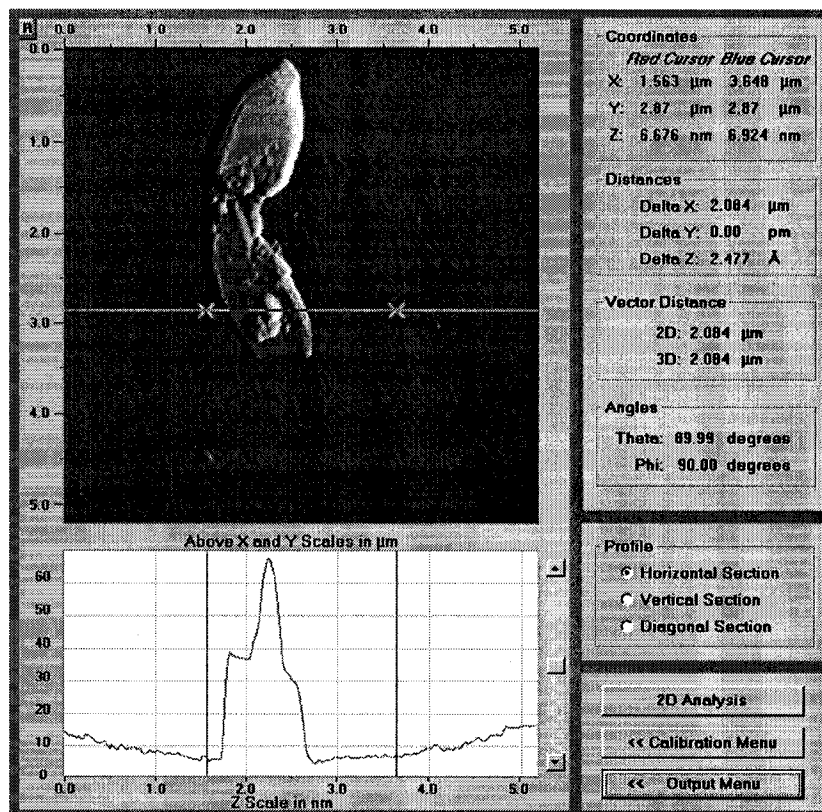


(a)

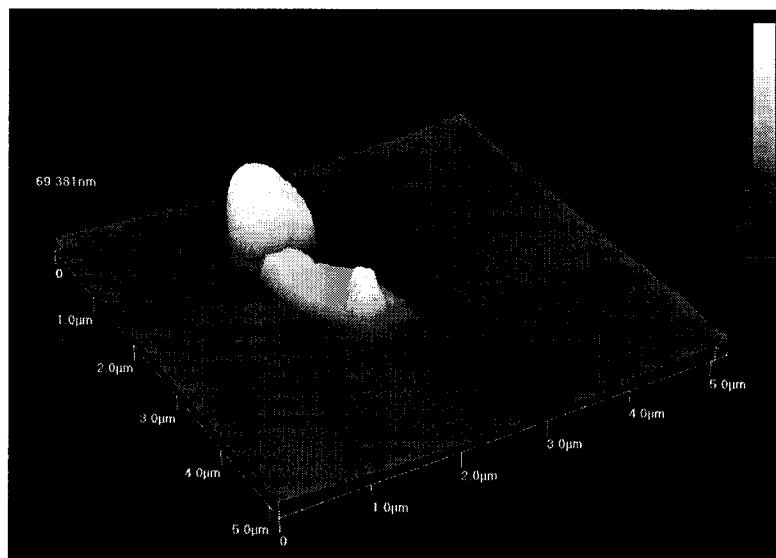


(b)

Figure 5.15 AFM image of fibronectin-coated surface with a layering architecture of $(\text{PAH/PSS})_s/\text{gelatin}$ on nanostrip treated glass substrate. (a) 2-D; (b) 3-D



(a)



(b)

Figure 5.16 AFM image of a single fibronectin molecule on the surface of 5-bilayer polyelectrolyte thin films. (a) 2-D; (b) 3-D.

Table 5.5 Roughness of fibronectin-coated polyelectrolyte thin films on glass substrates.

# of Bilayers	Layering Architecture	Roughness (nm)	
		Average	SD
20	(PAH/PSS) ₂₀ /FN	28.81	3.80
10	(PAH/PSS) ₁₀ /FN	23.80	1.54
5	(PAH/PSS) ₅ /FN	16.44	0.70
2	(PAH/PSS) ₂ /FN	13.51	2.54
1	(PAH/PSS) ₁ /FN	12.24	1.98

5.1.5.4 Comparison of the Roughness of PSS- and Fibronectin-coated Thin Films

In addition, AFM scans were taken for fibronectin-coated polyelectrolyte thin films on silicon substrate to compare the effect of bulk substrates on the surface roughness. Meanwhile, fibronectin-coated glass substrates were also incubated in fibronectin solution overnight for a second time to further investigate the adsorption properties of fibronectin. Figure 5.17 is a graph summarizing the roughness of PSS- and fibronectin-coated surfaces with different architectures.

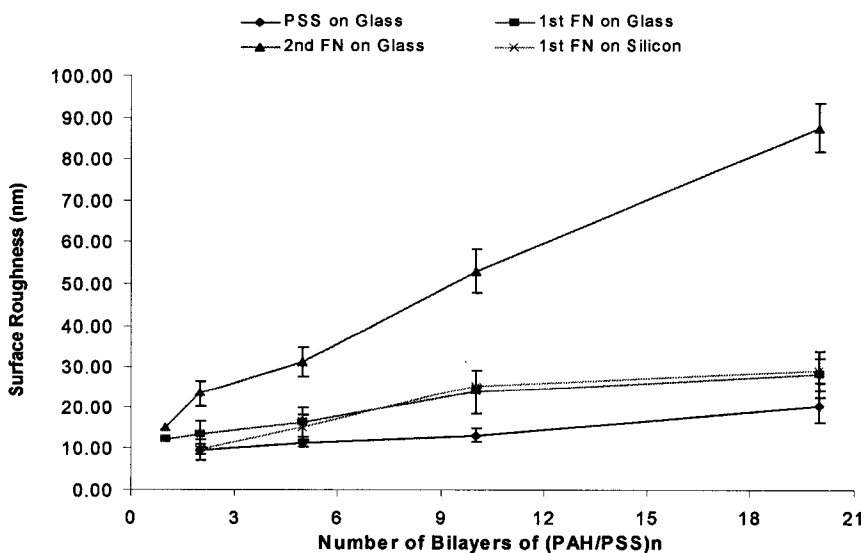


Figure 5.17 Surface roughness of PSS- and fibronectin-coated thin films

Figure 5.17 indicates the agreement of roughness of fibronectin-coated surfaces on glass substrate and silicon substrate, both show the offsets from the line of PSS-coated surfaces. For both PSS- and fibronectin-coated surfaces, the surface roughness increases as the number of bilayers of polymer thin films increases. The surfaces with second layer of fibronectin show a great increase of roughness and demonstrate the self-adsorption of fibronectin molecules.

5.2 Fabrication of Cell Culture Scaffolds

5.2.1 Fabrication of Multilayer Thin Film Patterns on Planar Base Substrates

Using LbL-LO technique, the protein/polyelectrolyte multilayer thin film patterns can be fabricated on the planar base substrate, such as glass, silicon, and PMMA. With this technique, the lateral dimension and vertical dimensions of the patterns, the layering architectures, and the surface properties of the patterns can be tightly controlled.

5.2.1.1 Polyelectrolyte and FITC-gelatin Thin Film Patterns on Glass Slides

3-D cell culture scaffolds were fabricated with LbL-LO technology in the order of (PDDA/PSS)₃/(PDDA/FITC-gelatin)₃, as shown in Figure 5.18. Before layering polyelectrolyte and FITC-gelatin films, the photoresist pattern was inspected in order to control the quality of the final FITC-gelatin patterns. Two types of patterns were designed for cell culture studies, strip patterns and square patterns, wherein the feature size ranged from 50 to 90 μm in both cases. In Figure 5.18(a), representative images of strip patterns are shown, from which it can be seen that the patterns have been faithfully

transferred from the mask to the photoresist, the prerequisite condition to obtain good polyelectrolyte and FITC-gelatin patterns after the layering process.

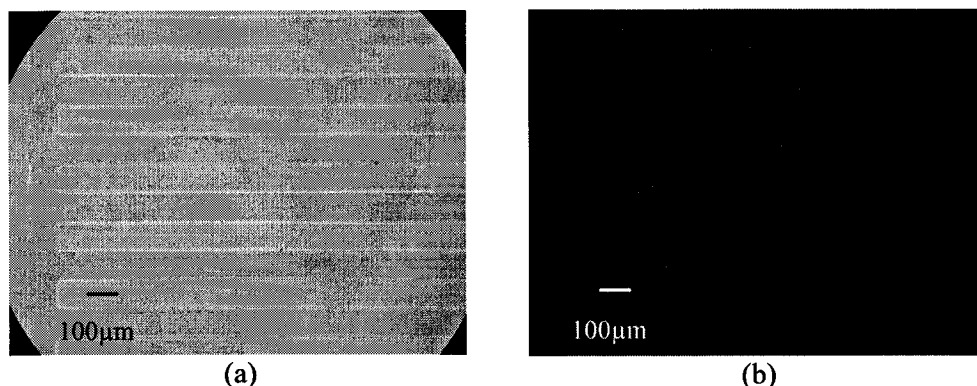


Figure 5.18 (a) Optical image of photoresist pattern before LbL; (b) Fluorescence image of FITC-gelatin pattern following the LbL-LO process

The characterization of fabrication results for protein nanofilms was facilitated by the inclusion of the fluorescent tag FITC. Figure 5.18 (b) shows fluorescence image of polyelectrolyte and FITC-gelatin patterns following the lift-off process, for which the layering architecture was $(\text{PDDA}/\text{PSS})_3/(\text{PDDA}/\text{FITC-gelatin})_3$. From the previous QCM measurements, it is estimated that the total thickness of these patterns is about 30 nm. As noted previously, the film thickness might be modulated when using PDDA and PSS solutions by adding salt, typically KCl or NaCl, to the polyion solutions. The FITC-gelatin patterns shown in Figure 5.18 (b) demonstrate the success of layering FITC-gelatin to the glass substrate and fabricating 3-D FITC-gelatin patterns on the glass substrate with LbL-LO technology.

Beside FITC-gelatin patterns, using the LbL-LO process, multiple polyelectrolyte and nanoparticle thin film patterns were also assembled on glass substrates with a variety of layering architectures and different material as the outermost layer. The main emphasis of this approach is to study the effect of architecture and surface materials on cell

behaviors. Cell culture scaffolds fabricated with different architectures and materials are shown in Figure 5.19.

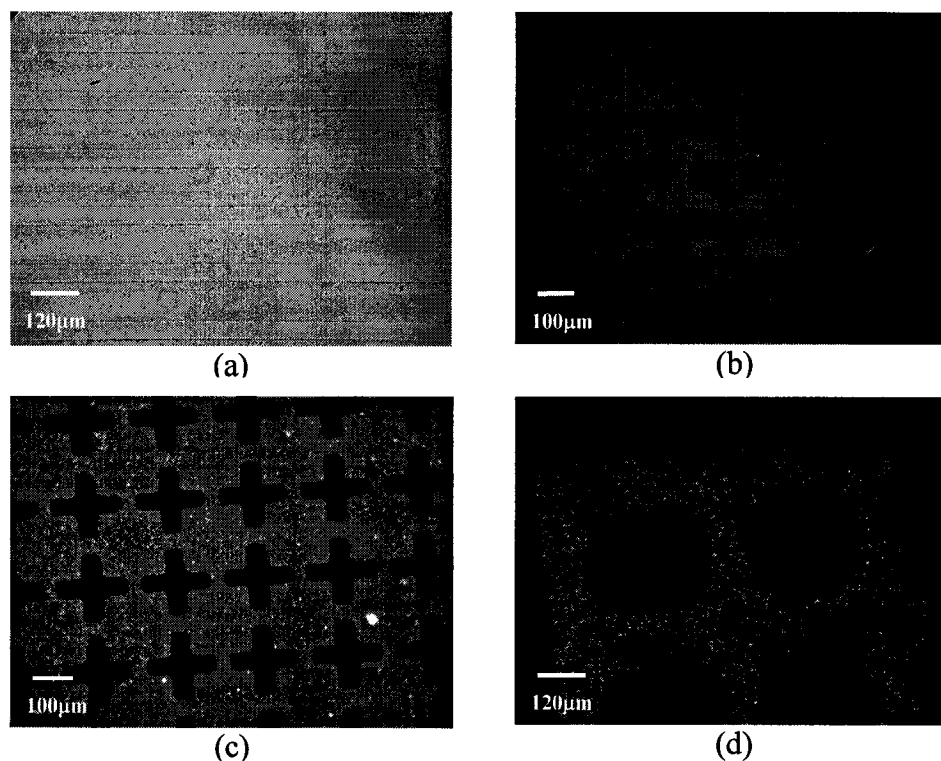


Figure 5.19 Optical and fluorescence images of polyelectrolyte, fluorescent particles and FITC-gelatin patterns on glass substrates fabricated with LbL-LO technology

- (a) Phase contrast image of polyelectrolyte channel patterns with architecture of $(\text{FITC-PAH/PSS})_2/(\text{FITC-PAH/gelatin})_3$.
- (b) Fluorescence image of FITC-Gelatin patterns with architecture of $(\text{PDDA/PSS})_3/(\text{PDDA/FITC-Gelatin})_3$.
- (c) Fluorescence image of FITC-PAH patterns with architecture of $(\text{FITC-PAH/PSS/Ru-PAH/PSS})_4/\text{PDDA}$.
- (d) Fluorescence image of fluorescent polyelectrolyte particle pattern with architecture of $(\text{PAH/PSS})_3/(\text{PAH/Particles})_3/\text{PAH}$.

Figure 5.19 (a) is a phase contrast image of gelatin thin film patterns on glass slides with layering architecture of $(\text{FITC-PAH/PSS})_2/(\text{FITC-PAH/Gelatin})_3$. For this sample, strip patterns were fabricated on the glass substrate. It is clear from the image that the polyelectrolyte film was too thin (about 30 to 50 nanometers thick) to be visible with an optical microscope in transmission and phase contrast modes; therefore, it was

necessary to couple fluorescent dyes or fluorescent particles with polyions in the fabrication process to facilitate observation of the patterned microstructures.

Figure 5.19(b) is a fluorescence image of such FITC-gelatin patterns. FITC-gelatin and polyions were deposited on the substrate in the order of (PDDA/PSS)₃/(PDDA/FITC-gelatin)₃, such that FITC-gelatin was made as the outermost layer. In this manner, cell attachments on FITC-gelatin and glass could be compared. Figure 5.19(c) is a similar fluorescence image of polyelectrolyte patterns with the architecture of (FITC-PAH/PSS/Ru-PAH/PSS)₄/PDDA. One purpose of choosing different architectures to build up these scaffolds is to investigate the possibility of layer-by-layer self-assembly with newly selected materials as layering elements. Also, choosing different materials as the outermost layer on the patterns allows study of the cell-material interaction in the *in vitro* environment.

In addition to fabricating cell culture scaffolds with polyions and gelatin, fluorescent particles were also alternately deposited with oppositely charged polyions on some of the scaffolds. Figure 5.19(d) is a fluorescence image of a nanofilm pattern with a layering architecture of (PAH/PSS)₃/(PAH/Particles)₃/PAH. In this scaffold, 20 nm negatively-charged fluorescent particles were used to assist in pattern visualization, so the overall thickness of the polyelectrolyte and particle films after the layering process was estimated to be around 100nm, larger than that of the films with conjugated polyelectrolyte and gelatin. Unlabeled PAH was designed to be the outermost layer for these particular cell culture scaffolds.

The images in Figure 5.19 demonstrate important basic features of LbL-LO technology; it is a simple and efficient approach to fabricate cell culture scaffolds coated

with patterned layers of nano-scale thickness, which has been proved by quartz crystal microbalance (QCM) measurement [21]. Using this technology, the surface properties can be modified by changing the outermost layer of patterns, which plays the main mediating role in reaction with living cells in the *in vitro* environment. With the modification of the micropatterned scaffolds, either in the topography of the structures or in the surface materials of the coating, it is possible to compare the cell behaviors on these different substrates. In addition, the successful assembly of fluorescent-labeled materials opens the door to integration of optical indicators, including fluorescent nanoparticle sensors into cell culture scaffolds. Thus, this work defines a platform process for producing micro/nanoscale structures with high vertical and lateral resolution while simultaneously controlling the composition for specific bio-material interactions and integrating opto-chemical transducers (indicators). Future studies will aim to more carefully define the limitations and relative advantages of these micro- and nano-manufacturing methods so as to develop an easy-to-use toolkit for generating customized complex biosystems.

5.2.1.2 Polyelectrolyte/gelatin Thin Film Squared Patterns on Cover Slips

A similar approach was employed to fabricate conjugated polyelectrolyte and gelatin thin films patterns on cover slip with a revised fabrication protocol. During this particular fabrication process, the main issue is to fix the cover slip on a solid support in a manner that allows it to be released at the end of the process. Standard microscopy glass slides were used as the solid supports for the fabrication of cell culture scaffolds with 3-D polyelectrolyte thin film patterns. As mentioned above, the 3-D polyelectrolyte thin film

patterns were fabricated using LbL-LO with the order of PDDA/(PSS/FITC-PAH)₂/(gelatin/FITC-PAH)₄/gelatin. The feature size of these square patterns is 50 μm x 50 μm in planar directions.

The characterization of fabrication results for these polyelectrolyte nanofilm patterns was facilitated by the inclusion of the fluorescent tag FITC. After layering process, fluorescence images were taken before and after lift-off step. In Figure 5.20, representative images of the square patterns before the lift-off step are shown with objective 10X and objective 40X lenses, respectively. From these images, both of the photoresist patterns and polyelectrolyte films adsorbed on the surface can be seen. It is clear that the patterns have been faithfully transferred from the mask to the photoresist, which is the first prerequisite to obtain good polyelectrolyte patterns after the layering process.

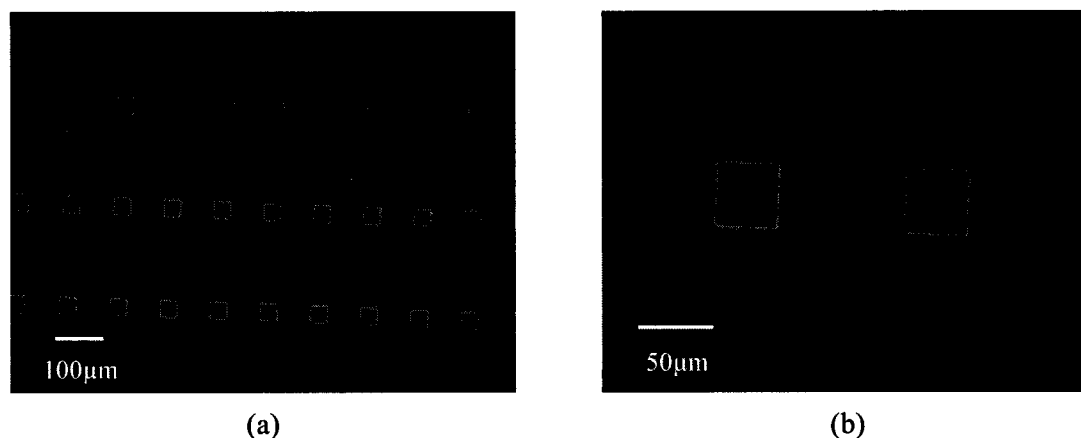


Figure 5.20 Fluorescence images of square patterns with size of 50 μm x 50 μm on glass cover slips before to lift-off step. Objectives: (a) 10X. (b) 40X

Figure 5.21 shows fluorescence images of polyelectrolyte patterns after lift-off step. The fluorescence patterns shown in Figure 5.21 demonstrate the success of layering polyelectrolyte films and fabricating 3-D polyelectrolyte patterns on the glass cover slips

with LbL-LO technology. According to the size of smooth muscle cells, it is satisfied to fabricate the square patterns with $50\mu\text{m}$ to study the cell attachment and growth on a specific area.

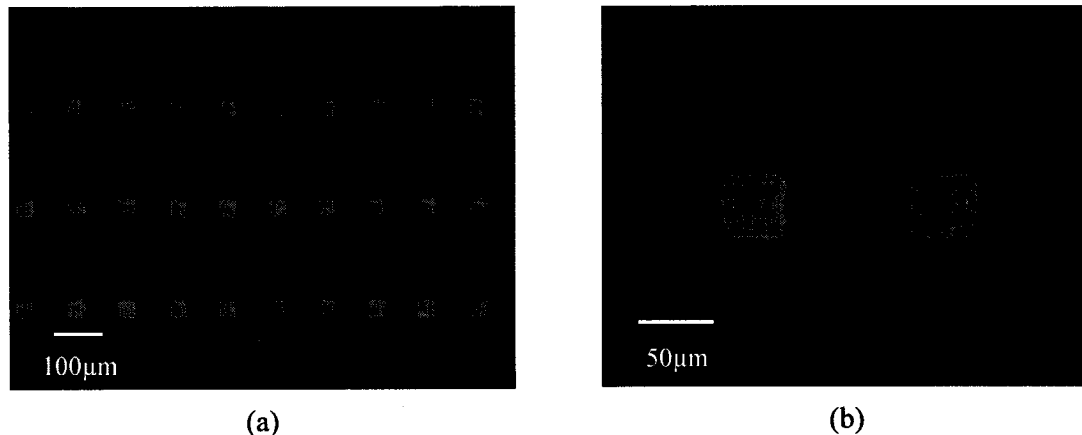


Figure 5.21 Fluorescence images of square patterns with size of $50\mu\text{m} \times 50\mu\text{m}$ on glass cover slip after lift-off step. Objectives: (a) 10X. (b) 40X

Figure 5.22 is a 3-D AFM graph showing measurements made on an edge of a gelatin-coated square pattern on PDDA-coated glass substrate. In this 3-D graph, it can be seen that the photoresist with polyelectrolyte thin films on its top was completely removed from PDDA-coated base glass substrate after lift-off, which results in the flat region on the left side of the image. It is apparently that the surface of gelatin-coated pattern is much rougher than the PDDA-coated surface. This gives an overall vision of the pattern structure at micron/submicron dimensions. However, it is also observed that the edge of the polyelectrolyte/gelatin pattern is not perfect straight as expected due to the electrostatic bond among the charged materials.

In addition, a 2-D AFM graph and image analysis is shown in Figure 5.23 for the same pattern. In this graph, similar to the 3-D graph, it can be seen that some of polyelectrolyte thin films were remaining bonded to the polyelectrolyte pattern at the

edge appearing as “flaps” or “wings” on the edges of the squares that showed otherwise be straight. This phenomenon is probably due to the strong molecular bond among the polyelectrolyte materials. The image analysis plot (bottom graph) shows the surface profile along the horizontal direction of the substrate. The thickness of the polyelectrolyte thin film pattern is 60 nm, which roughly matches the calculation from QCM measurement. As mentioned in the previous Experimental Theory section in chapter 3, the thickness of polyelectrolyte films is affected by several factors, number of layers, apparently; materials used; ionic strength of solutions, temperature etc. These factors may make the thickness varied somehow from sample to sample.

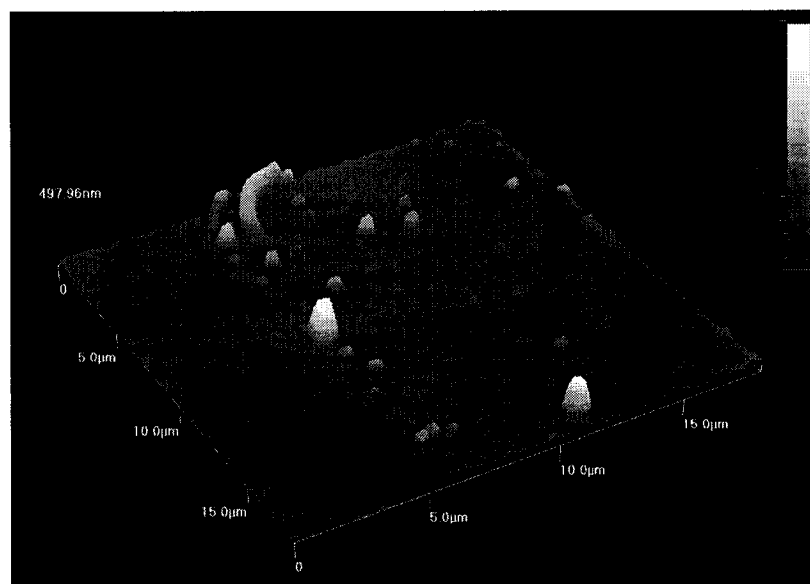


Figure 5.22 3-D AFM graph of gelatin-coated square pattern on glass substrate

Both the 2-D and 3-D AFM graphs show the relatively smooth surface of PDDA-coated base substrate and rougher surface of polyelectrolyte-patterned multilayer thin films. It also indicates that the more layers of polyelectrolyte film, the rougher surface as demonstrated by previous AFM studies on polyelectrolyte and

protein thin films. It is very helpful to know the surface topography of polyelectrolyte film patterns and analyze the possibility of fabrication techniques to design and optimize the engineered cell culture scaffolds with these technologies.

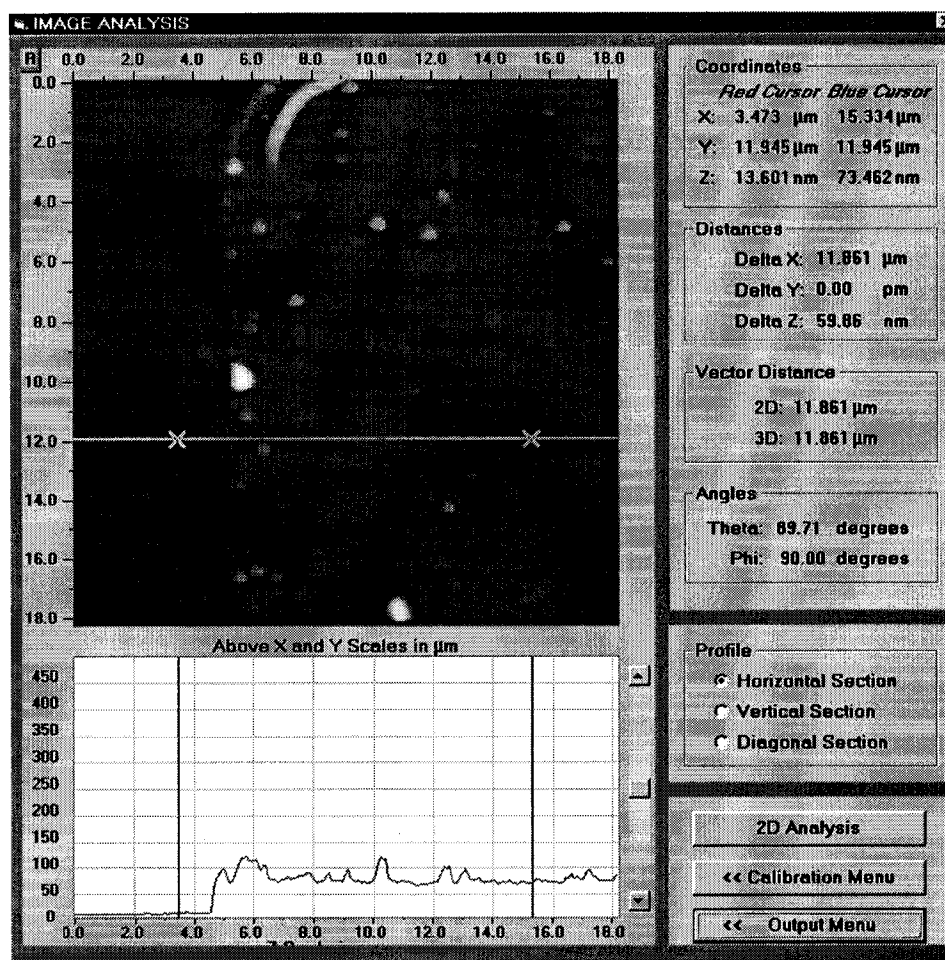


Figure 5.23 2-D AFM graph and image analysis of gelatin-coated square pattern

5.2.1.3 Polyelectrolyte/fibronectin Thin Film Patterns on Glass Slides

Based on the work presented above, it is clear that fibronectin is different from gelatin and other polyelectrolytes, and not easy to be applied to make multilayer fibronectin thin films with electrostatic layer-by-layer self-assembly due to its unknown

isoelectric point. However, the AFM study of fibronectin adsorption to thin films on planar surface described above (section 5.1.5) indicates that this molecule does self-adsorb on the surface of PSS-coated polyelectrolyte thin films. Using this fact, the LbL-LO technique was also performed to test if polyelectrolyte thin film patterns with one layer of fibronectin as the outermost surface could be achieved after lift-off process.

Figure 5.24 shows the fluorescence images of polyelectrolyte thin film patterns with one layer of fibronectin adsorbed as the outermost surface on PDDA-coated glass slide after lift-off process. The layering architecture is (FITC-PAH/PSS)₅+Fibronectin.

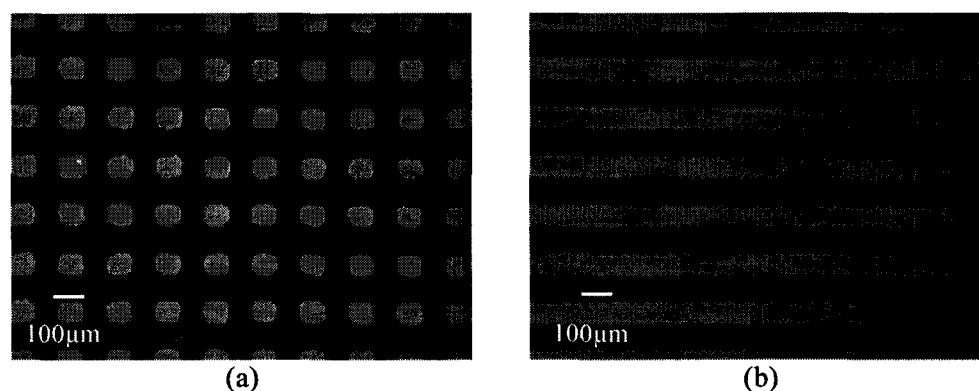


Figure 5.24 Fluorescence images of fibronectin-coated polyelectrolyte thin film
(a) Square; (b) Strip patterns following the LbL-LO process

Although these images in Figure 5.24 indicate the desired patterns can be achieved using LbL-LO technique, it was yet unknown whether the outermost fibronectin was still on the pattern surface after lift-off in acetone. At this point, AFM scans of the surface were performed to prove that fibronectin is on the pattern surface. Figure 5.25 is a 3-D AFM image, which shows the step of a fibronectin-coated pattern on the PDDA-coated glass substrate after lift-off process.

In Figure 5.25, it can be seen that the surface of fibronectin-coated pattern is much rougher than PDDA-coated glass surface, very similar to the surface of fibronectin

on planar substrate in Figure 5.15. This image seems to indicate that the material on the patterned surface is fibronectin from the point of surface roughness and surface appearance compared to the image in Figure 5.15. It is also apparent that the fibronectin on the patterned surface is shaped differently from that of fibronectin on planar glass surfaces without lift-off process. This image suggests that the lift-off process using acetone changes the conformation of fibronectin molecules adsorbed to the patterned surface. Fibronectin is most likely partially denatured in lift-off process. It is necessary to perform cell culture experiment to test if fibronectin is still functional as adhesive molecule for cell attachment even if it is denatured.

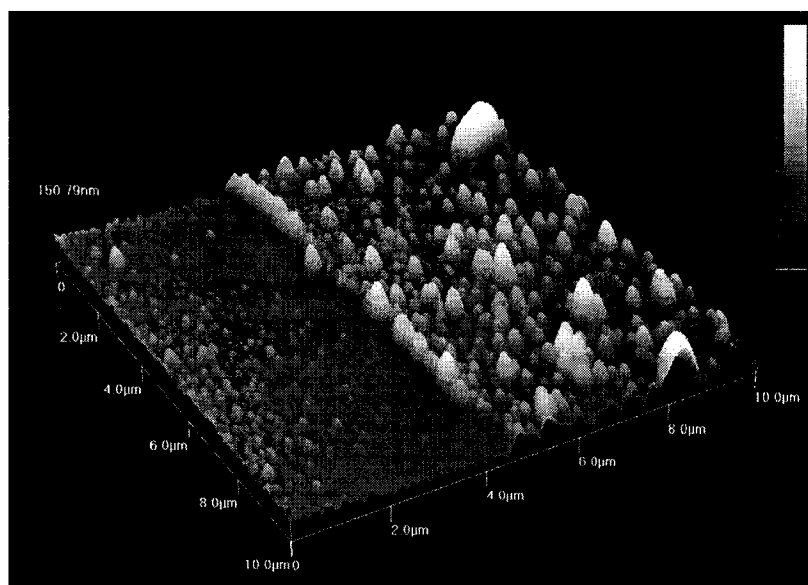


Figure 5.25 3-D AFM graph of fibronectin-coated polyelectrolyte patterns on glass substrate

5.2.1.4 Polyelectrolyte Thin Film Patterns on PMMA Substrates

The polyelectrolyte thin films could be assembled not only on nanostrip pretreated glass and silicon substrates but also on the O₂ plasma treated PMMA substrates using LbL-LO technique.

PMMA substrates were treated with O₂ plasma before LbL-LO process. Figure

5.26 contains fluorescence images of $(\text{PDDA/PSS})_2 / (\text{FITC-PLL/PSS})_2 / \text{FITC-PLL}$ on PMMA substrate. The difference from fabrication the polymer films on glass and silicon is MF319 developer instead of acetone has to be used in the lift-off process for PMMA substrate. The fabrication of polymer patterns on PMMA substrate provides an optional approach to fabricate the patterns on the optical clear substrate besides glass substrate.

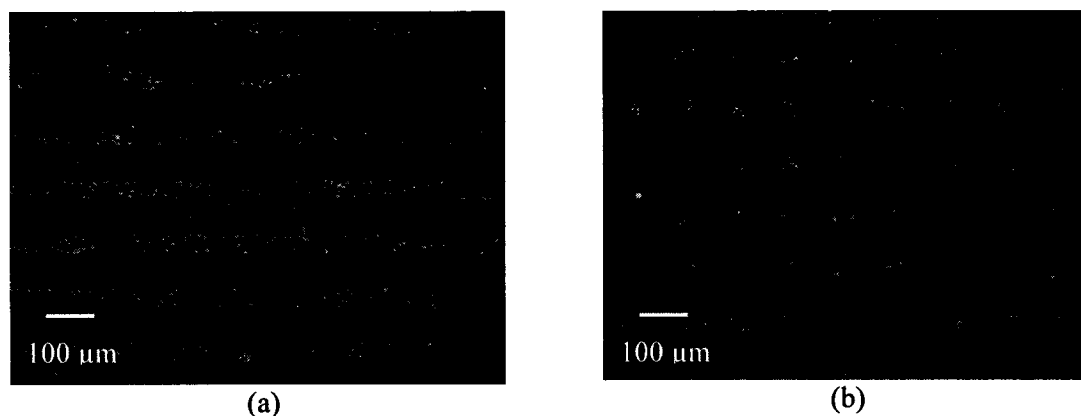


Figure 5.26 Fluorescent images of $(\text{PDDA/PSS})_2 / (\text{FITC-PLL/PSS})_2 / \text{FITC-PLL}$ patterns on PMMA substrate. (a) strip; (b) square patterns

5.2.2 Fabrication of PMMA Microchanneled Substrates

As many papers demonstrated that microchannelled PDMS substrate may control the alignment of cells, PMMA microchannels were fabricated using ICP and hot-embossing technique to investigate the cell growth on PMMA substrate. Using the generic photolithography, photoresist patterns were utilized as the mask for ICP etching on silicon substrate. Figure 5.27 contains SEM images of 100 μm silicon microchannels. It can be seen that the etched silicon bottom surface is smooth, which good for demolding in hot-embossing process. However, one may also notice the undercut at the bottom of the sidewall, which should be avoided. During the fabrication, if the undercut is too big, it may cause demolding failure.

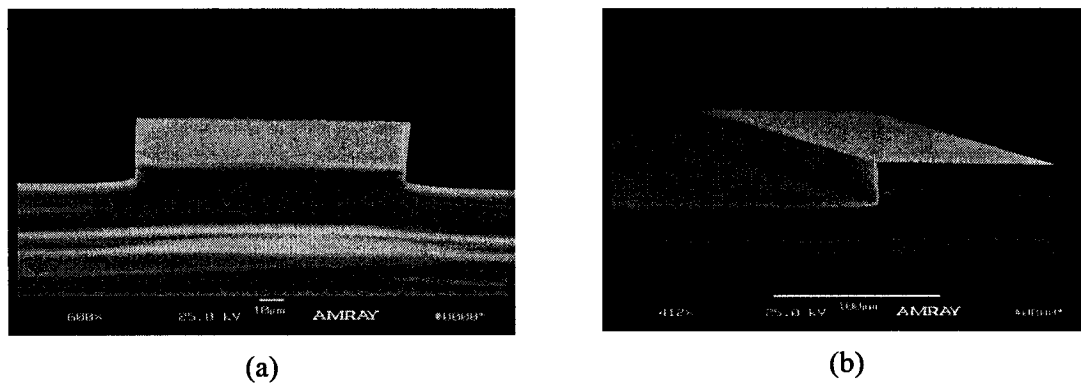


Figure 5.27 SEM images of 100 μ m channel patterns on silicon substrate

(a) front-view; (b) side-view

Figure 5.28 contains SEM images of 60 μ m channels on silicon mold and on PMMA substrates. In images of Figure 5.28 (a) and (b), less undercut is found, so the microchannel patterns are successfully transferred from silicon mold to PMMA substrates using hot-embossing technique, as shown in images of Figure 5.28 (c) and (d).

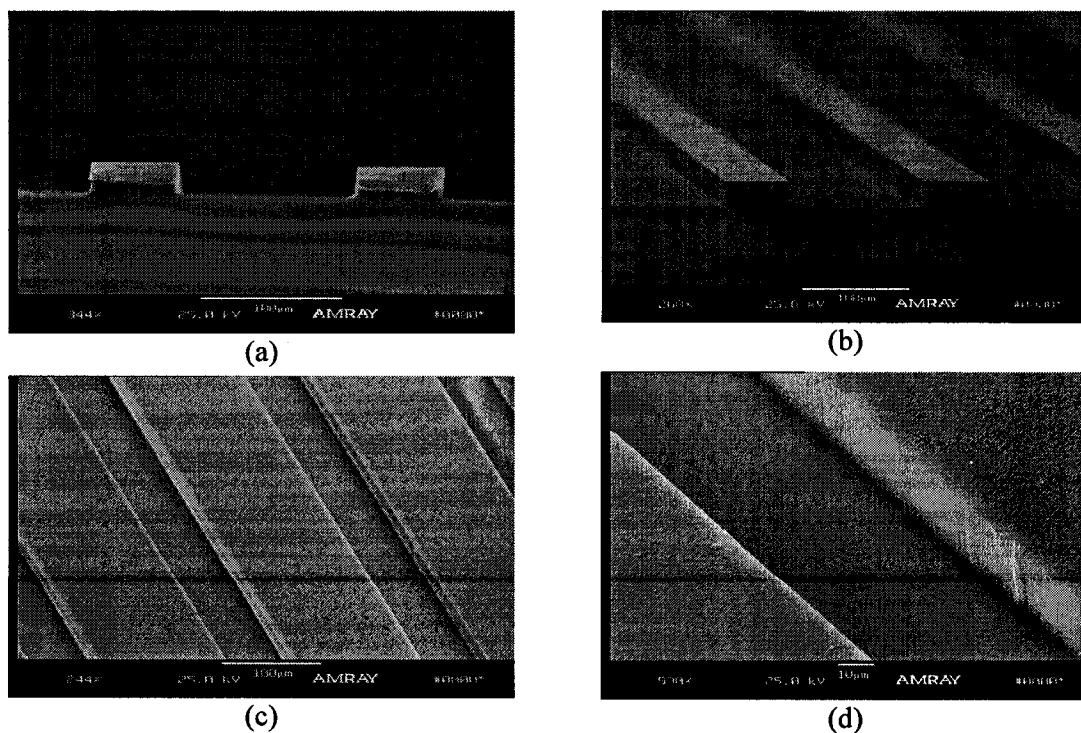


Figure 5.28 SEM images of 60 μ m channel patterns on (a, b) silicon; (c, d) PMMA

SU-8 photolithography, ICP etch, and hot-embossing provide useful tools to fabricate high aspect ratio microstructures, thus, wisely combine these microfabrication technologies with LbL self-assembly technique, almost all the desired cell culture scaffolds could be achieved.

5.2.3 Fabrication of 3-D Microfluidic Cell Culture System on Silicon Substrates

It is desirable to build up a microfluidic cell culture system with a combination of fabrication technologies to study the advanced cell-cell, cell-material, and cell-matrix interactions. Based on the previous investigation on the microfabrication and layer-by-layer self-assembly techniques, it was assumed that the multilayer polyelectrolyte thin film patterns not only can be fabricated on planar base substrate, but also can be fabricated on microstructured base substrate. With the combination of multiple micro/nanofabrication processes, including at least twice photolithography, ICP, and twice LbL self-assembly, the shapes and dimensions of the entire system can be precisely controlled.

Figure 5.29 contains two SEM images of square photoresist patterns in the channels on silicon substrate. These images show the intermediate fabrication results before LbL-LO process. As the photo resist patterns need to be made in the silicon channels rather than on the planar surfaces, it is necessary to adjust the spin speed when spin coating; otherwise, the photo resist coating may not be uniform and can not reach the bottom surface of the channel, as shown in Figure 5.29 (a). In Figure 5.29(b), photo resist is spin coated uniformly, so after development, it can be seen that resist patterns are made in the channels. Profilometer scan measurement shows the depth of the silicon channel is

around $30\mu\text{m}$, the depth of the square resist patterns is about $2\mu\text{m}$.

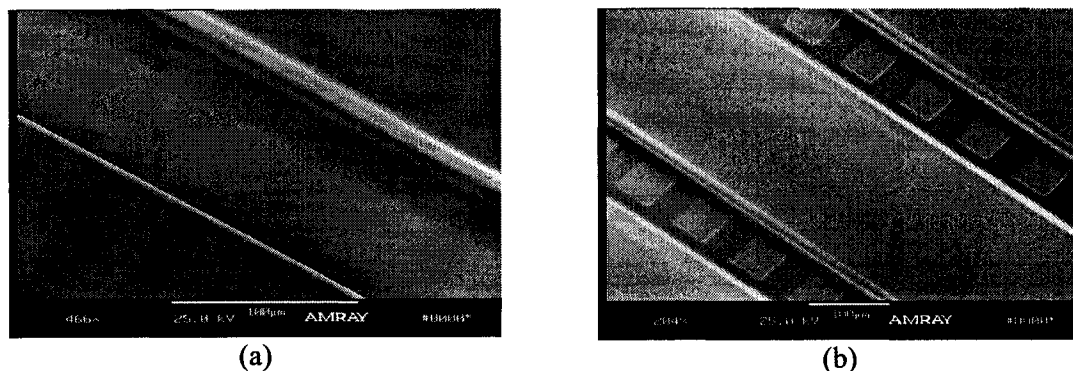


Figure 5.29 SEM images of $60\mu\text{m}$ silicon channel pattern and square PR 1813 photo resist patterns aligned in the channels with (a) non-uniform coating; (b) uniform coating

Fluorescence images in Figure 5.30 are square patterns in the channels of silicon substrate before and after lift-off step. The layering architecture of polyelectrolyte thin films is $(\text{FITC-PAH/PSS})_3$. During the LbL process, it was different from the fabrication of polymer thin films on the planar substrate. The key point of LbL is the adsorption of polyion molecules on the surface of substrate, so air bubbles in the microchannels must be removed with the assistance of a vacuum pump when incubation steps were performed.

There are several potential applications of this microfluidic cell culture system to study neuron cell growth. First, it can be used to study cell behavior individually (assume that neural cells grow on specific adhesive area with controlled alignment); second, it is designed to detect signal transduction (assume cells can grow side-by-side, physically separated, but chemically linked), thus, one would like to know how they “talk” to each other); third, control and understand injury of neural cells may probably achieved by this system in the near future.

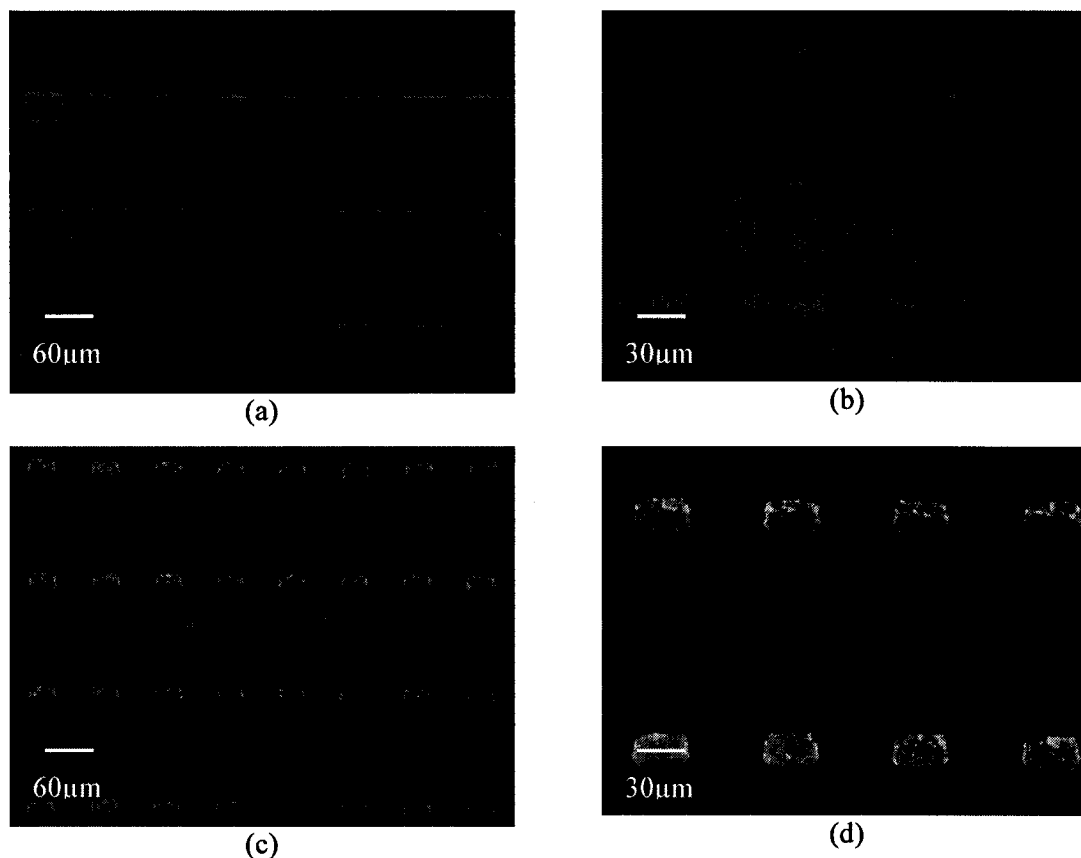


Figure 5.30 Fluorescent images of 3-D microfluidic cell culture system on silicon (a, b) before lift-off; (c, d) after lift-off

5.3 Cell Culture on Engineered Scaffolds

5.3.1 Culture RASMCs on Planar Substrates

Surface properties and underlying architectures of the scaffolds are important factors for cell landing and attachment. In this section, smooth muscle cells were cultured on the planar substrates to study the cell-material interactions.

5.3.1.1 Compare Cell Attachment on Plain Glass and FITC-gelatin-coated Surfaces

Smooth muscle cells cultured on the planar substrate surfaces of plain glass and FITC-gelatin were first compared. The architecture of FITC-gelatin deposited on the

substrate was (PDDA/PSS)₃/(PDDA/FITC-gelatin)₃. After 48 hours of cell passage, images of cells cultured on flat surfaces of plain glass and FITC-gelatin coating were collected with the same objective lens (10X) and focus depth (F4.0). Two representative optical images of cell culture are shown in Figure 5.31.

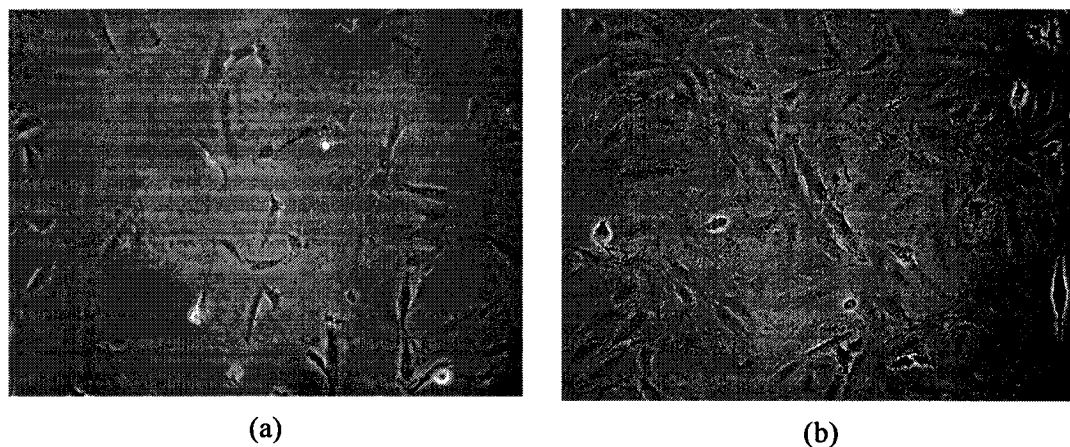


Figure 5.31 Optical images of cells cultured on a plain glass surface and FITC-Gelatin coated surfaces of glass substrates (Objective: 10X, F4.0).

(a) Cells cultured on the plain glass substrate.

(b) Cells cultured on the flat substrate with FITC-Gelatin as the outmost layer.

The image of Figure 5.31 (a) shows smooth muscle cells cultured on a plain glass substrate, while Figure 5.31 (b) is an image of cells cultured on the glass substrate with FITC-gelatin thin film coating as the outermost layer. Comparison of these two images clearly indicates that the FITC-gelatin coated surface shows greater cell attachment than the glass surface. The number of cells on FITC-gelatin coated surface is 115 ± 8.49 cells/image area, while the number of cells on plain glass surface is 52 ± 5.22 cells/image area. Statistical t-test analysis also indicates that there is a significant difference between the cell numbers on these two surfaces ($P < 0.01$). These results prove the hypothesis that cells attach preferentially to FITC-gelatin compared to plain glass.

It is observed that the quality of the phase contrast images in Figure 5.32 is not

satisfied and highly improved images are expected to be used in scientific articles, cell staining will be a useful technique for the observation of cells in culture.

5.3.1.2 Stain Cells on Control Tissue Culture Treated Dishes

As mentioned above, phase contrast images have not always turned out to be satisfied to observe and analyze the shape of cells on different material surfaces with different roughness; thus, it is necessary to stain the cells such that facilitate the study on cell morphology, cell viability, and other analysis for cells depending on the specific experimental purpose.

At first, FM 1-43 was chosen to stain the plasma membrane see the profile of cells. As shown in Figure 5.32, smooth muscle cells were cultured in 24-well cell culture plastic plate. With a combination procedure, cell membranes and nuclei were stained by FM 1-43 and Hoechst 33342.

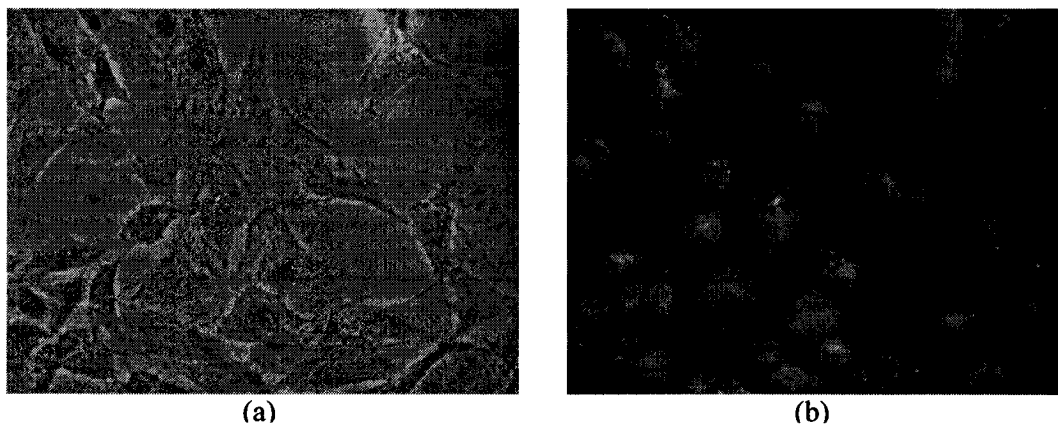


Figure 5.32 (a) Phase contrast; (b) Fluorescence image of RASMCs in 24-well cell culture plastic plates after being stained with FM 1-43 and Hoechst 33342

Figure 5.32 (b) is the fluorescence image of cells, which were stained by FM 1-43 and Hoechst 33342. From this, one can roughly see the profile of individual cells, but no

much improvement for observation than that of the phase contrast image in Figure 5.32 (a). Alexa Fluor 488 Phalloidin may be a suitable stain for studying the shape of cells, because F-actin is supposed to exist everywhere in the body of cells, especially in the pseudopodia which are important in describing the morphology of cells.

To study the focal adhesion of smooth muscle cells, anti-vinculin and goat anti-mouse IgG fluorescein secondary antibody were selected to stain vinculin in the cell membrane. Figure 5.33 shows a representative fluorescence image of smooth muscle cells, which were stained by goat anti-mouse IgG fluorescein secondary antibody and Hoechst 33342. In this image, the focal adhesions are revealed by the bright green spots. It is expected that the cell attachment on a specific surface is directly related to the number or the area of the focal adhesions.



Figure 5.33 Fluorescence images of cells in 24-well cell culture plates after being stained with goat anti-mouse IgG fluorescein secondary antibody

5.3.1.3 Investigation of Cell Morphology on Polyelectrolyte and Protein-coated Planar Surface with Different Layering Architectures

The polyelectrolyte thin film patterns were fabricated with different polyelectrolytes and proteins as the outermost surface layers, as shown in AFM images in Figure 5.12, 5.13, 5.15, and 5.17, such that the architectures of the polyelectrolyte films are identical except for the outermost layer. This fabrication was performed as an essential step toward determining the relative dependence of cell attachment on surface chemistry and underlying nanoarchitectures.

A. Cells on fibronectin-coated polyelectrolyte thin film substrates

Figure 5.34 and Figure 5.35 are fluorescence images of cells after 24 hours culture on fibronectin-coated multilayer polyelectrolyte thin films with layering architecture of (PAH/PSS) $_n$ + fibronectin ($n=1$, 1-bilayer; $n=20$, 20-bilayer). In Figure 5.34, smooth muscle cells were stained by Alexa Fluor 488 phalloidin to show F-actin in cells. The F-actin stain also facilitates visual of cell morphology to assess the dependence on the different number of underlying polyelectrolyte thin film substrates. It can be seen that cells show rounded shape on fibronectin-coated 1-bilayer polyelectrolyte thin film surface, while cells have a more spread-out elongated appearance on fibronectin-coated 20-bilayer thin film surface with more pseudopodia. Figure 5.35 shows cells stained by anti-vinculin and goat anti-mouse IgG fluorescein conjugated secondary antibody. The fluorescence images in this figure display the vinculin, contained in focal adhesions.

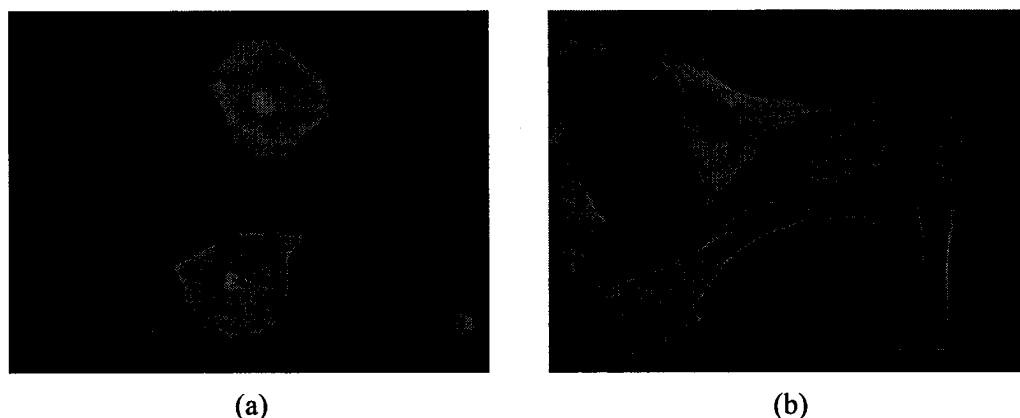


Figure 5.34 Fluorescence images of cells with Hoechst 33342 and Alexa Fluor 488 phalloidin stain cultured on fibronectin-coated multilayer polyelectrolyte thin films

(a) 1-bilayer; (b) 20-bilayer architecture



Figure 5.35 Fluorescence images of cells with Hoechst 33342 and goat anti-mouse IgG fluorescein conjugated secondary antibody stain cultured on fibronectin-coated multilayer polyelectrolyte thin films

(a) 1-bilayer; (b) 20-bilayer architecture

Cells show similar morphologies to those observed in Figure 5.34. However, it cannot be concluded from these data that more focal adhesions are on 20-bilayer films than on 1-bilayer film due to the limitation of this staining approach that too much non-specific vinculin is stained in cells around the nuclei.

Another phenomenon that should be noticed is the increasing background signal from the staining of the substrate with more layers of polyelectrolyte thin films.

In Figures 5.34 (b) and 5.35 (b), it can be seen that the 20-bilayer polymer thin films show blue color, which indicates they were stained by Hoechst 33342, while the 1-bilayer polymer thin film substrate does not show this nonspecific background stain. The possible reason for this phenomenon is much more Hoechst 33342 fluorescent molecules were absorbed by the 20-bilayer polymer films than 1-bilayer films so that the background stain was shown in 20-bilayer images. It also seems that fibronectin on 20-bilayer polymer thin film substrate can be stained by the goat anti-mouse IgG fluorescein conjugated secondary antibody, but it is not shown on the 1-bilayer polymer thin film substrate. The reason for this phenomenon needs to be further explored.

B. Cells on gelatin-coated polyelectrolyte thin film substrates

Figure 5.36 and Figure 5.37 are fluorescence images of smooth muscle cells after 12 hours culture on gelatin-coated multilayer polyelectrolyte thin films with layering architecture of (PAH/PSS) $_n$ + PAH/gelatin ($n=1$, 1-bilayer; $n=20$, 20-bilayer).

Similarly, in Figure 5.36, smooth muscle cells are stained by Alexa Fluor 488 phalloidin to show F-actin in cells, while Figure 5.37 shows cells stained by anti-vinculin and goat anti-mouse IgG fluorescein conjugated secondary antibody. It also can be seen that cells show elongated and more spread-out growth pattern on 20-bilayer thin film surface. Compared to the cells on fibronectin-coated polymer films, little difference can be seen except it appears that the “fingers” of the cells in the pseudopodia are less sharp on the gelatin-coated films than those on fibronectin-coated films by the phalloidin stained cells.

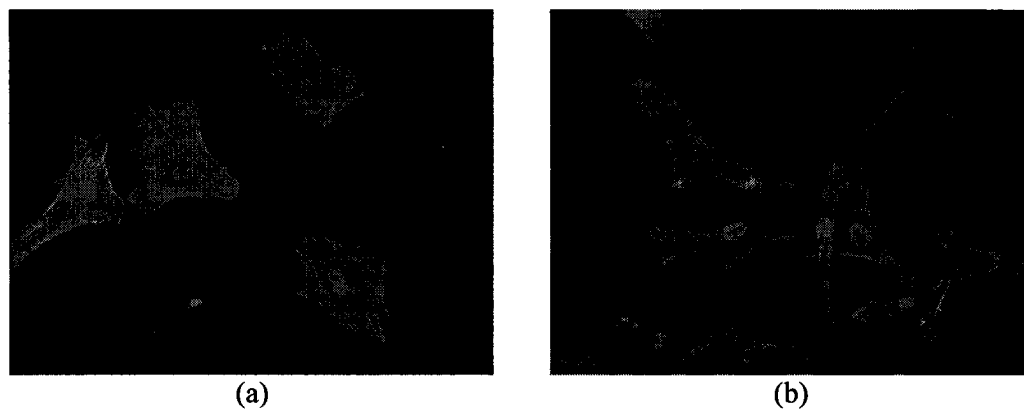


Figure 5.36 Fluorescence images of cells cultured on gelatin-coated multilayer polyelectrolyte thin films with Hoechst 33342 and Alexa Fluor 488 phalloidin stain

(a) 1-bilayer; (b) 20-bilayer architecture

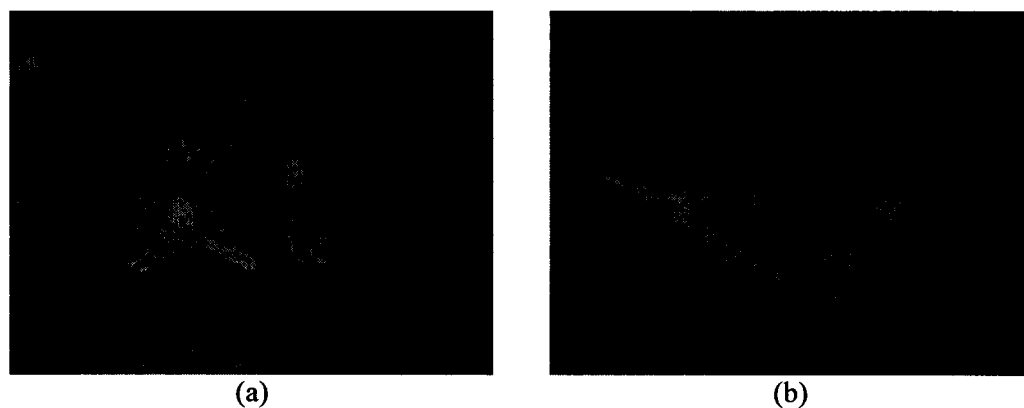


Figure 5.37 Fluorescence images of cells cultured on gelatin-coated multilayer polyelectrolyte thin films with Hoechst 33342 and goat anti-mouse IgG fluorescein conjugated secondary antibody stain

(a) 1-bilayer; (b) 20-bilayer architecture

C. Cells on PSS-coated polyelectrolyte thin film substrates

Figure 5.38 and Figure 5.39 are fluorescence images of smooth muscle cells after 36 hours culture on the multilayer polyelectrolyte thin films with layering architecture of (PAH/PSS) $_n$, ($n=1$, 1-bilayer; $n=20$, 20-bilayer). In Figure 5.38, smooth muscle cells are stained by Alexa Fluor 488 phalloidin to show F-actin in cells, while Figure 5.39 shows cells stained by anti-vinculin and goat anti-mouse IgG

fluorescein conjugated secondary antibody.

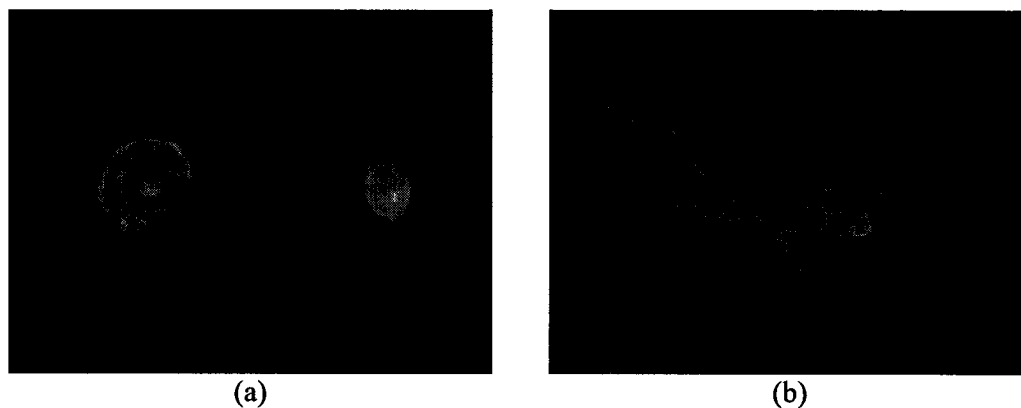


Figure 5.38 Fluorescence images of cells cultured on multilayer polyelectrolyte thin films with PSS as outermost layer with Hoechst 33342 and Alexa Fluor 488 phalloidin stain

(a) 1-bilayer; (b) 20-bilayer architecture

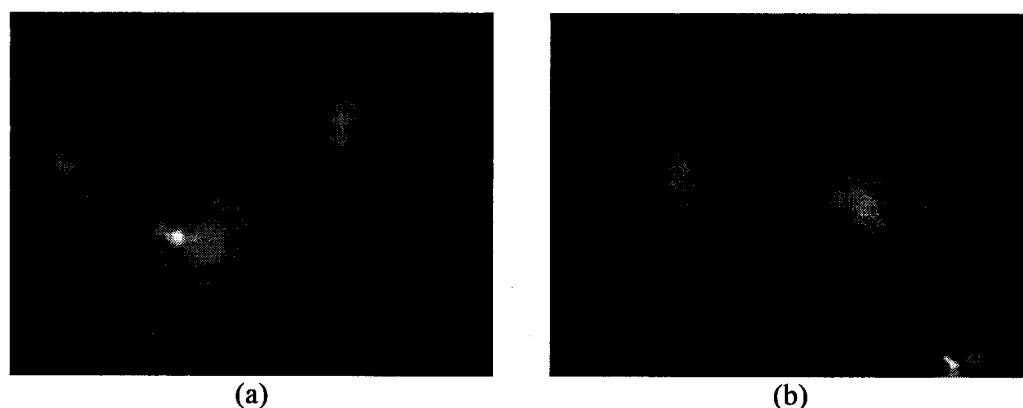


Figure 5.39 Fluorescence images of cells cultured on multilayer polyelectrolyte thin films with PSS as the outermost layer with Hoechst 33342 and goat anti-mouse IgG fluorescein conjugated secondary antibody stain

(a) 1-bilayer; (b) 20-bilayer architecture

Figure 5.38 and 5.39 show a more spread-out pattern on 20-bilayer polyelectrolyte thin film PSS surface than that on 1-bilayer PSS surface. However, the morphologies of cells are rather different from those on fibronectin and gelatin-coated surfaces with the same number of layers of underlying polymer thin films. In

Figure 5.39 (a), cells are small, like round-ball shape, obviously are not spread out. Although cells are spread out more on the 20-bilayer substrate, they still show the round shape, and exhibit fewer pseudopodia than those seen on fibronectin and gelatin-coated 20-bilayer thin film substrates.

Comparing these images of cells on 1-bilayer and 20-bilayer polymer thin films with fibronectin, gelatin, and PSS coatings as outermost surfaces, it seems that both fibronectin and gelatin have better adhesion for the attachment of smooth muscle cells than PSS coating surface. Furthermore, with the same outermost surface material, 20-bilayer polymer films are better for cell spread out than 1-bilayer film substrate. Smooth muscle cells were also cultured on 2-bilayer, 5-bilayer, and 10-bilayer polymer films with fibronectin, gelatin, and PSS coatings. Little difference was observed for the cell morphologies on 2-bilayer and 1-bilayer films, and those on 10-bilayer and 20-bilayer films. Based on the data collected, 10-bilayer films may be the critical architecture for a better attachment and further growth of smooth muscle cells from the aspect of qualitatively analysis.

Figure 5.40 and Figure 5.41 show the measurements of the roundness and number of pseudopodia of smooth muscle cells on PSS-, fibronectin-, and gelatin-coated multilayer polyelectrolyte thin films. In Figure 5.40, it is seen that the roundness of smooth muscle cells on all PSS-, fibronectin-, and gelatin-coated thin films decreases with increasing the number of layers of the underlying architectures. In Figure 5.41, the number of pseudopodia of cells increases with increasing of number of underlying architectures for fibronectin-coated thin films; there is a sharp increase of number of pseudopodia for PSS-coated films when the underlying architecture increases from 1-

bilayer to 2-bilayer, then changing little to 5-, 10-, and 20-bilayer films; The number of pseudopodia on gelatin-coated thin films keeps constant for all different number of underlying architectures.

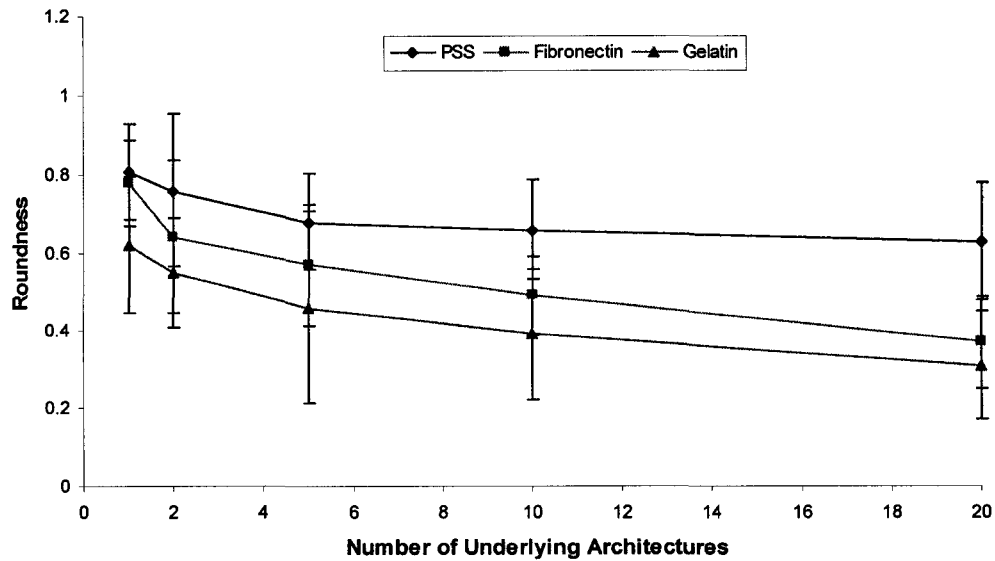


Figure 5.40 Roundness of smooth muscle cells on PSS-, fibronectin-, and gelatin-coated multilayer polyelectrolyte thin films

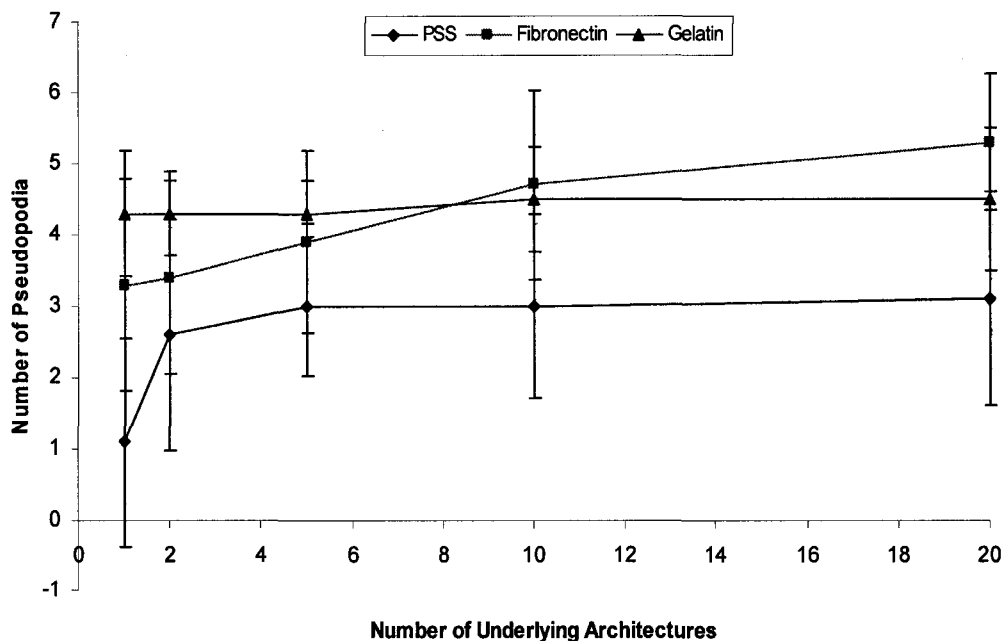


Figure 5.41 Number of pseudopodia of smooth muscle cells on PSS-, fibronectin-, and gelatin-coated multilayer polyelectrolyte thin films

The student t-test statistical analysis results, showed in Table 5.6, indicate that

there are significant differences between the roundness of cells on 1-bilayer and 20-bilayer polymer thin films for all three PSS-, fibronectin-, and gelatin-coated surfaces, which agree with the qualitative analysis above. For fibronectin-coated thin films, there is significant difference of cell roundness on all 1-, 2-, 5-, 10-, and 20-bilayer thin films except 2-bilayer to 5-bilayer films, and 5-bilayer to 10-bilayer films. It appears that underlying architectures are critical for cell morphologies. For gelatin-coated thin films, it seems the roundness of cell decreases gradually, with no clear critical layer that indicates the change. For PSS-coated thin films, 1-, 2-, 10-bilayer are critical numbers for cells showing significant change in roundness.

Table 5.6 Probability of T-test of cell roundness and number of pseudopodia on different number of underlying polyelectrolyte architectures (m=n=15).

	Roundness of Cells			Number of Pseudopodia		
	PSS	Fibronectin	Gelatin	PSS	Fibronectin	Gelatin
1- Vs. 2-bilayer	0.1956	0.0105*	0.1127	0.0110*	0.4495	0.5000
1- Vs. 5-bilayer	0.0031**	4E-05**	0.0258*	0.0010**	0.1239	0.5000
1- Vs. 10-bilayer	0.0015**	1E-08**	4E-04**	0.0007**	0.0058**	0.2539
1- Vs. 20-bilayer	0.0005**	6E-11**	4E-06**	0.0005**	0.0001**	0.2821
2- Vs. 5-bilayer	0.1028	0.1036	0.1234	0.2126	0.1383	0.5000
2- Vs. 10-bilayer	0.0677*	0.0064**	0.0040**	0.2413	0.0056**	0.2112
2- Vs. 20-bilayer	0.0295*	4E-05**	3E-05**	0.1853	0.0001**	0.2539
5- Vs. 10-bilayer	0.3488	0.0833	0.1708	0.5000	0.0525	0.1912
5- Vs. 20-bilayer	0.1729	0.0004**	0.0225*	0.3901	0.0016**	0.2418
10- Vs. 20-bilayer	0.2867	0.0029**	0.0850	0.4025	0.1098	0.5000

Note: * P<0.05; ** P<0.01.

Compared with the cell roundness, statistical analysis results of the number of pseudopodia of cells in Table 5.6 show agreement to Figure 5.41. For PSS-coated surfaces, 2-bilayer is the essential architecture for increasing the number of pseudopodia.

There is no significant difference for cells on gelatin-coated surface with different underlying architecture. For fibronectin-coated surfaces, 10-bilayer and 20-bilayer architectures are more important for increasing the number of cell pseudopodia.

Table 5.7 contains statistical analysis data of the comparison of cell morphologies on these three coating materials. By measuring the cell roundness and number of pseudopodia, the cell adhesion on these scaffolds can be indirectly inferred.

Table 5.7 Probability of paired T-test of cell roundness and number of pseudopodia on different coating materials (n=5).

	PSS-Fibronectin	PSS-Gelatin	Fibronectin-Gelatin
Roundness	0.0109*	0.0003**	0.0016**
Number of Pseudopodia	0.0034**	0.0033**	0.2435

Note: * P<0.05; ** P<0.01.

The data in Table 5.7 indicate significant differences between PSS- and fibronectin-coated films, PSS- and gelatin-coated films for either cell roundness or cell pseudopodia. The roundness of cells on fibronectin-coated surface is different from that on gelatin-coated surface, but the number of pseudopodia does not show significant difference. The statistical analysis demonstrates that both fibronectin and gelatin have cell adhesive properties, whereas PSS does not. Because cells show different roundness on fibronectin- and gelatin-coated thin films, they clearly have different responses to these two materials, which may be manifest in behavior during further growth. Long-term effects of materials on cell response need to be studied more thoroughly in the future.

5.3.2 Culture Cells on Patterned Substrates

Using microfabrication and LbL-LO techniques, multilayer thin film patterns can be fabricated on the planar or microstructured substrates. The surface topography, surface

material, and the underlying architectures can be controlled to study the cell alignment and attachment on these *in vitro* scaffolds.

5.3.2.1 Cells Cultured on Polyelectrolyte Thin Film Patterned Glass Substrate

Polyelectrolyte thin film patterns with different surface materials and layering architectures were fabricated to study cell attachment, alignment, and growth. Figure 5.42 contains images of cells cultured on glass substrates with different polyelectrolyte patterns. In Figure 5.42(a), the cell culture pattern was layered alternately with polyions and 20 nm fluorescent particles in the order of (PAH/PSS)₃/(PAH/nanoparticles)₃/PAH. The outermost layer of the pattern was PAH, while the glass surface was the nonpatterned region. It is observed from the image that cells could grow on the glass surface instead of the patterned surface with PAH coating.

The scaffolds in Figure 5.42(b), (c), and (d) have similar layering architectures except the outermost layer of the polyelectrolyte thin films was varied. In Figure 5.42(b), the cell culture pattern was layered with (FITC-PAH/PSS/Ru-PAH/PSS)₄/PDDA on the glass substrate. As PDDA was the outermost layer on the pattern, similarly as in Figure 5.42(a), smooth muscle cells grew on the glass surface, while no cells were observed on the PDDA coated surface.

In Figure 5.42(c), the layering architecture of the cell culture pattern was (FITC-PAH/PSS/Ru-PAH/PSS)₄/PEI, so PEI was the outermost layer of the pattern. It was observed that a few cells grew on PEI coated surface, but the cell density was much lower than that on the glass surface.

In Figure 5.42(d), the thin film pattern was layered with (FITC-PAH/PSS/Ru-

PAH/PSS)₄, so PSS was the outermost layer. Smooth muscle cells grew on both patterned PSS coated surface and nonpatterned glass surface. Little difference between the cell densities on these two surfaces was seen from this image.

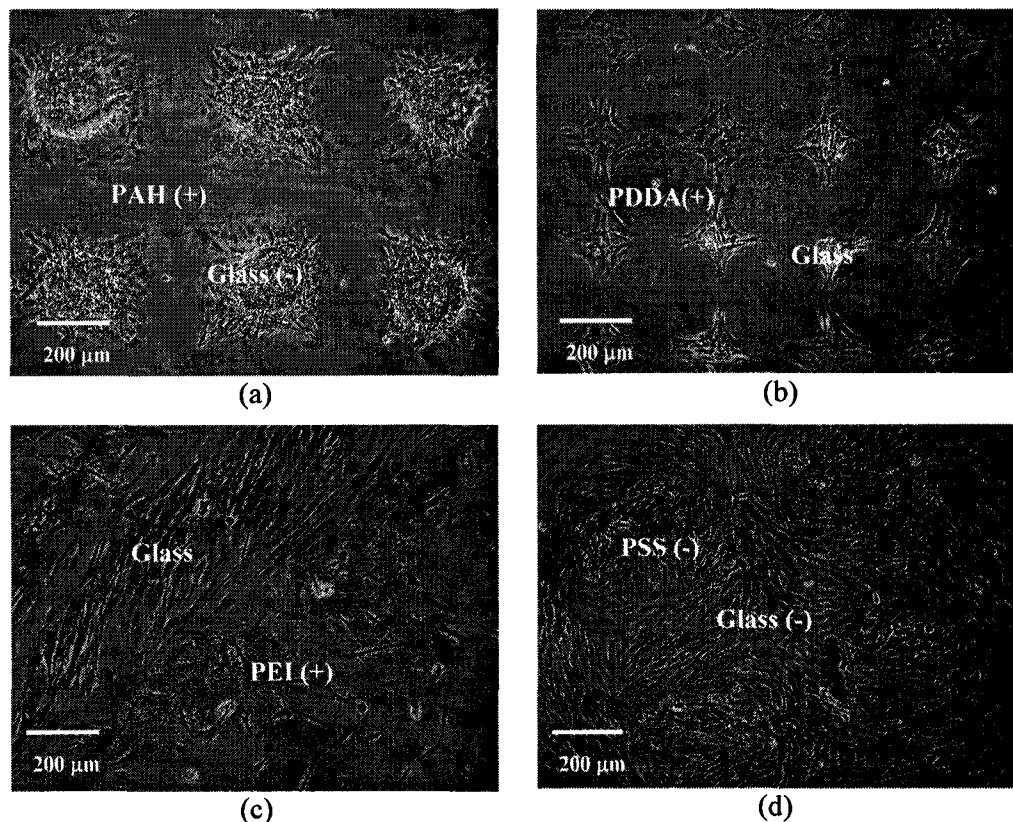


Figure 5.42 Optical images of cells cultured on the polyelectrolyte patterns with a variety of LbL architectures

- (a) Cells cultured on the polyelectrolyte pattern with (PAH/PSS)₃/(PAH/Fluorescent particles)₃/PAH.
- (b) Cells cultured on the pattern with layering order of (FITC-PAH/PSS/Ru-PAH/PSS)₄/PDDA.
- (c) Cells cultured on the pattern with layering order of (FITC-PAH/PSS/Ru-PAH/PSS)₄/PEI.
- (d) Cells cultured on the pattern with layering order of (FITC-PAH/PSS/Ru-PAH/PSS)₄.

These images suggest that surface charge polarities of polyelectrolyte thin films may affect the attachment and the proliferation of smooth muscle cells. PAH, PDDA, and PEI are all positively charged polyions, while PSS is a negatively charged polyion and the nanostrip treated glass surface is also negatively charged. In this study, smooth muscle cells appear to prefer to grow on the negatively charged surface, rather than on the positively charged surface. It was found that positively charged chitosan could

modify poly(L-lactic acid) (PLLA) surface and improve its cytocompatibility to human endothelial cells [2]. Also, one reported that poly-L-lysine (PLL) precoating with human autologous extracellular matrix could improve cell attachment of myofibroblasts [212]. Although different cell types may exhibit different response to the same surface materials, also cells may display different behavior to different materials with same surface charge polarity, these finding indicate that charge polarity is not the only factor of polymer surface chemistry to affect cell adhesion, other factors, such as the charge intensity and charge distribution, may also influence the growth of cells. The most important requirement is the cell adhesive materials used in the *in vitro* cell culture systems to make the cells land and grow, then further to investigate the other factors which make cells behave like in their *in vivo* environment.

5.3.2.2 Cells Cultured on Gelatin or FITC-gelatin Patterned Glass Substrate

A. Cells on gelatin-coated square pattern on cover slip

To study cell initially selective landing, RASMCs were cultured on the engineered cell culture scaffold with gelatin-coated polyelectrolyte thin film patterns on PDDA-coated glass substrate. The polyelectrolyte thin film patterns had a layering architecture of PDDA/(PSS/FITC-PAH)₂/(gelatin/FITC-PAH)₄/gelatin. The initial attraction of gelatin-coated polyelectrolyte thin film patterns was clearly shown in Figure 5.43. Just in 30 minutes after cell culture, most of the cells were attracted to the gelatin-coated square patterns. Compared to PDDA-coated planar surface, it was apparent that gelatin worked as an adhesive material, and PDDA could be used as a cell-repulsive material for cell initially selective attachment.

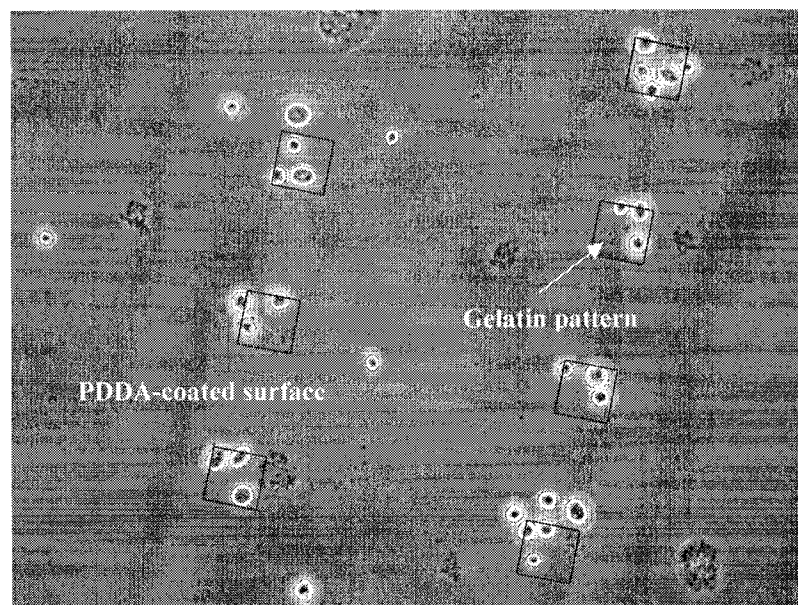


Figure 5.43 Initial attraction of SMCs to gelatin-coated patterns in 30 minutes after cell passage.

To compare cell initially selective landing on different materials, smooth muscle cells were cultured on two types of gelatin-coated polyelectrolyte-patterned substrates. Both of the cell culture scaffolds were built up with gelatin-coated polyelectrolyte square patterns as adhesive regions, which had the same pattern size, $50\mu\text{m} \times 50\mu\text{m}$ and same layering architecture as mentioned above. The difference was that in one scaffold, gelatin-coated polyelectrolyte patterns were deposited on PDDA-coated glass surface, used as the cell-repulsive region, and the second scaffold was fabricated with these gelatin-coated square patterns on plain glass surface, which was used as the control region. After 3 hours of cell culture, cells were observed and optical phase contrast images were taken, shown in Figure 5.44.

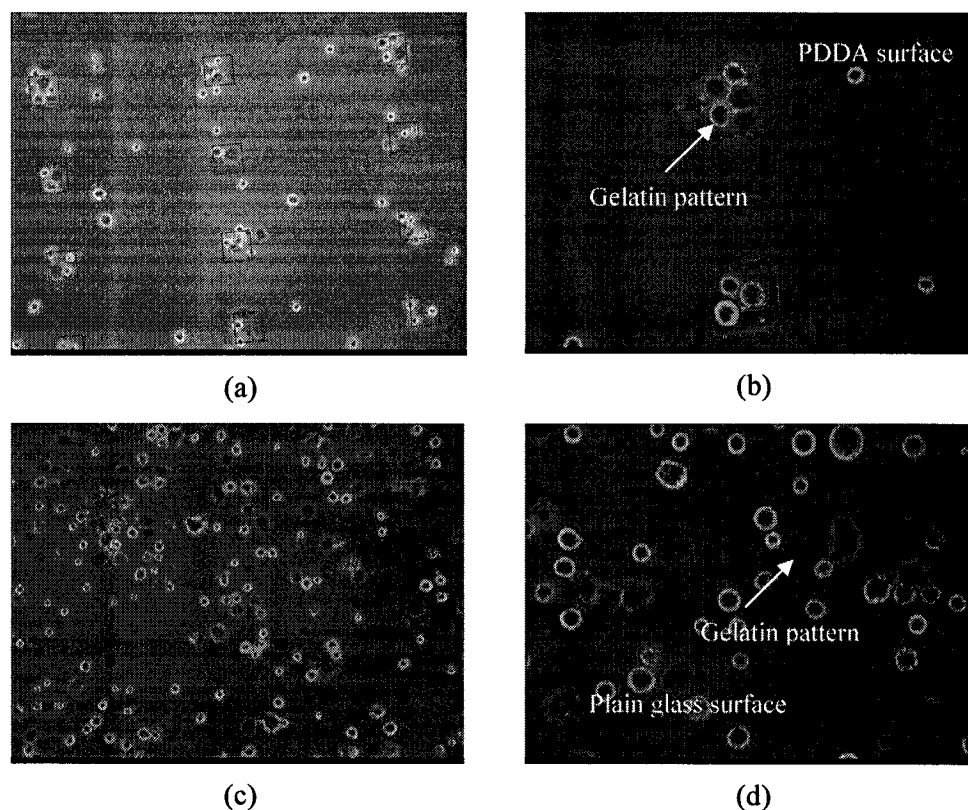


Figure 5.44 Optical images of SMCs transferred onto two types of substrates after 3 hours

(a,b) gelatin-coated pattern with PDDA-coated nonadhesive surface.

(c,d) gelatin-coated pattern with control plain glass surface.

(a, c) objective 10X; (b, d) objective 40X.

Figure 5.44 (a) and (b) are images of cells cultured on gelatin-coated polyelectrolyte patterns with PDDA-coated intermediate regions. Figure 5.44 (b) is a zoom-in image of that in Figure 5.44 (a). As also shown in Figure 5.43, smooth muscle cells were still strongly attracted by gelatin-coated patterns, but repelled by PDDA-coated regions. In Figure 5.44 (c) and (d), same as in Figure 5.44 (a) and (b), Figure 5.44 (d) is a magnified image of 5.44 (c), smooth muscle cells were cultured on the substrate with gelatin-coated square patterns, while the planar surface was just plain glass without any polyelectrolyte coatings. It was observed that smooth muscle cells could attach on both surfaces of gelatin-coated patterns and plain glass substrate,

indicating that there was not much adhesive difference between gelatin-coated patterns and control plain glass surface for the attraction of cell initial attachment. These images indicate that PDDA-coated surface can be used as cell-repulsive intermediate regions to control the position of cell initial landing, further to control the cell growth pattern.

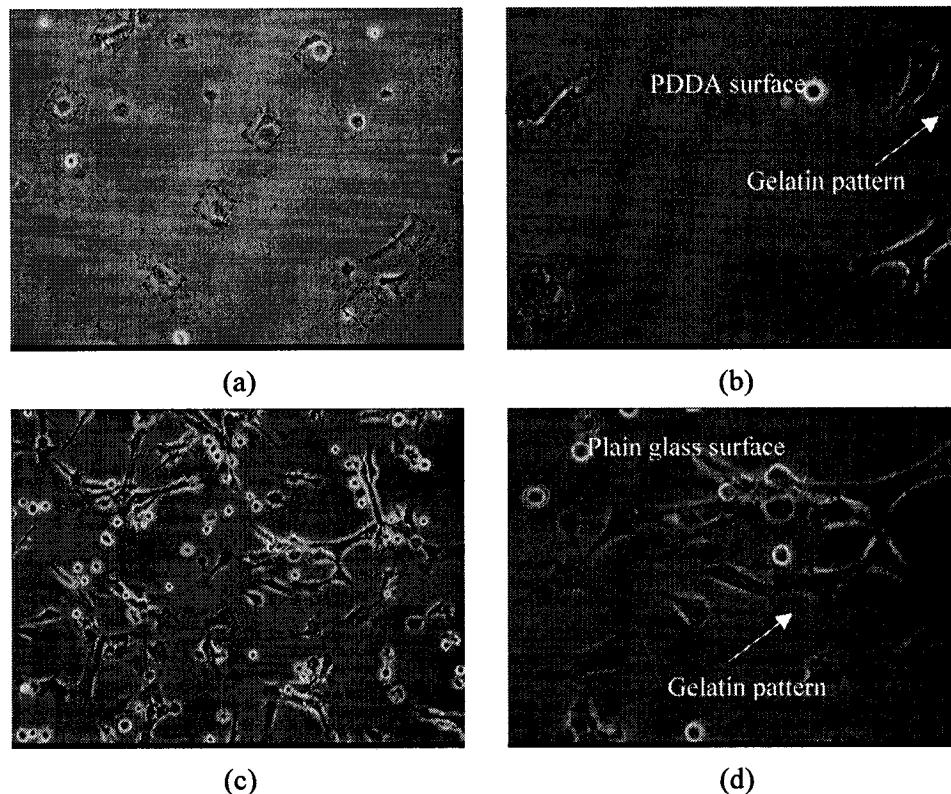


Figure 5.45 Optical images of SMCs cultured on two types of substrates after 15 hours

(a,b) gelatin-coated pattern with PDDA-coated nonadhesive surface.

(c,d) gelatin-coated pattern with control plain glass surface.

(a,c) objective 10X; (b,d) objective 40X

Cell culture images were taken continuously after 15 hours to compare the further cell growth on these two types of cell culture scaffolds. As shown in Figure 5.45, similar phenomena were observed over longer times. Smooth muscle cells began to spread and grow on the gelatin-coated square patterns instead of on the large area of PDDA-coated planar surface after initial landing shown in Figure 5.45 (a) and

(b). In contrast, shown in Figure 5.45 (c) and (d), smooth muscle cells grew everywhere on the entire surface no matter the gelatin-coated patterns or the control plain glass. The results from Figures 5.44 and 5.45 give an insight for future design strategy of cell culture systems that carefully selecting biomaterials as cell-adhesive or cell-repulsive materials is a critical issue when studying cell behavior in an *in vitro* engineered ECM.

Further, in the same batch of experiments, it was observed that the “degradation” of cell-repulsive function of PDDA-coated regions was time-dependent, shown in Figure 5.46, which could be seen that smooth muscle cells began to migrate from gelatin-patterned adhesive patterns to PDDA-coated regions after 40 hours of cell culture, although their pseudopodia still preferred to attach on the gelatin-coated patterns, as shown in Figure 5.46 (c). After 70 hours of cell culture, more and more cells grew on PDDA-coated regions. The true mechanism of this “degradation” of PDDA coating is not clear. One possible reason for this “degradation” is the size of a single smooth muscle cell is much larger than that of a gelatin-coated square pattern. So, after attaching on the gelatin-coated pattern surface, cells would like to spread out to survive and to perform normal function, thus they had to migrate to the “uncomfortable” surfaces. Another possibility is that gelatin and PDDA were gradually “dissolved” or “broken down” in the cell culture media, thus changing the local physical stresses of gelatin and PDDA coated surfaces, so the adhesive and repulsive properties disappeared with time. This feature of time-dependent culture of cell attachment needs to be studied in more detail doing future research work.

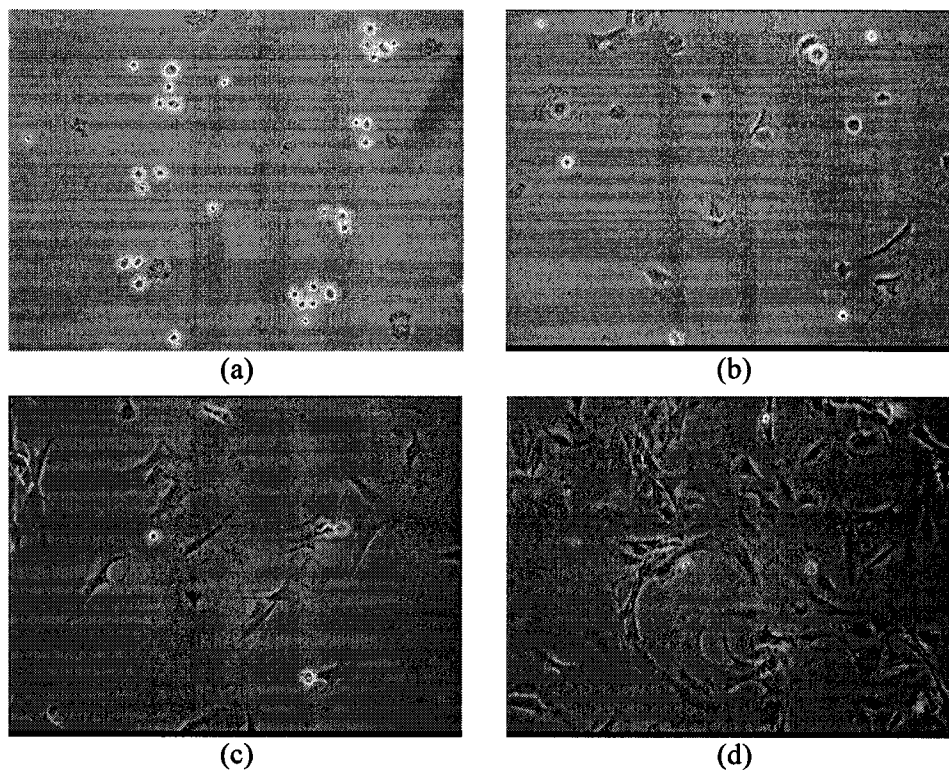


Figure 5.46 Time-dependent of degradation of PDDA-coated nonadhesive region. SMCs cultured on substrate with gelatin-coated adhesive square patterns and PDDA-coated nonadhesive region after (a) 30 minutes; (b) 15 hours; (c) 40 hours; (d) 70 hours

B. Cells on FITC-gelatin coated patterns on glass slide

Two types of FITC-gelatin coated patterns were designed and fabricated: one was a square pattern, and the other was the strip pattern. Smooth muscle cells were cultured on these FITC-gelatin patterns to investigate cell attachment and alignment on these two patterned microstructures. As was observed in all previous cases, smooth muscle cells initially landed and grew on the FITC-gelatin coated patterned surfaces in the first few days. Because the glass surface also permits the growth of cells, as shown in Figure 5.31(a), after several days cells could spread out and grow on both the FITC-gelatin patterned surface and glass surface when cell numbers increased greatly.

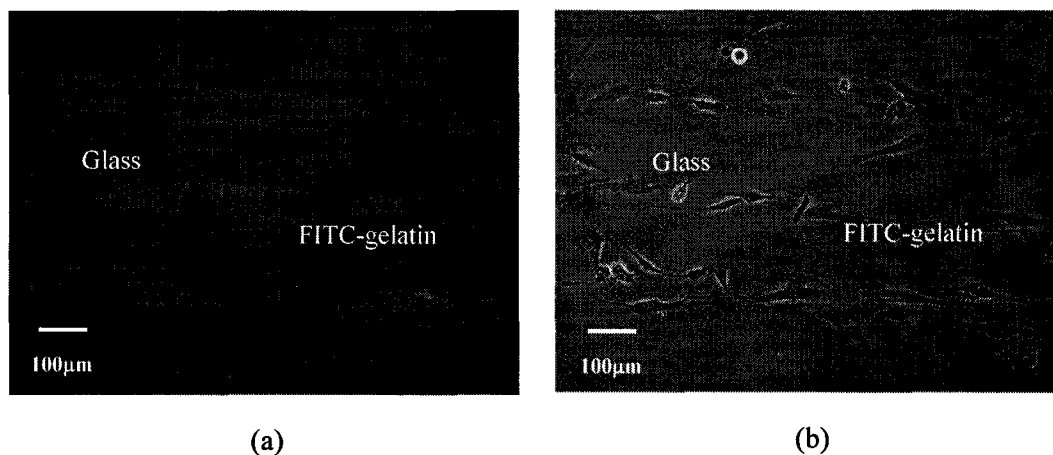


Figure 5.47 Cell culture on FITC-gelatin patterned glass substrate
 (a) Fluorescence image of FITC-gelatin patterns; (b) Optical image of Cell culture

For cells cultured on the strip patterns, an interesting cell growth pattern on FITC-gelatin patterned surface was observed, as shown in Figure 5.47 (b). These images were taken on the second day after cell passage. In Figure 5.47 (b), it can be seen that most of the cells initially landed on the pattern surface with FITC-gelatin coating instead of on the surface of plain glass. The width of the FITC-gelatin regions of the rectangular pattern in the image was 70 μm . The similar cell growth patterns were also observed on the surface of FITC-gelatin coated rectangular patterns in a range of widths from 50 to 100 μm . Furthermore, edge effects were found at the interface of FITC-gelatin patterns and glass surfaces: the cells appear to align with the edge of FITC-gelatin regions.

These cell culture results further demonstrate that both gelatin and FITC-gelatin coating are cell-adhesive materials for smooth muscle cells and can be used to attract cells for initial landing. Secondly, strip patterns with cell-adhesive surface material have a better control for cell alignment.

C. Cells on FITC-gelatin coated strip patterns on glass slide

Cell staining may greatly facilitate the visualization of the cell shape when cells are cultured on the engineered scaffolds. Figure 5.48 shows the fluorescence images of RASMCs cultured on gelatin-coated glass substrate.

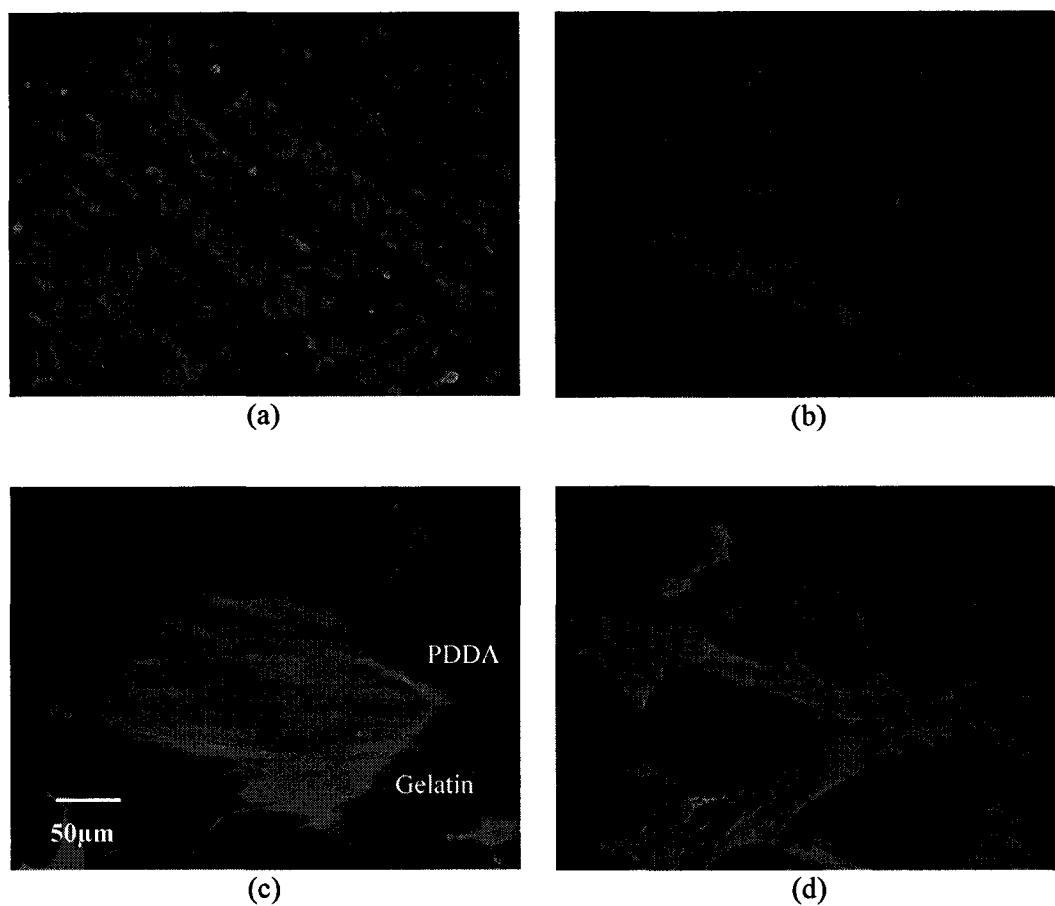


Figure 5.48 Fluorescence images of cells on gelatin-coated thin film patterned glass substrate after staining by Alexa Fluor 488 Phalloidin. Fluorescence strip pattern with gelatin coating is 120µm in width; background with PDDA coating is 60µm wide
(a,b,c,d show the images with different magnifications.)

The thin film patterns in these images have a layering architecture of PSS+(FITC-PAH/PSS)+(FITC-PAH/gelatin)₃, and the base background of glass surface was coated with one layer of PDDA. It can be obviously observed that cells

prefer to grow on gelatin-coated surfaces rather than on PDDA-coated surfaces, which agrees with the previous observation of cells cultured on FITC-gelatin coated thin film patterns. In addition, in Figure 5.48 (d), one may notice that cells can cross the narrow PDDA-coated region. This happening is considered that the “communication” of the cells to each other depends on the sizes of both the patterns and the cells.

5.3.2.3 Cells Cultured on Fibronectin Patterned Glass Substrate

Smooth muscle cells were cultured on the fibronectin-coated polyelectrolyte thin film pattern fabricated on glass substrate as described in section 5.2.1.3. It was observed that after 2 days culture, cells most preferred to grow on fibronectin-coated pattern surfaces just like the cells cultured on gelatin-coated pattern surfaces. But, it was also found that fibronectin was different from gelatin for the initial attachment of smooth muscle cells. That is, smooth muscle cells are initially attracted to land by gelatin-coated surface, while fibronectin does not appear to attract smooth muscle cells to land on its surface.

Figure 5.49 contains images of smooth muscle cells on fibronectin-coated and gelatin-coated polymer thin film surfaces after 12 hours of culture with the same seeding density of 5×10^4 cells/well. These scaffolds have the similar layering architectures: (FITC-PAH/PSS)₅ + Fibronectin and (FITC-PAH/PSS)₅ + FITC-PAH/gelatin, respectively. In Figure 5.49 (a), it can be seen that smooth muscle cells have to land on PDDA-coated surface initially and there is not a single cell on fibronectin-coated pattern surface after 12 hours culture. However, after 12 hours cell culture, smooth muscle cells

have landed and attached on gelatin-coated pattern surface, and further begin to spread out and grow along the gelatin-coated strip patterns, as shown in Figure 5.49 (b). Comparing Figure 5.49 (a) and (b), there seems to be a better initial attraction for smooth muscle to attract to gelatin than fibronectin.

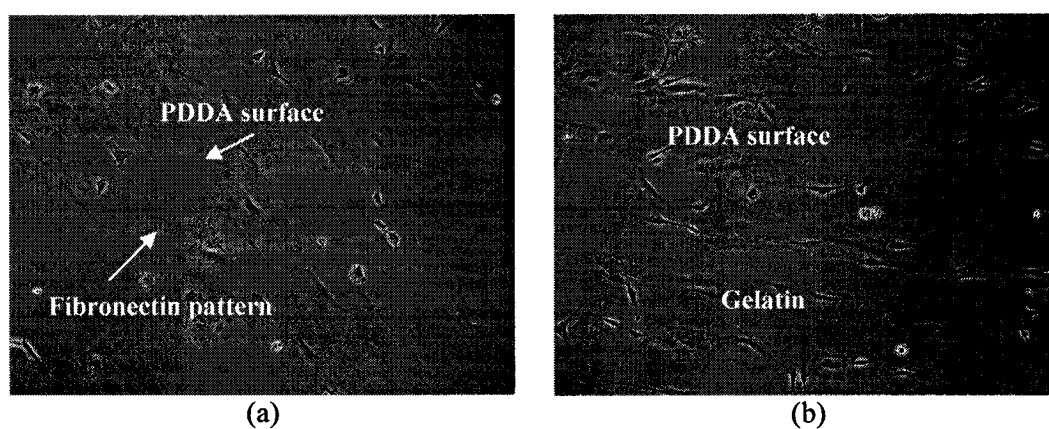


Figure 5.49 Optical images of cells on (a) fibronectin-coated; (b) gelatin-coated thin film patterns on PDDA-coated glass substrates after 12 hours culture. (10X objective)

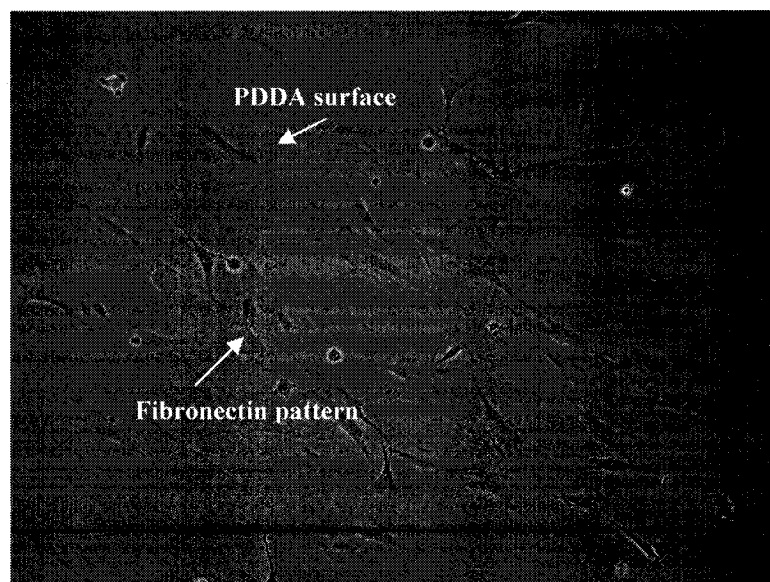


Figure 5.50 Optical images of cells on fibronectin-coated film patterns on PDDA-coated glass substrates after 24 hours culture. (10X objective)

Figure 5.50 shows smooth muscle cells landing on PDDA-coated surface begin to migrate to fibronectin-coated pattern surface after 24 hours culture. Figure 5.51 contains the images of cells cultured on fibronectin-coated square and strip patterns. These images indicate fibronectin is still a cytophilic protein for the growth of smooth muscle cells.

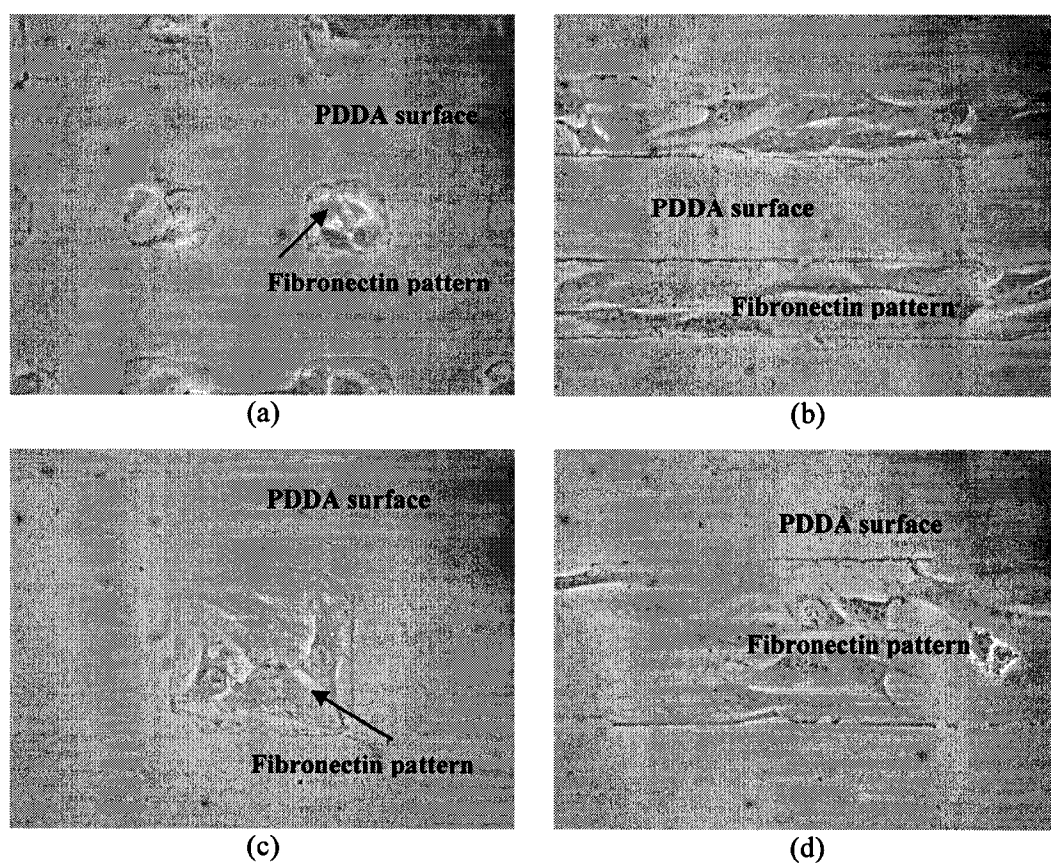


Figure 5.51 Optical images of cells on fibronectin-coated thin film patterns on PDDA-coated glass substrates after 2 days culture. (40X objective)

(a) 60µm square; (b) 60µm strip; (c) 120µm square; (d) 120µm strip patterns

The images in Figure 5.49 to Figure 5.51 indicate that both gelatin and fibronectin are cell-adhesive materials for cell further growth, but they have different effects on the initial landing of smooth muscle cells.

Figure 5.52 shows fluorescence images of the same smooth muscle cells cultured on fibronectin-coated pattern after co-staining by Alexa Fluor 488 phalloidin and Hoechst

33342. With the Hoechst 33342 nuclear stain, it is easier to distinguish the individual cells on the patterns. An interesting phenomenon shown in Figure 5.52 (a) is that some cells cross PDDA-coated surface to adhere on the two neighboring fibronectin-coated square patterns. It is not known whether cells were on both patches, and they generated a physical connection with one another, or if cells on one patch moved to another one to need for surface area to grow.

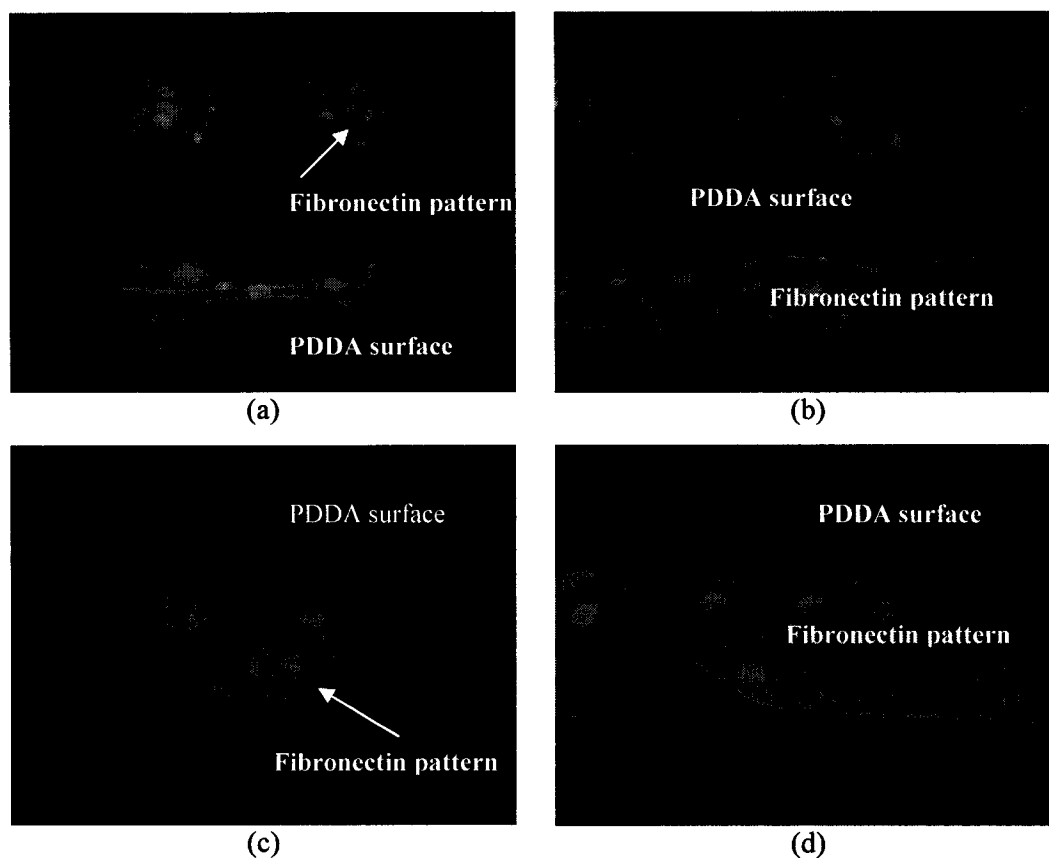


Figure 5.52 Fluorescence images of cells on fibronectin-coated thin film patterns on PDDA-coated glass substrates after stained by Alexa Fluor 488 Phalloidin and Hoechst 33342

(a) 60µm square; (b) 60µm strip; (c) 120µm square; (d) 120µm strip patterns

Although it is possible that the conformation of fibronectin has been changed and partially denatured during lift-off process in acetone, it is still functional for the final cell attachment and growth based on these cell culture results on fibronectin-coated polymer

patterns. However, the initial non-attractive landing of cells may be one of the effects due to the denaturation of fibronectin in acetone. LbL-LO technology needs to be further studied, especially, when it is applied in biological research work.

5.4 Cell Culture on other Substrates

5.4.1 Cells Cultured on Microchanneled PMMA Substrates

SMCs cultured on 60 μ m channeled PMMA substrates showed a different behavior compared with previous study on glass and PDMS substrates. Cells cultured on plain PMMA substrates could attach, grow, and be aligned in the channels, as shown in Figure 5.53(a); however, in Figure 5.53(b), cells cultured on gelatin-coated PMMA substrates could not even attach on the surface of substrates. This surprising phenomenon suggests that the properties of patterned PMMA must be further explored.

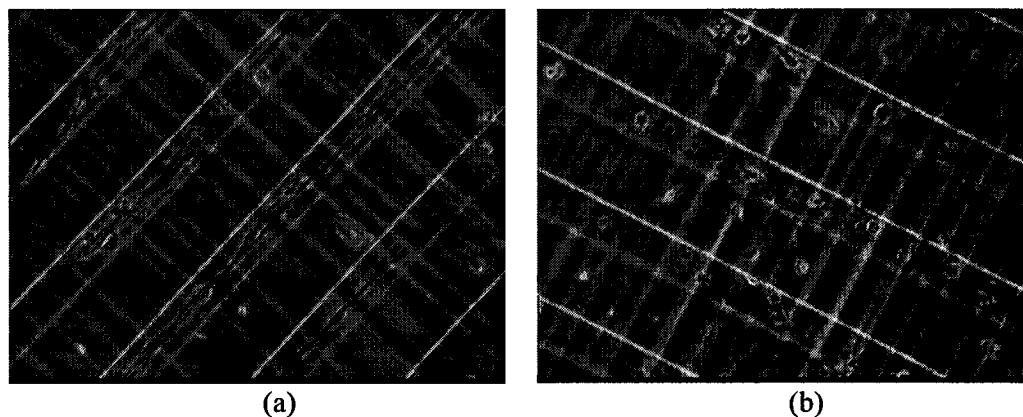


Figure 5.53 Cells cultured on (a) plain; (b) gelatin-coated 60 μ m channeled PMMA substrates

5.4.2 Cells Cultured in 3-D Silicon Microfluidic Cell Culture Systems

It is impossible to see the cells with phase contrast microscope when they are cultured on the opaque substrates, such as silicon wafer. So, it is required to stain the cells for the observation purpose.

Figure 5.54 shows RASMCs grown in the 60 μ m wide and 30 μ m deep channels with 40 μ m x 40 μ m PSS-coated square patterns after stained by Hoechst 33342 and Propidium Iodide.



Figure 5.54 Cellular nuclei stain of cells in 60 μ m silicon channeled substrate

In Figure 5.54, the nuclei of living cells can be clearly seen on the square patterns in the channel. It is observed a couple of cells on the top surface of silicon substrate are dead, as shown in Figure 5.54 (b). These two images indicate that smooth muscle cells can grow in the PSS-patterned silicon channels.

In Figure 5.55, smooth muscle cells are cultured on the 60 μ m wide and 30 μ m deep channeled silicon substrate. After stained by Alexa Fluor 488 phalloidin, it can be observed that most of the cells grow in the channels and align along the channels.

Cell culture patterns on the 3-D channeled silicon substrates indicate that the

physical barrier is also important for the study on cell behavior in an *in vitro* cell culture system. However, for most of biological studies, cells are cultured on optical clear substrates, the 3-D microfluidic cell culture systems are necessary to be transferred and fabricated on glass or PMMA substrates in the near future for observation purpose.

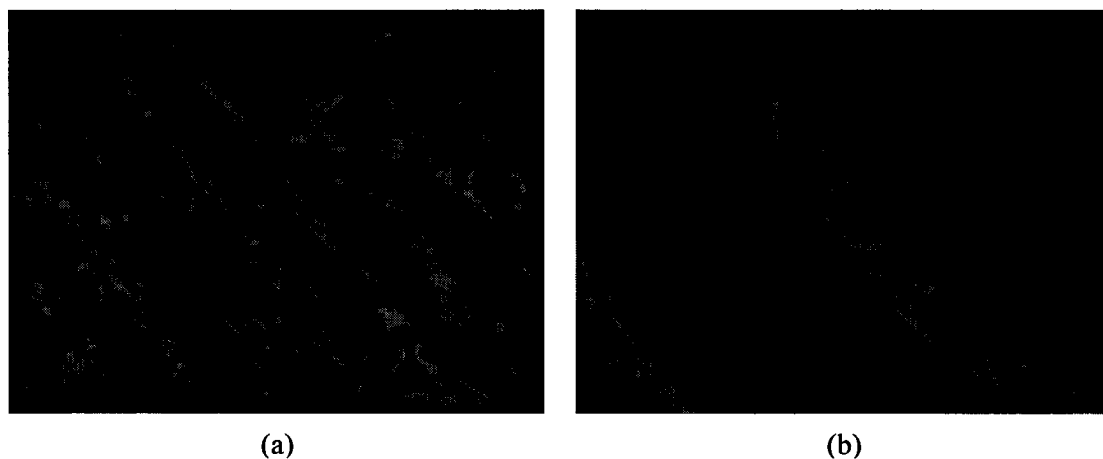


Figure 5.55 F-actin stain of cells cultured in 60µm channeled silicon substrate with Alexa Fluor 488 phalloidin

In summary, this chapter described and analyzed the experimental results involving surface properties of various biomaterials, fabrication results of engineered cell culture scaffolds using all kinds of microfabrication and nanopatterning techniques, and cell culture investigation for the fabricated scaffolds.

First, the assembly properties of gelatin and fibronectin were investigated to confirm that both the proteins could be adsorbed on the polyelectrolyte thin film surfaces. This assembly is the basis to study cell-material interactions in the *in vitro* cell culture systems. Smooth muscle cells were cultured on various engineered cell culture scaffolds, including planar substrates and patterned substrates with different surface materials and with different surface topographies. Cell culture results indicate that negatively charged

polyelectrolyte may have a better cell attachment than positively charged one; gelatin and fibronectin may work as the cell-adhesive materials for the attachment of smooth muscle cells; underlying polyelectrolyte architectures may affect the cell morphology, thus influence the attachment and focal adhesion of cells; strip patterns with adhesive coatings may increase the alignment of smooth muscle cells. The detailed research conclusion will be given in the next chapter.

CHAPTER 6

CONCLUSIONS

Organisms are the most complicated and ordered structures in the world; the explorations of mechanisms of biolife will likely last forever. With the development of modern technologies, however, people have been gaining more and more knowledge about the mechanisms of organism function, delving ever deeper into the molecular and submolecular levels. As understanding improves, scientists and researchers are becoming involved in the field of tissue engineering, making efforts to fix or replace failing body parts with artificial organs. The work in this project is also focused on developing new ways to study the effect of important factors on the regulation of cell growth in an *in vitro* environment. Surface materials and underlying architectures of the *in vitro* cell culture scaffolds were investigated to the attachment and alignment of smooth muscle cells.

As proteins play an important role in the current biomedical engineering, biomaterial, and biosensor fields, and studies on materials have been developed into the nanometer range, it is necessary to take further steps toward better understanding of protein and synthetic polymer properties for potential application to cell and tissue culture. As a first step in this work, the electrostatic assembly properties of FITC-gelatin or gelatin were studied with QCM, zeta-potential analyzer, UV-Vis spectroscopy, and fluorescence spectroscopy. The surface properties, such as surface roughness and surface

hydrophobicity, of gelatin, fibronectin, and polymer materials were measured with AFM and contact angle systems. The experimental results indicate that the charge polarity of gelatin varies as pH shifts away from its isoelectric point, and its charge density changes with both pH and the composition of buffer solution. After labeling gelatin with FITC, the conjugate is still negatively charged and can also be alternately layered with positively charged polyions.

In addition, contact angle measurement indicates the surface hydrophobicity is not only affected by the outermost layer materials, but also by the underlying materials and base substrates. There is little difference in surface hydrophobicity between polyelectrolyte PAH and conjugate FITC-PAH when deposited with the same layering architecture on the same base glass substrate, which indicate that conjugated polymer material does not make the surface properties different from the original polymer material. This facilitates the fabrication and inspection of cell culture scaffolds due to the interchangeable usage of the conjugated materials and original material. AFM measurement shows that the surface roughness increases with increasing number of layers of fibronectin and polymer materials on different base substrates. Cell attachment is affected by the difference of surface roughness of the scaffolds.

The extracellular matrix is of critical importance for modulating cell function *in vivo*. Fabrication of engineered cell culture scaffolds mimicking *in vivo* ECM in an *in vitro* environment for culture of specific cells with a desired growth pattern is still a major challenge in the area of tissue engineering. In this work, 2-D and 3-D cell culture scaffolds were fabricated to investigate microfabrication and layer-by-layer nanopatterning techniques and study the effect of microstructure, surface material, and

underlying architecture on the attachment and alignment of smooth muscle cells. Taking advantage of the property of fluorescent probes, FITC-gelatin, FITC-PAH, and Ru-PAH patterned cell culture scaffolds were fabricated with micromaching and layer-by-layer self-assembly approaches to facilitate the recognition of nanofilm patterns.

Currently, a new approach, using layer-by-layer and lift-off (LbL-LO) to fabricate the cell culture scaffolds, provides a unique opportunity to study cell behavior on micro/nano-patterned structures with modified surface properties. From our investigation, it can be concluded that LbL-LO is very efficient to make polyelectrolyte ultrathin film patterns with charged polyions and proteins. Positively charged PAH and PDDA coatings are repulsive cell growth, while negatively charged PSS and pretreated glass surfaces are cell adhesive. Gelatin, a negatively charged denatured collagen, shows the cytophilic properties for smooth muscle cells, and FITC-gelatin-coated patterns align cell growth along the main axis of the strip patterns.

However, the effect of polyelectrolyte patterns with different outermost surface molecules on the attachment and the growth of smooth muscle cells is not only due to the polarity of surface charge. Other factors, such as charge density, charge distribution, protein integrin-peptide of the surface materials, and even the properties of the underlying material and bulk substrate also influence the cell behavior. Smooth muscle cells were cultured on fibronectin, gelatin, and PSS-coated surfaces with 1-bilayer and 20-bilayer of PAH/PSS underlying architectures on glass substrates. The cell culture results indicate that both fibronectin and gelatin are cell adhesive proteins, on which cells show a preferred attachment than on PSS-coated surfaces. Comparing cell morphologies on these coated multilayer polymer films, cells show more spread-out patterns and have

more pseudopodia on 20-bilayer underlying substrates with fibronectin and gelatin coatings. Student's t-test statistical analyses support the hypothesis that the roundness of cells increases with increasing the number of underlying architectures, which indicate that the more layers of polyelectrolyte thin films, the better adhesion of smooth muscle cells. Furthermore, the statistical analyses show that there are significant differences in the cells roundness and number of pseudopodia between on gelatin-, fibronectin-, and PSS-coated multilayer thin films.

The initial attachment of smooth muscle cells on fibronectin and gelatin-coated thin film patterns after seeding was also studied. It was observed that smooth muscle cells preferred to land on gelatin-coated pattern surfaces and grew there. In contrast, cells landed on surfaces other than fibronectin, including the apparently cytophobic PDDA surface, and then migrated to fibronectin-coated region. This demonstrates that even though both cell adhesive materials, they have different effects on cell behavior.

The study of *in vitro* cell culture still has a long way to go to mimic the cell behavior in an *in vivo* environment. It is believed that this study on the fabrication methods of *in vitro* cell culture scaffolds lays the groundwork for many future potential applications, and will eventually benefit a variety of research and development efforts in cell biology, tissue engineering, and biomaterials.

REFERENCES

1. J. D. Mendelsohn, S. Y. Yang, J. Hiller, A. I. Hochbaum, and M. F. Rubner, "Rational Design of Cytophilic and Cytophobic Polyelectrolyte Multilayer Thin Films", *Biomacromolecules*, Vol. 4, 96-106, 2003.
2. Y. Zhu, C. Gao, T. He, X. Liu, and J. Shen, "Layer-by-Layer Assembly to Modify Poly(L-lactic acid) Surface toward Improving its Cytocompatibility to Human Endothelial Cells", *Biomacromolecules*, Vol. 4, 446-452, 2003.
3. Y. Li, D. A. Kniss, L. C. Lasky, S-T. Yang, Culturing and differentiation of murine embryonic stem cells in a three-dimensional fibrous matrix, *Cytotechnology*, Vol. 41, n. 1, pp. 23-35, 2003.
4. V. Stary, L. Bacakova, J. Hornk, V. Chmelk, "Bio-compatibility of the surface layer of pyrolytic graphite", *Thin Solid Films*, Vol. 433, n. 1, 191-198, 2003.
5. J. L. Környei, Z. Vértes, K. A. Kovács, P. M. Göcze, M. Vértes, "Developmental changes in the inhibition of cultured rat uterine cell proliferation by opioid peptides", *Cell Proliferation*, Vol. 36, n. 3, 151-163, 2003
6. P. Tyroen-Tóth, D. Vautier, Y. Haikel, J. Voegel, P. Schaaf, J. Chluba, and J. Ogier, "Viability, adhesion, and bone phenotype of osteoblast-like cells on polyelectrolyte multilayer films", *Journal of Biomedical Materials Research*. Vol. 60, 657-667, 2002.
7. A. A. Lee, D. A. Graham, S. D. Cruz, A. Ratcliffe, and W. J. Karlon, "Fluid Shear Stress-Induced Alignment of Cultured Vascular Smooth muscle Cells", *Journal of Biomechanical Engineering*. Vol. 124, 37-43, 2002.
8. J. Nishida, K. Nishikawa, S. Nishimura, S. Wada, T. Karino, T. Nishikawa, K. Ijiro, and M. Shimomura, "Preparation of Self-Organized Micro-Patterned Polymer Films Having Cell Adhesive Ligands." *Polymer Journal*. Vol. 34(3), 166-174, 2002.
9. L. Griscom, P. Degenaar, B. LePioufle, E. Tamiya, and H. Fujita, "Techniques for patterning and guidance of primary culture neurons on micro-electrode arrays", *Sensors and Actuators B Chemical*. Vol. 83, 15-21, 2002.
10. D. W. Hutmacher, "Scaffold Design and fabrication technologies for engineering tissues — state of the art and future perspectives", *Journal of Biomaterials Science Polymer Edition*, Vol. 12(1), 107-124, 2001.

11. C. M. Agrawal and R. B. Ray, "Biodegradable polymeric scaffolds for musculoskeletal tissue engineering", *Journal of Biomedical Materials Research*. Vol. 55, 141-150, 2001.
12. R. S. Bhati, D. P. Mukherjee, K. J. McCarthy, S. H. Rogers, D. F. Smith, and S. W. Shalaby, "The growth of chondrocytes into a fibronectin-coated biodegradable scaffold", *Journal of Biomedical Materials Research*. Vol. 56, 74-82, 2001.
13. E. W. Raines, "The extracellular matrix can regulate vascular cell migration, proliferation, and survival: relationships to vascular disease", *International Journal of Experimental Pathology*. Vol. 81, 173-182, 2000.
14. L. Kam and S. G. Boxer, "Cell adhesion to protein-micropatterned-supported lipid bilayer membranes", *Journal of Biomedical Materials Research*, Vol. 55, 487-495, 2000.
15. B. S. Kim and D. J. Mooney, "Engineering smooth muscle tissue with a predefined structure". *Journal of Biomedical Materials Research*, Vol. 41, 322-332, 1998.
16. A. Folch, S. Mezzour, M. Du"ring, O. Hurtado, M. Toner, R. Mu"ller, "Stacks of Microfabricated Structures as Scaffolds for Cell Culture and Tissue Engineering", *Biomedical Microdevices*, Vol 2, n. 3, 207-214, 2000.
17. T. A. Desai, J. Deutsch, D. Motlagh; W. Tan, B. Russell, "Microtextured Cell Culture Platforms: Biomimetic Substrates for the Growth of Cardiac Myocytes and Fibroblasts", *Biomedical Microdevices*, Vol. 2, n.2, 123-129, 1999.
18. J. D. Snyder, T. A. Desai, "Microscale three-dimensional polymeric platforms for *in vitro* cell culture systems", *Journal of Biomaterials Science, Polymer Edition*, Vol. 12, n. 8, 921-932, 2001.
19. S. N. Bhatia and C. S. Chen, "Tissue Engineering at the Micro-Scale", *Biomedical Microdevices*, Vol. 2 n.2, 31-144, 1999.
20. J. A. Schmidt and A. F. Recum, "Macrophage Response to Microtextured Silicone", *Biomaterials*, Vol. 13, n.5, 1059-1069, 1992.
21. M. Lampin, R. Warocquier-Clerout, M. F. Sigot-Luizard, "Correlation between Substratum Roughness and Wettability, Cell Adhesion, and Cell migration", *Journal of Biomedical Material Research*, Vol. 36, n.1, 99-108, 1997.
22. E. T. den Baber, J. E. de Ruijter, J. A. Jansen, "Effect of Parallel Surface Microgrooves and Surface Energy on Cell Growth", *Journal of Biomedical Materials Research*, Vol. 29, 511-518, 1995.

23. P. Clark, P. Connolly, A. S. G. Curtis, "Cell Guidance by Ultrafine Topography *in vitro*", *Journal of Cell Science*, Vol. 99, 73-77, 1991.
24. E. T. den Braber, J. E. de Ruijter, J. A. Jansen, "Quantitative Analysis of Cell Proliferation and Orientation on Substrata with Uniform Parallel Surface microgrooves", *Biomaterials*, Vol. 17, n.11, 1093-1099, 1996.
25. X. F. Walboomers, W. Monaghan, J. A. Jansen, "Attachment of fibroblasts on smooth and microgrooved polystyrene", *Journal of Biomedical Material Research*, Vol. 46, n.2, 212-20, 1999.
26. G. Kneditschek, F. Schneider, K. F. Weibezahn, "A Tissue-Like Culture System Using Microstructures: Influence of Extracellular Matrix Material on Cell Adhesion and Aggregation", *Journal of Biomechanical Engineering*, Vol. 121, 35-39, 1999.
27. A. M. Green, J. A. Jansen, J. P. C. M. van der Waerden, "Fibroblast response to microtextured silicone surfaces: Texture orientation into or out of the surface", *Journal of Biomedical Materials Research*, Vol.28, 647-653, 1994.
28. Y. A. Rovensky, I. L. Slavnaya, and J. M. Vasiliev, "Behavior of fibroblast-like cells on grooved surfaces", *Experimental Cell Research*, Vol. 65, 193-201, 1971.
29. Y. A. Rovensky and I. L. Slavnaya, "Spreading of fibroblast like cells on grooved surfaces", *Experimental Cell Research*, Vol. 84, 199-206, 1973.
30. G. A. Dunn and J. P. Jansen, "A new hypothesis of contact guidance in tissue cells". *Experimental Cell Research*, Vol.101, 1-14, 1976.
31. N. G. Maroudas, "Growth of fibroblasts on linear and planar anchorages of limiting dimensions", *Experimental Cell Research*, Vol. 81, 104-110, 1973
32. D. M. Brunette, G. S. Kenner, and T. R. L. Gould, "Grooved titanium surfaces orient growth and migration of cells from human gingival explants", *Journal of Dental Research*. Vol. 62, 1045-1048, 1983.
33. K. D. Chesmal and J. Black, "Cellular responses to Chemical and morphologic aspects of biomaterial surfaces. I. A novel *in vitro* system", *Journal of Biomedical Material Research*, Vol. 29, 1089-1099, 1995.
34. D. G. White, H. P. Hershey, J. J. Moss, H. Daniels, R. S. Tuan; V. D. Bennett, "Functional analysis of fibronectin isoforms in chondrogenesis: Full-length recombinant mesenchymal fibronectin reduces spreading and promotes condensation and chondrogenesis of limb mesenchymal cells", *Differentiation*, Vol. 71, n. 4-5, 251-261, 2003.

35. Y. Adan, Y. Goldman, R. Haimovitz, K. Mammon, T. Eilon, S. Tal, A. Tene, Y. Karmel, M. Shinitzky, "Phenotypic differentiation of human breast cancer cells by 1,3 cyclic propanediol phosphate", *Cancer Letters*, Vol. 194, n. 1, 67-79, 2003.
36. M. H. Prado da Silva, G. D. A. Soares, C. N. Elias, S. M. Best, I. R. Gibson, L. DiSilvio, M. J. Dalby, "In vitro cellular response to titanium electrochemically coated with hydroxyapatite compared to titanium with three different levels of surface roughness", *Journal of Materials Science: Materials in Medicine*, Vol. 14, n. 6, 511-519(9), 2003.
37. C. M. Celluzzi, C. Welbon, "A simple cryopreservation method for dendritic cells and cells used in their derivation and functional assessment", *Transfusion*, Vol. 43, n. 4, 488-494(7), 2003.
38. M. Jechlinger, S. Grünert, H. Beug, "Mechanisms in Epithelial Plasticity and Metastasis: Insights from 3D Cultures and Expression Profiling", *Journal of Mammary Gland Biology and Neoplasia*, Vol. 7, n. 4, 415-432(18), 2002.
39. M. K. Haynes, E. L. Hume, J. B. Smith, Phenotypic Characterization of Inflammatory Cells from Osteoarthritic Synovium and Synovial Fluids, *Clinical Immunology*, Vol. 105, n. 3, 315-325(11), 2002.
40. M. Yoshigi, S. Karnik, D. Y. Di, E. B. Clark, and H. J. Yost., "Quantitative Analysis of Cytoskeletal Remodeling in Vascular Smooth muscle Cells During Phenotypic Modulation", *Computers in Cardiology*, Vol. 27, 205-206, 2000.
41. G. Csucs, R. Michel, J. W. Lussi, M. Textor, G. Danuser, "Microcontact printing of novel co-polymers in combination with proteins for cell-biological applications", *Biomaterials*, Vol. 24, n. 10, 1713-1720(8), 2003.
42. J. D. Mendelsohn, C. J. Barrett, V. V. Chan, A. J. Pal, A. M. Mayes and M. F. Rubner, "Fabrication of Microporous Thin Films from Polyelectrolyte Multilayers", *Langmuir*, Vol. 16 (11), 5017 -5023, 2000.
43. D. L. Elbert, C. B. Herbert and J. A. Hubbell, "Thin Polymer Layers Formed by Polyelectrolyte Multilayer Techniques on Biological Surfaces", *Langmuir*, Vol. 15(16), 5355-5362, 1999.
44. Y. M. Lvov, K. Ariga, I. Ichinose, T. Kunitake, "Assembly of Multicomponent Protein Films by Means of Electrostatic Layer-by-Layer Adsorption", *J. Am. Chem. Soc.*, 1Vol. 17, 6117-6123, 1995.
45. Y. M. Lvov, "Electrostatic Layer-by-Layer Assembly of Proteins and Polyions, In book: Protein Architecture: Interfacial Molecular Assembly and Immobilization Biotechnology", Ed: Y.M. Lvov and H. Möhwald, M.Dekker Publ., New York, 125-167, 2000.

46. P. He, N. Hu and G. Zhou, "Assembly of Electroactive Layer-by-Layer Films of Hemoglobin and Polycationic Poly(diallyldimethylammonium)", *Biomacromolecules*, Vol. 3(1), 139 -146, 2002.
47. S. Kaihara, J. Borenstein, R. Koka, S. Lalan, E. R. Ochoa, M. Ravens, H. Pien, B. Cunningham, and J. P. Vacanti, "Silicon Micromachining To tissue Engineer Branched Vascular Channels for Liver Fabrication", *Tissue Engineering*, Vol. 6(2), 105-117, 2000.
48. J. Deutsch, D. Motlagh, B. Russell, and T. A. Desai, "Fabrication of Microtextured Membranes for Cardiac Myocyte Attachment and Orientation", *Journal of Biomedical Materials Research*, Vol. 53, 267-275, 2000.
49. T. Matsuda and Y. Nakayama, "Surface microarchitectural design in biomedical applications: *In vitro* transmural endothelialization on microporous segmented polyurethane films fabricated using an excimer laser", *Journal of Biomedical Materials Researc.*, Vol. 31, 235-242, 1996.
50. G. D. Pins, M. Toner, and J. R. Morgan, "Microfabrication of an analog of the basal lamina: biocompatible membranes with complex topographies", *FASEB Journal*, Vol. 14, 593-602, 2000.
51. J. Tan, H. Shen, K. L. Carter, and W. Mark Saltzman, "Controlling human polymorphonuclear leukocytes motility using microfabrication technology", *Journal of Biomedical Materials Research*, Vol. 51, 694-702, 2000.
52. J. R. Anderson, D. T. Chiu, R. J. Jackman, O. Cherniavskaya, J. C. McDonald, H. Wu, S. H. Whitesides, and G. M. Whitesides, "Fabrication of Topologically Complex Three-Dimensional Microfluidic Systems in PDMS by Rapid Prototyping", *Analytical Chemistry*, Vol. 72, 3158-3164, 2000.
53. D. C. Duffy, J. C. McDonald, O. J. A. Schueller, and G. M. Whitesides, "Rapid Prototyping of Microfluidic Systems in Poly(dimethylsiloxane)", *Analytical Chemistry*, Vol. 70, 4974-4984, 1998.
54. A. W. Feinberg, C. A. Seegert, A. L. Gibson, A. B. Brennan, "Engineering micrometer and nanometer scale features in polydimethylsiloxane elastomers for controlled cell function", *Materials Research Society Symposium - Proceedings*, Vol. 711, 181-186, 2002
55. J. T. Elliott, A. Tona, J. T. Woodward, P. L. Jones, A. L. Plant, "Thin Films of Collagen Affect Smooth muscle Cell Morphology", *Langmuir*, Vol.19 (5), 1506 - 1514, 2003.
56. Y. Ito, "Surface micropatterning to regulate cell functions", *Biomaterials*, Vol. 20. 2333-2342, 1999.

57. J. H. Fitton, B. A. Dalton, G. Beumer, G. Johnson, H. J. Griesser, J. G. Steele, "Surface topography can interfere with epithelial tissue migration", *Journal of Biomedical Material Research*, Vol. 42, 245-57, 1998.
58. J. H. Lee, S. J. Lee, G. Khang, H. B. Lee, "Interaction of fibroblasts on polycarbonate membrane surfaces with different micropore sizes and hydrophilicity". *Journal of Biomaterials Science Polymer Edition*, Vol. 10, 283-94, 1999.
59. T. G. van Kooten, J. F. Whitesides, A. F. von Recum, "Influence of silicone (PDMS) surface texture on human skin fibroblast proliferation as determined by cell cycle analysis", *Journal of Biomedical Material Research*, Vol. 43, 1-14, 1998.
60. T. S. T. Matsuda, "Development of surface photochemical modification method for micropatterning of cultured cells", *Journal of Biomedical Material Research*, Vol. 29: 749-56, 1995.
61. N. Dontha, W. B. Nowall, and W. G. Kuhr, "Generation of biotin/avidin/enzyme nanostructures with maskless photolithography", *Analytical Chemistry*, Vol. 69(14), 1997.
62. K. M. DeFife, E. Colton, Y. Nakayama, T. Mastuda, J. M. Anderson, "Spatial regulation and surface chemistry control of monocyte/macrophage adhesion and foreign body giant cell formation by photochemically micropatterned surface", *Journal of Biomedical Material Research*, Vol. 45: 148-54, 1999.
63. H. Mirzadeh, M. Dadsetan, "Influence of laser surface modifying of polyethylene terephthalate on fibroblast cell adhesion", *Radiation Physics and Chemistry*, Vol. 67, no. 3, 381-385(5), 2003.
64. M. V. Risbud, R. Dabhade, S. Gangal, R. R. Bhonde, "Radio-frequency plasma treatment improves the growth and attachment of endothelial cells on poly(methyl methacrylate) substrates: implications in tissue engineering", *Journal of Biomaterials Science, Polymer Edition*, Vol. 13, n. 10, 1067-1080(14), 2002.
65. Y. Zhu, C. Gao, J. Shen, "Surface modification of polycaprolactone with poly(methacrylic acid) and gelatin covalent immobilization for promoting its cytocompatibility", *Biomaterials*, Vol. 23, n. 24, 4889-4895(7), 2002.
66. F. R. Pu; Williams R.L.; Markkula T.K.; Hunt J.A., "Effects of plasma treated PET and PTFE on expression of adhesion molecules by human endothelial cells in vitro", *Biomaterials*, Vol. 23, n. 11, 2411-2428(18), 2002.
67. S. Metz, M. O. Heuschkel, B. Valencia Avila, R. Holzer, D. Bertrand, Renaud, "Microelectrodes with three-dimensional structures for improved neural interfacing", *Annual Reports of the Research Reactor Institute*, Vol. 1, 765-768, 2001.

68. X. Liu, R. McC, B. Douglas, R. R. Carter, L. A. Bullara, T. G. H. Yuen, W. F. Agnew, "Stability of the interface between neural tissue and chronically implanted intracortical microelectrodes", *IEEE Transactions on Rehabilitation Engineering*, Vol. 7, n 3, 315-326, 1999.
69. X. T. Cui, D. C. Martin, "Surface modification of neural recording microelectrodes with conducting polymers", *Materials Research Society Symposium - Proceedings*, Vol. 698, 101-106, 2002
70. G. W. Brodland, H. H. Chen, "Mechanics of cell sorting and envelopment", *Journal of Biomechanics*, Vol. 33, n 7, 845-851, 2000.
71. H. Chen, H. Chang, "Electrophoretic separation of small DNA fragments in the presence of electroosmotic flow using poly(ethylene oxide) solutions", *Analytical Chemistry*, Vol. 71, n. 10, 2033-2036, 1999.
72. M. Zborowski, L. Sun, L. R. Moore, J. J. Chalmers, "Rapid cell isolation by magnetic flow sorting for applications in tissue engineering", *ASAIO Journal*, Vol. 45, n 3, 127-130, 1999.
73. C. S. Chen, M. Mrksich, S. Huang, G. M. Whitesides, D. E. Ingber, "Micropatterned surfaces for control of cell shape, position, and function", *Biotechnology Progress*, Vol. 14, n 3, 356-363, 1998.
74. D. E. Ingber, "Engineering cell shape and function through control of substrate adhesion", *Polymer Surfaces and Interfaces: Characterization, Modification and Application*, 413, 1997.
75. A. Folch and M. Toner, "Microengineering of cellular interactions", *Annu. Rev. Biomed. Eng.*, Vol.2, 227-256, 2000.
76. J. T. Elliott, A. Tona, J. T. Woodward, P. L. Jones, A. L. Plant, "Thin Films of Collagen Affect Smooth muscle Cell Morphology", *Langmuir*, Vol.19 (5), 1506 - 1514, 2003.
77. M. Radhika, M. Babu, P. K. Sehgal, "Cellular proliferation on desamidated collagen matrices", *Comparative Biochemistry and Physiology -- Part C: Pharmacology, Toxicology and Endocrinology*, Vol.124(2), 131-139, 1999.
78. S. N. Stephansson, B. A. Byers, A. J. Garca, "Enhanced expression of the osteoblastic phenotype on substrates that modulate fibronectin conformation and integrin receptor binding", *Biomaterials*, Vol. 23(12), 2527-2534, 2002.
79. K. E. Healy, "Molecular engineering of materials for bioreactivity", *Curr. Opin. Solid State Mater. Sci.*, Vol. 4, 381-387, 1999.

80. J. M. Anderson, "Biological Responses to Materials", *Annu. Rev. Mater. Res.*, Vol. 31, 81-110, 2001.
81. C. D. McFarland, *et al.*, "Protein adsorption and cell attachment to patterned surfaces", *Journal of Biomedical Materials Research*, Vol. 49: 200-210, 2000.
82. J. Hyun, H. Ma, Z. Zhang, T. P. Beebe, and A. Chilkoti, "Universal Route to Cell Micropatterning Using an Amphiphilic Comb Polymer", *Advanced Materials*, Vol. 15, n. 7-8, 576-579, 2003.
83. P. T. Hammond and G. M. Whitesides, "Formation of Polymer Microstructures by Selective Deposition of Polyion Multilayers Using Patterned Self-Assembled Monolayers as a Template", *Macromolecules*, Vol. 28, 7569-71, 1995.
84. Y. Wang, W. Du, W. B. Spillman and R. O. Claus, "Biocompatible Thin Film Coatings Fabricated Using the Electrostatic Self-Assembly Process", *Biomedical Instrumentation Based on Micro- and Nanotechnology, Proceedings of SPIE*, Vol. 4265, pp.142-151, 2001.
85. B. T. Houseman and M. Mrksich, "The Role of Ligand Density in the Enzymatic Glycosylation of Carbohydrates Presented on Self-Assembled Monolayers of Alkanethiolates on Gold", *Angew. Chem., Int. Ed. Engl.*, Vol. 38, 782-785, 1999.
86. C. S. Kwok, P. D. Mourad, L. A. Crum and B. D. Ratner, "Surface Modification of Polymers with Self-Assembled Molecular Structures: Multitechnique Surface Characterization", *Biomacromolecules*, Vol. 1(1), 139 -148, 2000.
87. M. N. Yousaf, M. Mrksich, "Diels-Alder Reaction for the Selective Immobilization of Protein to Electroactive Self-Assembled Monolayers", *J. Am. Chem. Soc.*, Vol. 121, 4286-4287, 1999.
88. C. H. Hodneland, M. Mrksich, "Biomolecular Surfaces that Release Ligands under Electrochemical Control", *J. Am. Chem. Soc.*, Vol. 122, 4235-4236, 2000.
89. Y. M. Lvov and G. Decher, "Assembly of Multilayer Ordered Films by Alternating Adsorption of Oppositely Charged Macromolecules", *Crystallography Reports*, Vol. 39, 696-716, 1993.
90. I. P. Hayward, K. R. Bridle, G. R. Campbell, P. A. Underwood and J. H. Campbell, "Effect of Extracellular Matrix Proteins on Vascular Smooth muscle Cell Phenotype", *Cell Biology International*, Vol.19, n.10, pp839-846, 1995.
91. L. Griscorn, P. Degenaar, M. Denoual, and F. Morin, Culturing of Neurons in Microfluidic Arrays, *Proceedings of 2nd Annual International IEEE-EMBS Special Topic Conference on Microtechnologies in Medicine and Biology*, Madison, MI, USA, May 2-4, 2002, 160-163, 2002.

92. D. T. Chiu, N. L. Jeon, S. Huang, R. S. Kane, C. J. Wargo, I. S. Choi, D. E. Ingber and G. M. Whitesides, "Patterned Deposition of cells and Proteins onto Surfaces by Using Three-dimensional Microfluidic Systems", *Applied Physical Sciences*, Vol. 97, 2408-2413, 2000.
93. C. H. Thomas, J. -B. Lhoest, D. G. Castner, C. D. McFarland, and K. E. Healy, "Surfaces Designed to Control the Projected Area and Shape of Individual Cells", *Transactions of the ASME*, Vol. 121, 40-48, 1999.
94. J. V. Moyano, A. Maqueda, J. P. Albar, A. Garcia-Pardo, "A Synthetic Peptide from the Heparin-Binding Domain III (Repeats III4-5) of Fibronectin Promotes Stress-Fibre and Focal-Adhesion Formation in Melanoma Cells", *Biochemical Journal*, Vol. 371, 565-571, 2003.
95. A. Ramamurthi, I. Vesely, "Smooth muscle Cell Adhesion on Crosslinked Hyaluronan Gels", *Journal of Biomedical Materials Research*, Vol. 60, 196-205, 2002.
96. A. S. Goldstein, P. A. Dimilla, "Effect of Adsorbed Fibronectin Concentration on Cell Adhesion and Deformation under Shear on Hydrophobic Surfaces", *Journal of Biomedical Materials Research*, Vol. 59, 665-675, 2002.
97. V. Marchi-Artzner, B. Lorz, U. Hellerer, M. Kantlehner, H. Kessler, E. Sackmann, "Selective Adhesion of Endothelial Cells to Artificial Membranes with A Synthetic RGD-Lipopeptide", *Chemistry - A European Journal*, Vol. 7, 1095-1101, 2001.
98. H. Ai, Y. M. Lvov, D. K. Mills, and S. A. Jones, "Micropatterning of Micro/Nanospheres on PDMS by Using Layer-by-Layer Self-Assembly", *Proceedings of 2nd Annual International IEEE-EMBS Special Topic Conference on Microtechnologies in Medicine and Biology*, Madison, MI, USA, May 2-4, 2002, 144-147, 2002.
99. B. C. Wheeler, J. M. Corey, G. J. Brewer and D. W. Branch, "Microcontact Printing for Precise Control of Nerve Cell Growth in Culture", *Journal of Biomechanical Engineering*, Vol.121, pp.73-78, 1999.
100. M. Li, K. K. Kondabatni, T. Cui and M. J. McShane, "Fabrication of 3-D Gelatin-patterned Glass Substrates with Layer-by-Layer and Lift-Off (LbL-LO) Technology", *IEEE Transactions on Nanotechnology*, submitted, 2003.
101. F. Hua, T. Cui, and Y. M. Lvov, "Lithographic Approach to Pattern Self-Assembled Multilayers", *Langmuir*, Vol. 18, 6712-6715, 2002.

- 102.F. Hua, Y. M. Lvov and T. Cui, "Spatial Patterning of Colloidal Nanoparticle-based Thin Film by a Combinative Technique of Layer-by-layer Self-assembly and Lithography", *Journal of Nanoscience and Nanotechnology*, Vol.2, No.3, 357-361, 2002.
- 103.F. Hua, J. Shi, Y. M. Lvov, and T. Cui, "Patterning of Layer-by-layer Self-assembled Multiple Types of Nanoparticle Thin Films by Lithographic Technique", *Nano Letters*, Vol.2, No.11, 1119-1222, 2002.
- 104.D. Wisser, J. Steffes, "Skin replacement with a collagen based dermal substitute, autologous keratinocytes and fibroblasts in burn trauma", *Burns*, Vol. 29, n. 4, 375-380(6), 2003.
- 105.R. Wiechula, "The use of moist wound-healing dressings in the management of split-thickness skin graft donor sites: a systematic review", *International Journal of Nursing Practice*, Vol. 9, n. 2, S9-S17(1), 2003.
- 106.B. A. Rubis, D. Danikas, M. Neumeister, W.G. Williams, H. Suchy, S.M. Milner, "The use of split-thickness dermal grafts to resurface full thickness skin defects", *Burns*, Vol. 28, no. 8, 752-759(8), 2002.
- 107.B. P. Chan, I. E. Kochevar, R. W. Redmond, "Enhancement of Porcine Skin Graft Adherence Using a Light-Activated Process", *Journal of Surgical Research*, Vol. 108, no. 1, 77-84(8), 2002.
- 108.A. Kinsner, E. Lesiak-Cyganowska, D. Śladowski, "In vitro reconstruction of full thickness human skin on a composite collagen material", *Cell and Tissue Banking*, Vol. 2, no. 3, 165-171(7), 2001.
- 109.Y. M. Bello, A. F. Falabella, W. H. Eaglstein, "Tissue-Engineered Skin: Current Status in Wound Healing", *American Journal of Clinical Dermatology*, Vol. 2, no. 5, 305-313(9), 2001.
- 110.B. L. Seal, T. C. Otero, A. Panitch, "Polymeric biomaterials for tissue and organ regeneration", *Materials Science and Engineering: R: Reports*, Vol. 34, no. 4, 147-230(84), 2001.
- 111.T. W. Lin, "An alternative method of skin grafting: the scalp microdermis graft", *Burns*, Vol. 21, no. 5, 374-378(5), 1995.
- 112.E. Khor, L. Y. Lim, "Implantable applications of chitin and chitosan", *Biomaterials*, Vol. 24, no. 13, 2339-2349(11), 2003.
- 113.M. D. Timmer, C. G. Ambrose, A. G. Mikos, "In vitro degradation of polymeric networks of poly(propylene fumarate) and the crosslinking macromer poly(propylene fumarate)-diacrylate", *Biomaterials*, Vol. 24, no. 4, 571-577(7), 2003.

- 114.D. H. Carter, A. J. Scully, D. A. Heaton, M. P. J. Young, J. E. Aaron, "Effect of deproteination on bone mineral morphology: implications for biomaterials and aging", *Bone*, Vol. 31, no. 3, 389-395(7), 2002.
- 115.S. C. Mendes, M. Sleijster, A. van den Muysenberg, J. D. de Bruijn, C. A. van Blitterswijk, "A cultured living bone equivalent enhances bone formation when compared to a cell seeding approach", *Journal of Materials Science: Materials in Medicine*, Vol. 13, no. 6, 575-581(7), 2002.
- 116.L. C. Jones, C. Frondoza, D. S. Hungerford, "Effect of PMMA particles and movement on an implant interface in a canine model", *The Journal of Bone and Joint Surgery*, Vol. 83, no. 3, 448-458(11), 2001.
- 117.K. S. Khan, P. M. O Connell, D. A. O Farrell, "Muscle strength following anterior cruciate ligament reconstruction: comparison between hamstring and patellar tendon graft", *Irish Journal of Medical Science*, Vol. 172, no. 1, 51, 2003.
- 118.Y. Oya, S. Kobayasi, K. Nakanura, J. Shimizu, S. Murayama, I. Kanazawa, "Skeletal muscle pathology of chronic graft versus host disease accompanied with myositis, affecting predominantly respiratory and distal muscles, and hemosiderosis", *Clinical Neurology*, Vol. 41, no. 9, 612-616, 2001.
- 119.A. Amore, P. Cirina, M. Chiesa, G. Conti, L. Peruzzi, R. Coppo, "Graft endothelium and chronic allograft nephropathy: insight from in vitro trans-differentiation of smooth muscle cells induced by mismatched lymphocytes", *Transplantation Proceedings*, Vol. 33, no. ER7-8, pp. 3347-3348, 2001.
- 120.K. Kurotobi, Y. Suzuki, M. Kaibara, M. Iwaki, H. Nakajima, H. Suzuki, "In Vitro and In Vivo Study of Ion-Implanted Collagen for the Substrate of Small Diameter Artificial Grafts", *Artificial Organs*, Vol. 27, no. 6, pp. 582-586(5), 2003.
- 121.S. L. Mitchell, L. E. Niklason, "Requirements for growing tissue-engineered vascular grafts", *Cardiovascular Pathology*, Vol. 12, no. 2, pp. 59-64(6), 2003.
- 122.R. R. Mitry, R. D. Hughes, M. M. Aw, C. Terry, G. Mieli-Vergani, R. Girlanda, P. Muiesan, M. Rela, N. D. Heaton, A. Dhawan, "Human Hepatocyte Isolation and Relationship of Cell Viability to Early Graft Function", *Cell Transplantation*, Vol. 12, no. 1, 69-74(6), 2003.
- 123.K. Kosaka, H. Fujiwara, K. Tatsumi, S. Yoshioka, T. Higuchi, Y. Sato, T. Nakayama, S. Fujii, "Human peripheral blood mononuclear cells enhance cell-cell interaction between human endometrial epithelial cells and BeWo-cell spheroids", *Human Reproduction*, Vol. 18, no. 1, 19-25(7), 2003.

- 124.T. Yamamoto, K. Hartmann, B. Eckes, T. Krieg, "Mast cells enhance contraction of three-dimensional collagen lattices by fibroblasts by cell-cell interaction: role of stem cell factor/c-kit", *Immunology*, Vol. 99, no. 3, 435-439(5), 2000.
- 125.M. Montes, D. McIlroy, A. Hosmalin, A. Trautmann, "Calcium responses elicited in human T cells and dendritic cells by cell-cell interaction and soluble ligands", *International Immunology*, Vol. 11, no. 10, 1725-1726(2), 1999.
- 126.C. Armour, K. Garson, M. W. McBurney, "Cell-Cell Interaction Modulates myoD-Induced Skeletal Myogenesis of Pluripotent P19 Cells *in Vitro*", *Experimental Cell Research*, Vol. 251, no. 1, 79-91(13), 1999.
- 127.S. Donadio, C. Dubois, G. Fichant, L. Roybon, J. C. Guillemot, C. Breton, C. Ronin, "Recognition of cell surface acceptors by two human α -2,6-sialyltransferases produced in CHO cells", *Biochimie*, Vol. 85, no. 3, 311-321(11), 2003.
- 128.S. Godefroy, N. Corvaia, D. Schmitt, J. Aubry, J. Bonnefoy, P. Jeannin, M. Staquet, "Outer membrane protein A (OmpA) activates human epidermal Langerhans cells", *European Journal of Cell Biology*, Vol. 82, no. 4, pp. 193-200(8), 2003.
- 129.R. Casadio, M. Compiani, A. Facchiano, P. Fariselli, P. Martelli, I. Jacoboni, I. Rossi, "Protein structure prediction and biomolecular recognition: from protein sequence to peptidomimetic design with the human β 3 integrin", *SAR and QSAR in Environmental Research*, Vol. 13, no. 3-4, pp. 473-486(14), 2002.
- 130.V. Das, B. Nal, A. Roumier, V. Meas-Yedid, C. Zimmer, J. Olivo-Marin, P. Roux, P. Ferrier, A. Dautry-Varsat, A. Alcover, "Membrane-cytoskeleton interactions during the formation of the immunological synapse and subsequent T-cell activation", *Immunological Reviews*, Vol. 189, no. 1, pp. 123-135(13), 2002.
- 131.X. Fernandez-Busquets, W. J. Kuhns, T. L. Simpson, M. Ho, D. Gerosa, M. Grob, M. M. Burger, "Cell adhesion-related proteins as specific markers of sponge cell types involved in allogeneic recognition", *Developmental and Comparative Immunology*, Vol. 26, no. 4, pp. 313-323(11), 2002.
- 132.L. Mulard, "Proteoglycans", *Biochimie*, Vol. 78, no. 3, pp. 215-216(2), 1996.
- 133.R. Gorodetsky, A. Vexler, M. Shamir, J. An, L. Levdansky, I. Shimeliovich, G. Marx, "New cell attachment peptide sequences from conserved epitopes in the carboxy termini of fibrinogen", *Experimental Cell Research*, Vol. 287, no. 1, 116-129(14), 2003.
- 134.X. Lu, D. Lu, M. F. Scully, V. V. Kakkar, "Modulation of Integrin-binding Selectivity by Mutation within the RGDLoop of Snake Venom Proteins: A Novel Drug Development Approach", *Current Medicinal Chemistry - Cardiovascular & Hematological Agents*, Vol. 1, no. 2, 189-196(8), 2003.

- 135.B. Felding-Habermann, "Integrin adhesion receptors in tumor metastasis", *Clinical and Experimental Metastasis*, Vol. 20, no. 3, 203-213(11), 2003.
- 136.G. F. Guidetti, F. Greco, A. Bertoni, C. Giudici, M. Viola, R. Tenni, E. M. Tira, C. Balduini, M. Torti, "Platelet interaction with CNBr peptides from type II collagen via integrin $\alpha_2\beta_1$ ", *Biochimica et Biophysica Acta (BBA)/Molecular Cell Research*, Vol. 1640, no. 1, 43-51(9), 2003.
- 137.C. Yin, K. Liao, H. Mao, K. W. Leong, R. Zhuo, V. Chan, "Adhesion contact dynamics of HepG2 cells on galactose-immobilized substrates", *Biomaterials*, Vol. 24, no. 5, 837-850(14), 2003.
- 138.D. E. Solomon, "An in vitro examination of an extracellular matrix scaffold for use in wound healing", *International Journal of Experimental Pathology*, Vol. 83, no. 5, 209-216(8), 2002.
- 139.R. Lange, F. Luthen, U. Beck, J. Rychly, A. Baumann, B. Nebe, "Cell-extracellular matrix interaction and physico-chemical characteristics of titanium surfaces depend on the roughness of the material", *Biomolecular Engineering*, Vol. 19, no. 2, 255-261(7), 2002.
- 140.C. S. Izzard, L. R. Lochner., "Cell-to-substrate contacts in living fibroblasts: an interference reflexion study with an evaluation of the technique", *Journal of Cell Science*, Vol.21(1), 129-59, 1976.
- 141.J. Wehland, M. Osborn, K. Weber, "Cell-to-substratum contacts in living cells: a direct correlation between interference-reflection and indirect-immuno-fluorescence microscopy using antibodies against actin and alpha-actinin", *Journal of Cell Science*, Vol. 37, 257-73, 1979.
- 142.L. Leyton, P. Schneider, C. V. Labra, C. Ruegg, C. A. Hetz, A. F. G. Quest, C. Bron, "Thy-1 binds to integrin β_3 on astrocytes and triggers formation of focal contact sites", *Current Biology*, Vol. 11, no. 13, 1028-1038(11), 2001.
- 143.T. Sugiyama, Y. Matsuda, K. Mikoshiba, "Inositol 1,4,5-trisphosphate receptor associated with focal contact cytoskeletal proteins", *FEBS Letters*, Vol. 466, no. 1, 29-34(6), 2000.
- 144.T. E. O'Toole, "Integrin signaling: Building connections beyond the focal contact?", *Matrix Biology*, Vol. 16, no. 4, 165-171(7), 1997.
- 145.S. Manenti, F. Malecaze, J. M. Darbon, "The major myristoylated PKC substrate (MARCKS) is involved in cell spreading, tyrosine phosphorylation of paxillin, and focal contact formation", *FEBS Letters*, Vol. 419, no. 1, 95-98(4), 1997.

- 146.E. Oberdörster, D. M. Cottam, F. A. Wilmot, M. J. Milner, J. A. McLachlan, "Interaction of PAHs and PCBs with Ecdysone-Dependent Gene Expression and Cell Proliferation", *Toxicology and Applied Pharmacology*, Vol. 160, no. 1, 101-108(8), 1999.
- 147.M. Napolitano, D. Bellavia, M. Maroder, M. Farina, A. Vacca, L. Frati, A. Gulino, I. Screpanti, "Modulation of cytokine gene expression by thymic lympho-stromal cell to cell interaction: effect of retinoic acid", *Thymus*, Vol. 24, no. 4, pp. 247-258(12), 1997.
- 148.J. W. Lim, H. Kim, K. H. Kim, "Cell adhesion-related gene expression by *Helicobacter pylori* in gastric epithelial AGS cells", *The International Journal of Biochemistry and Cell Biology*, Vol. 35, no. 8, pp. 1284-1296(13), 2003.
- 149.I. Takahashi, K. Onodera, Y. Sasano, I. Mizoguchi, J. W. Bae, H. Mitani, M. Kagayama, H. Mitani, "Effect of stretching on gene expression of $\beta 1$ integrin and focal adhesion kinase and on chondrogenesis through cell-extracellular matrix interactions", *European Journal of Cell Biology*, Vol. 82, no. 4, pp. 182-192(11), 2003.
- 150.N. Boudreau and M. Bissell, "Extracellular matrix signaling: integration of form and function in normal and malignant cells", *Current Opinion in Cell Biology*, Vol. 10, 640-646, 1998.
- 151.W. G. Hill, G. S. Harper, T. Rozaklis, J. J. Hopwood, "Sulfation of Chondroitin/Dermatan Sulfate by Cystic Fibrosis Pancreatic Duct Cells Is Not Different from Control Cells", *Biochemical and Molecular Medicine*, Vol. 62, no. 1, 85-94(10), 1997.
- 152.A. Huttenlocher, R. R. Sandborg and A. F. Horwitz, "Adhesion in cell migration", *Current Opinion in Cell Biology*, Vol. 7, 697-706, 1995.
- 153.K. Van Oostveldt, M. J. Paape, H. Dosogne, C. Burvenich, "Effect of apoptosis on phagocytosis, respiratory burst and CD18 adhesion receptor expression of bovine neutrophils", *Domestic Animal Endocrinology*, Vol. 22, no. 1, 37-50(14), 2002.
- 154.A. Mezzogiorno, V. Esposito, "Potential Role for High and Low Molecular Weight Tissue Transglutaminases in Transforming Mammalian Cell Properties, Current Drug Targets – Immune", *Endocrine & Metabolic Disorders*, Vol. 1, no. 3, 223-232(10), 2001.
- 155.C. Miller, S. Jeftinija, S. Mallapragada, "Micropatterned Schwann Cell-Seeded Biodegradable Polymer Substrates Significantly Enhance Neurite Alignment and Outgrowth", *Tissue Engineering*, Vol. 7, no. 6, 705-715(11), 2001.

- 156.C. Neidlinger-Wilke, E. Grood, L. Claes, R. Brand, "Fibroblast orientation to stretch begins within three hours", *Journal of Orthopaedic Research*, Vol. 20, no. 5, 953-956(4), 2002.
- 157.C. Neidlinger-Wilke, E. S. Grood, J. H. Wang, R. A. Brand, L. Claes, "Cell alignment is induced by cyclic changes in cell length: studies of cells grown in cyclically stretched substrates", *Journal of Orthopaedic Research*, Vol. 19, no. 2, 286-293(8), 2001.
- 158.J. H. Wang, E. S. Grood, J. Florer, R. Wenstrup, "Alignment and proliferation of MC3T3-E1 osteoblasts in microgrooved silicone substrata subjected to cyclic stretching", *Journal of Biomechanics*, Vol. 33, no. 6, 729-735(7), 2000.
- 159.K. Takakuda, H. Miyairi, "Tensile behaviour of fibroblasts cultured in collagen gel", *Biomaterials*, Vol. 17, no. 14, 1393-1397(5), 1996.
- 160.J. H. Wang, F. Jia, T. W. Gilbert, S. L. Woo, "Cell orientation determines the alignment of cell-produced collagenous matrix", *Journal of Biomechanics*, Vol. 36, no. 1, 97-102(6), 2003.
- 161.E. Eisenbarth, P. Linez, V. Biehl, D. Velten, J. Breme, H. F. Hildebrand, "Cell orientation and cytoskeleton organisation on ground titanium surfaces", *Biomolecular Engineering*, Vol. 19, no. 2, 233-237(5), 2002.
- 162.T. L. Shen, J. L. Guan, "Differential regulation of cell migration and cell cycle progression by FAK complexes with Src, PI3K, Grb7 and Grb2 in focal contacts", *FEBS Letters*, Vol. 499, no. 1, 176-181(6), 2001.
- 163.V. Petit, J. P. Thiery, "Focal adhesions: structure and dynamics", *Biology of the Cell*, Vol. 92, no. 7, 477-494(18), 2000.
- 164.S. E. Mutsaers, J. E. Bishop, G. McGrouther, G. J. Laurent, "Mechanisms of Tissue Repair: from Wound Healing to Fibrosis", *The International Journal of Biochemistry and Cell Biology*, Vol. 29, no. 1, 5-17(13), 1997.
- 165.R. J. Faull, J. M. Stanley, S. Fraser, D. A. Power, D. I. Leavesley, "HB-EGF is produced in the peritoneal cavity and enhances mesothelial cell adhesion and migration", *Kidney International*, Vol. 59, no. 2, 614-624(11), 2001.
- 166.M. A. Kharitonova, E. M. Levina, Y. A. Rovensky, "Cytoskeletal Control of Cell Length Regulation", *Russian Journal of Developmental Biology*, Vol. 33, no. 1, 43-51(9), 2002.
- 167.C. G. Galbraith, M. P. Sheetz, "Forces on adhesive contacts affect cell function", *Current Opinion in Cell Biology*, Vol. 10, no. 5, pp. 566-571(6), 1998.

- 168.J. Bartkova, B. Gron, E. Dabelsteen, J. Bartek, "Cell-cycle regulatory proteins in human wound healing", *Archives of Oral Biology*, Vol. 48, no. 2, pp. 125-132(8), 2003.
- 169.L. J. Smink, "Acetylation can regulate cell-cycle progression", *Trends in Molecular Medicine*, Vol. 7, no. 9, pp. 384-384(1), 2001.
- 170.E. Ruoslahti, J. C. Reed 1994. "Anchorage dependence, integrins, and apoptosis", *Cell*, Vol. 77(4), 477-78, 1994.
- 171.E. Ruoslahti, A. Vaheri, "Cell-to-cell contact and extracellular matrix", *Current Opinion in Cell Biology*, Vol. 9, no. 5, 605-607(3), 1997.
- 172.S. S. Shiratori, M. F. Rubner, "pH-Dependent Thickness Behavior of Sequentially Adsorbed Layers of Weak Polyelectrolytes", *Macromolecules*, Vol. 33, 4213-4219, 2000.
- 173.Y. Lvov, Z. Lu, X. Zu, J. Schenkman, J. Rusling, "Direct electrochemistry of myoglobin and cytochrome P450cam in alternate layer-by-layer films with DNA and other polyions", *J. Am. Chem Soc.*, Vol.120, 4073-4080, 1998.
- 174.H. Ai, M. Fang, S. Jones, Y. Lvov, "Electrostatic Layer-by-Layer Nano-Assembly on Biological Microtemplates: Platelets", *Biomacromolecules*, Vol.3, 560-564, 2002.
- 175.M. Ferreira, J. H. Ceung, M. F. Rubner, "Molecular self-assembly of conjugated polyions: a new process for fabricating multilayer thin film heterostructures", *Thin Solid Films*, Vol. 244, 806-809, 1994.
- 176.P. Leclere, A. Calderone, K. Mullen, J. L. Bredas, R. Lazzaroni, "Conjugated polymer chains self-assembly: a new method to generate (semi)-conducting nanowires?", *Materials Science and Technology*, Vol. 18, no. 7, 749-754, 2002.
- 177.S. Ghosh, J. Rasmusson, O. Inganas, "Supromolecular Self-Assembly for Enhanced Conductivity in Conjugated Polymer Blends: Ionic Crosslinking in Blends of Poly(3,4-ethylenedioxythiophene)-Poly(styrenesulfonate) and Poly(vinylpyrrolidone)", *Advanced materials*, Vol. 10, no. 14, 1097, 1998.
- 178.K. Ariga, Y. Lvov, T. Kunitake, "Assembling alternate dye-polyion molecular films by electrostatic layer-by-layer adsorption", *J. Am. Chem. Soc.*, Vol. 119, 2224-2231, 1997.
- 179.K. Ariga, M. Onda, Y. Lvov, T. Kunitake, "Alternate layer-by-layer assembly of organic dye and proteins is facilitated by premixing with polyions", *Chemistry Letters*, Vol. 26, 25-26, 1997.

- 180.T. M. Cooper, A. L. Campbell, R. L. Crane, "Formation of polypeptide-dye multilayers by electrostatic self-assembly technique", *Langmuir*, Vol.11, 2713-2718, 1995.
- 181.G. Decher, J. M. Calvert, J. Schmitt, "Metal Nanoparticle/Polymer Superlattice Films: Fabrication and Control of Layer Structure", *Advanced materials*, Vol. 9, no. 1, 61, 1997.
- 182.Y. Lvov, B. Munge, I. Ichinose, S. Suib, J. Rusling, "Films of manganese oxide nanoparticles with polycations and myoglobin from alternate-layer adsorption", *Langmuir*, Vol.16, 8850-8857, 2000.
- 183.X. Q. Zhang, Y. Wei, W. Y. Yang, X. Z. You, "Preparation and characterization of self-assembly organic multilayer films on silica surface", *Applied Surface Science*, Vol. 84, no. 3, pp. 267-271(5), 1995.
- 184.A. Singh, Y. Lvov, J-M. Lehn, "Formation of supramolecular assemblies by complementary association of octadecyloxy tartaric acid and bispyridyls", *Polymer Preprints*, Vol. 40, 1138-1139, 1999.
- 185.M. Onda, Y. Lvov, K. Ariga, T. Kunitake, "Molecularly flat films of linear polyions and proteins obtained by the alternate adsorption method", *Japan J. Appl. Physics*, Vol.36, L1608-1611, 1997.
- 186.D. Chang-Yen, Y. Lvov, M. McShane, B. Gale, "Electrostatic Self-Assembly of a Ruthenium-Based Oxygen Sensitive Dye", *Sensors and Actuators B*, Vol.87, 336-345, 2002.
- 187.M. Alloisio, S. Sottini, D. Cavallo, C. Dell'Erba, C. Cuniberti, G. Dellepiane, B. Gallot, "Self-assembly of polydiacetylene nanowires in ultra-thin films", *Materials Science and Engineering: C*, Vol. 23, no. 1, 297-300(4), 2003.
- 188.G. Decher, "Fuzzy Nanoassemblies: Toward Layered Polymeric Multicomposites", *Science*, Vol. 277, 1232-1237, 1997.
- 189.E. T. den Braber, H. V. Jansen, M. J. de Boer, H. J. E. Groes, M. Elwenspoek, L. A. Ginsel, J. A. Jansen, "Scanning electron microscopic, transmission electron microscopic, and confocal laser scanning microscopic observation of fibroblasts cultured on microgrooved surfaces of bulk titanium substrata", *J Biomed Mater Res.*, Vol. 40, 425-33, 1998.
- 190.T. Matsuda, K. Inoue, "Novel photoreactive surface modification technology for fabricated devices", *Trans Am Soc Artif Intern Organs*, Vol. 36, 161-4, 1990.

- 191.R. Shinghvi, A. Kumar, G. P. Lopez, G. N. Stephanopoulos, D. I. C. Wang, G. M. Whitesides, D. E. Ingber, "Engineering cell shape and function", *Science*, Vol. 264: 296-8, 1994.
- 192.C. S. Chen, M. Mrksich, S. Huang, G. M. Whitesides, D. E. Ingber, "Geometric control of cell life and death", *Science*, Vol. 276, 1425-8, 1997.
- 193.M. Mrksich, C. S. Chen, Y. Xia, L. E. Dike, D. E. Ingber, G. M. Whitesides, "Controlling cell attachment on contoured surfaces with self-assembled monolayers of alkanethiolates on gold", *Proc Natl Acad Sci USA*, Vol. 93, Vol. 10775-8, 1996.
- 194.P. Fromherz, H. Schaden, T. Vetter, "Guided outgrowth of leech neurons in culture", *Neurosci Lett*, Vol. 129, 77-80, 1991.
- 195.B. Lom, K. E. Healy, P. E. Hockberger, "A versatile technique for patterning biomolecules onto glass coverslips", *J Neurosci Meth*, Vol. 50, 385-97, 1993.
- 196.T. Sugawara, T. Matsuda, "Photochemical surface derivatization of a peptide containing Arg-Gly-Asp (RGD)", *Journal of Biomedical Materials Research*, Vol. 29, 1047-52, 1995.
- 197.M. Huber, P. Heiduschka, S. Kienle, C. Pavlidis, J. Mack, T. Walk, G. Jung, S. Thanos, "Modification of glassy carbon surfaces with synthetic laminin-derived peptides for nerve cell attachment and neurocite growth", *Journal of Biomedical Materials Research*, Vol. 41, 278-88, 1998.
- 198.A. S. Blawas, W. M. Reichert, "Protein Patterning", *Biomaterials*, Vol. 19, 595-609, 1998.
- 199.S. K. Ravi, S. Takayama, E. Ostuni, D. E. Ingber and G. M. Whitesides, "Patterning proteins and cells using soft lithography", *Biomaterials*, Vol. 20, 2363-2376, 1999.
- 200.L. Kam, S. G. Boxer, "Cell Adhesion to Protein-Micropatterned-Supported Lipid Bilayer Membranes", *Journal of Biomedical Materials Research*, Vol. 55, 487-495, 2001.
- 201.C. D. McFarland, C. H. Thomas, C. DeFilippis, J. G. Steele, K. E. Healy, "Protein adsorption and cell attachment to patterned surfaces", *Journal of Biomedical Materials Research*, Vol. 49, 200-210, 2000.
- 202.J. D. Bronzino, "The Biomedical Engineering Handbook, Section IV: Biomaterials", *CRC Press and IEEE Press*, 581-597, 1995.

- 203.K. D. Dee, D. A. Puleo, R. Bizios, "A Introduction to Tissue-Biomaterial Interactions", *Wiley-Liss*, 37-52, 2002.
- 204.N. A. Kotov, "Layer-by-Layer Self-Assembly: the contribution of hydrophobic interactions", *Nanostructured Materials*, Vol. 12, 789-796, 1999.
- 205.M. Madou, *Fundamentals of Microfabrication*, *CRC Press*, New York, 1997.
- 206.<http://www.dbanks.demon.co.uk/ueng/plith.html>.
- 207.<http://www.mal.eecs.uic.edu/eecs449/lectures/LIGA.html>.
- 208.<http://lmn.web.psi.ch/mntech/hotemb.htm>
- 209.<http://www.engr.washing.edu/~cam/Softlithdescription.html>.
210. <http://www.probes.com/handbook/>
- 211.J. R. Lakowicz, "Principles of Fluorescence Spectroscopy", *Kluwer Academic/Plenum Publishers*, 1999.
- 212.Q. Ye; G. Zund; S. Jockenhoewel, A. Schoeberlein, S. P. Hoerstrup, J. Grunenfelder, P. Benedikt, M. Turina, "Scaffold precoating with human autologous extracellular matrix for improved cell attachment in cardiovascular tissue engineering", *ASAIO Journal*, Vol. 46, n 6, p 730-733, 2000.

APPENDIX A

MATERIALS, CHEMICALS, AND SUPPLIES

A.1 Polyelectrolytes, Buffers, and Microspheres

- Poly(sodium 4-styrenesulfonate) (PSS), Average Mwca 1,000,000 powder, ALDRICH-434574, Aldrich Chem Co.
- Poly(diallyldimethylammonium chloride) (PDDA) solution, mol wt (high molecular weight) Average Mwca 400,000-500,000 20 wt. % in water, ALDRICH-409030, Aldrich Chem Co.
- Poly(allylamine hydrochloride) (PAH), Average Mwca 15,000 by GPC vs. PEG std., ALDRICH-283215, Aldrich Chem Co.
- Poly(ethyleneimine) solution (PEI, Ethyleneimine polymer solution), SIGMA-P3143, Sigma Chemical Co.
- Phosphate Buffered Saline (PBS) tablet, SIGMA-P4417, Sigma Chemical Co.
- Trizma[®]hydrochloride, reagent grade minimum99% (redox titration) crystalline, SIGMA-T3253, Sigma Chemical Co.
- Trizma[®]base, Primary Standard and Buffer minimum99.9% (titration) crystalline, SIGMA-T1503, Sigma Chemical Co.
- Potassium chloride (KCl), minimum99.0%, SIGMA-P4504, Sigma Chemical Co.
- Sodium bicarbonate (NaHCO₃), minimum99.5% crystalline, SIGMA-S8875, Sigma Chemical Co.
- Polystyrene Particles: Diameter 0.52 μm, Catalog # 1100-1197, SERADYN World Class Technology.
- Silica Particles: Diameter 0.2 μm, Catalog code SS02N, Bangs Laboratories, Inc.

A.2 Cell Culture Medium, Serum and Proteins

- HyQ[®]RPMI-1640 Medium Powder, with 2.05 mM L-glutamine, phenol red, no sodium bicarbonate, Catalog # SH30011.03, Hyclone.
- Hanks'Balanced Salt Solutions (HBSS), powder Modified cell culture, tested, SIGMA-H2387, Sigma Chemical Co.
- Fetal Bovine Serum (FBS) – Premium, Catalog # S11110, Atlanta biologicals.
- Antibiotic-Antimycotic (100X) (ABAM), Catalog # 15240062, Invitrogen Life Technologies.

- Trypsin, 2.5% (10X), Catalog # 15090046, Invitrogen Life Technologies.
- Gelatin bovine skin, Type B powder cell culture, tested, SIGMA-G9391, Sigma Chemical Co.
- Fibronectin (FN) from bovine plasma, Lyophilized powder cell culture, tested, SIGMA-F4759, Sigma Chemical Co.
- Anti-Vinculin, clone V284, CATALOG # 05-386, Upstate Cell Signaling Solutions.
- Albumin bovine serum (BSA), pH 7 minimum 98% (electrophoresis) Lyophilized powder, SIGMA-A7906, Sigma Chemical Co.
- Ribonuclease A from bovine pancreas, Lyophilized powder, SIGMA-R6513, Sigma Chemical Co.
- Poly-L-lysine hydrobromide (PLL), mol wt 70,000-150,000, SIGMA-P1274, Sigma Chemical Co.
- Triton[®]X-100, SIGMA-X100, Sigma Chemical Co.

A.3 Dyes and Fluorescence Labeled Probes

- Bis(2,2'-bipyridine)-4'-methyl-4-carboxybipyridine-ruthenium N-succinimidyl ester-bis (hexafluorophosphate) (Ru(bpy)₂(mcbpy-O-Su-ester)(PF₆)₂), FLUKA-96631, Fluka Chemical Co.
- Fluorescein isothiocyanate isomer I (FITC), suitable for protein labeling minimum 90% (HPLC) powder, SIGMA-F7250, Sigma Chemical Co.
- FluoSpheres[®] carboxylate-modified microspheres, 0.02 μm, yellow-green fluorescent (505/515), F-8787, Molecular Probes.
- Trypan Blue Solution (0.4%), SIGMA-T8154, Sigma Chemical Co.
- Vybrant[®] Apoptosis Assay Kit #5 Hoechst 33342/propidium iodide, V-13244, Molecular Probes.
- Alexa Fluor[®] 488 phalloidin, A-12379, Molecular Probes.
- N-(3-triethylammoniumpropyl)-4-(4-(dibutylamino)styryl)pyridinium dibromide (FM[®] 1-43), T-3163, Molecular Probes.
- Anti-Mouse IgG (Fc specific)-FITC antibody produced in goat, Affinity isolated antibody Buffered aqueous solution, SIGMA-4143, Sigma Chemical Co.

A.4 Photoresists, Chemicals and other Microfabrication Materials

- Positive photo resist S1813: MICROPOSIT[®] S1800[®] SERIES PHOTORESISTS, Shipley Company.
- Positive photo resist developer MF 319: MICROPOSIT[™] MF[™]-300 SERIES DEVELOPERS, Shipley Company.
- Negative photo resist SU-8 50: NANO[™]SU-8, MicroChem Inc.
- SU-8 developer and SU-8 2000 thinner: MicroChem Inc.
- N,N-Dimethylformamide (DMF), for molecular biology minimum 99%, SIGMA-D4551, Sigma Chemical Co.
- Polydimethylsiloxane (PDMS): SYLGARD[®] 184 SILICONE ELASTOMER KIT, Dow Corning Corporation.
- Poly(methyl methacrylate) (PMMA): ROHAGLAS[®] PMMA Film Clear 99530 (# 3055), CYRO Industries.
- Fisherbrand* Plain Glass Microslides, Catalog # 12-550A, Fisher Scientific International Inc.
- Fisherbrand* Cover Glasses, Catalog # 12-540A, Fisher Scientific International Inc

APPENDIX B

EQUIPMENT AND INSTRUMENTATION

B.1 Microfabrication Equipments

- Photoresist spinning, baking and development capabilities (CEE Model 1100)
- Dual-side Mask Aligner (Electronic Vision)
- Inductively Coupled Plasma Etch System (ICP, ALCATEL A601E)
- Hot-embossing Tool (JENOPTIK Microtechnik)
- Micro Reactive Ion Etcher (RIE, Technics Series 800)

B.2 Metrological Systems

- Scanning Electron Microscope (SEM, AMRAY model 1830)
- Stylus Profilometer (Tencor Alpha Step 500)
- Atomic Force Microscope (AFM, Q-Scope™ 350, Quesant Instrument Corporation).
- White light Interferometric Roughness-Step-Tester Microscope (WYKO RST Plus)
- Contact-Angle Measurement System (OCA, Data Physics, Future Digital Scientific Corp.)
- Zeta Potential Analyzer (Zeta Plus, Brookhaven Instruments Corp.)
- Quartz Crystal Microbalance (QCM, Iwatsu, SC-7201, Universal Counter)
- UV-Visible Spectrophotometer (Agilent Technologies)
- Fluorescence Spectrometer (QM-4, Photon Technology International)
- Hemocytometer (C.A. Hausser & Son)

B.3 Inspection Microscopes and Cameras

- Research System Microscope (OLYMPUS AX70)
- CCD Camera (SONY, CCD-IRIS)
- Inverted Epifluorescence Microscope (Nikon ECLIPSE TS100/TS100-F)
- Digital Camera (Nikon COOLPIX 995)

APPENDIX C

EXPERIMENTAL TECHNIQUES

C.1 Microfabrication Protocols

C.1.1 Generic PR 1813 photolithography

- Pretreatment: Nanostrip incubation at room temperature for 1 hour; or O₂ plasma, 250mTorr, 15msccm, 10min.
- Prebake: 165 °C, 10 minutes.
- Spin coating PR 1813: 1000 rpm, 100 r/s, 10 sec; 2000-3000 rpm, 500 r/s, 40-50 sec.
- Soft bake: 115 °C, 3-5 min
- Expose: Aligner UV, 8 sec; or UV lamp, 2 min
- Develop: MF 319, 1-2 min.
- Hard bake: 165 °C, 20 minutes.

C.1.2 Generic SU-8 25 photolithography

- Glass/silicon substrate pretreatment: incubation in nanostrip at room temperature for 1 hour.
- Prebake: 250 °C, 40 min.
- Spin coating SU-8: 1200 rpm, 300 r/s, 10 sec; 2000 rpm, 500 r/s, 30 sec.
- Soft bake: 65 °C, 20 min; ramp to 95 °C 30 min.
- Exposure: 50 sec.
- Post-exposure bake: 65 °C, 10 min; ramp to 95 °C, 20 min.
- Development: incubation in SU-8 developer for 1 min with inspection.
- Hard bake: 165 °C, 20 minutes.

C.1.3 Inductive Coupled Plasma (ICP) Etching

- Recipe: Bosch Big
- Power: 1800 W
- Bias: 30 W
- SF₆: 300 sccm / 7 sec
- C₄F₈: 50 sccm / 3 sec
- Time: 5 min

C.1.4 Hot Embossing

- Intialize ForceControl(true/false=0)
- Close Chamber()
- Heating(Top=130.0°C, Bottom=130.0°C)
- Wait Time(Time=60.00s)
- Position relative(Position=19.00000mm, Velocity=30.00000mm/min, MaxForce=3000N)
- Wait Time(Time=60.00s)
- Evacuate Chamber()
- Wait Time(Time=60.00s)
- Touch Force(Force=500N)
- Wait Time(Time=60.00s)
- Heating(Top=150.0°C, Bottom=135.0°C)
- Temperature>=(Temperature=130.0deg, Channel=10)
- Temper(Top=130.0deg,Bottom=130.0deg)
- Wait Time(Time=120.00s)
- Force-Force controled(Force=20000N, Velocity=0.500000mm/min)
- Wait Time(Time=120.00s)
- Cooling(Top=60.0deg,Bottom=60.0deg)
- Temperature<=(Temperature=80.0deg,Channel=12)
- DemoldingAdv(Stretch=1.00000mm,Velocity=1.50000mm/min)
- Cooling(Top=40.0deg, Bottom=40.0deg)
- Open Chamber()
- Unlock door()
- Cooling(Top=30.0deg, Bottom=30.0deg)

C.2 Cell Staining Protocols

C.2.1 Hoechst 33342 / Propidium Iodide

- Rinse cells in PBS*. (*Two quick rinse and two five-min rinses.)
- Apply a 100µg/mL solution of RNase A in PBS for 20 minutes at 37°C**.

- Rinse cells in PBS*. (**RNase treatment to remove RNA, the cause of cytoplasmic staining, is optional.)
- Apply a 1:1000 dilution of Hoechst 33342 stock in PBS (10 μ g/mL) for 20 minutes at 37°C.
- Rinse cells in PBS*.
- Apply a 1:500 dilution of propidium iodide stock in PBS (2 μ g/mL) for 5 minutes at 37°C.
- Rinse cells in PBS*.

C.2.2 Alexa Fluor® 488 phalloidin

- Dilute powder in 1.5 mL MtOH for stock solution.
- Make working solution (10 mL / 400 mL of stock solution in PBS)
- Remove media and rinse cells in PBS*
- Fix the sample in 3.7% formaldehyde (4% paraformaldehyde) solution in PBS for 10 min.
- Rinse cells with PBS*.
- Rinse cells in 0.1% Triton-X 100 in PBS for 3-5 min. (permeabilization)
- Rinse cells with PBS*.
- Incubate sample in working solution at 37°C for 20 min.
- Rinse cells with PBS*.

C.2.3 FM 1-43

- Dissolve 1 mg FM 1-43 in 2 mL DI water (concentration 0.5 mg/mL, about 1 mM) for stock solution.
- Make 20 μ M working solution (1 mL / 50 mL of stock solution in PBS):
- 20 μ L stock in 1 mL 1x PBS.
- Remove media and rinse cells in PBS*.
- Incubate sample in working solution at 37°C for 2.5 min.
- Rinse cells with PBS*.
- Fix the sample in 3.7% formaldehyde (4% paraformaldehyde) solution in PBS for 15 min.

- Rinse cells with PBS*.
- Incubate sample in 1:1000 dilution of Hoechst 33342 stock in PBS (10 μ g/mL) for 20 minutes at 37°C.
- Rinse cells with PBS*.

C.2.4 Anti-mouse IgG fluorescein secondary antibody

- Remove media and rinse cells in PBS*.
- Fix cells with 4% paraformaldehyde in PBS for 10 minutes at room temperature.
- Rinse cells with PBS*.
- Incubate with 0.25% Triton X-100 in PBS for 5 minutes.
- Rinse cells with PBS*.
- Incubate 8% BSA in PBS for 1 hour at room temperature.
- Rinse cells with PBS*.
- Incubate the cells with 10 μ g/ml anti-Vinculin in 1% BSA in PBS for 1 hour at room temperature.
- Rinse cells with PBS*.
- Incubate the cells with a 1:100 dilution of goat anti-mouse IgG fluorescein conjugated secondary antibody in 1% BSA in PBS for 1 hour at room temperature.
- Rinse cells with PBS*.
- Incubate sample in 1:1000 dilution of Hoechst 33342 stock in PBS (10 μ g/mL) for 20 minutes at 37°C.
- Rinse cells with PBS*

C.3 Cell Counting with Trypan Blue

- Prepare a cell suspension
 - Rinse cells with HBSS at room temperature for 10 min, twice.
 - Trypsinize cells at 37°C for 5 min and Suspend.
 - Spin down at 1000 rpm for 5 min.

- Remove trypsin supernatant.
- Add 5 ml HBSS and resuspend.
- Take 1 ml of a very well mixed HBSS/cell suspension.
- Combine 100 μ l 0.4% Trypan blue and 0.8 ml HBSS with cell suspension
- Fully resuspend.
- Place a cover slip over hemocytometer.
- Apply one drop of solution on the edge of cover slip and allow capillary action to draw it under cover slip.
- Count living cells (clear, the dead cells will be stained with tryphan blue) at 4 corners and 1 center square of hemocytometer. Do this for both sides of hemocytometer.
- Calculate cell density as follows:

$$\text{Cells per mL} = \text{cells counted} \times 10 \times 1000$$